学位論文

Symmetries and quantum phases in one-dimensional spin systems

（１次元スピン系における対称性と量子相）

平成２６年１２月博士（理学）申請

東京大学大学院理学系研究科
物理学専攻

藤　陽平

Abstract

We investigate disordered phases realized in one-dimensional quantum spin systems. We revisit an effective field theory proposed by Schulz [Phys. Rev. B **34**, 6372 (1986)], which encapsulates several essential properties in low energy, from the point of view of symmetry. Although this effective theory was originally derived by perturbation theory, we find that it is fully consistent with the symmetry of the Hamiltonian and thus uniquely identified in the non-perturbative sense. This theory explains many possible phase transitions known to occur among valence-bond-solid phases, which are typical disordered phases in one-dimensional spin systems. Furthermore, this theory indicates that the phase transitions only occur under one of four symmetries: time reversal, bond-centered inversion, dihedral group of spin rotations, and site-centered inversion combined with a spin rotation. Surprisingly, the first three symmetries are consistent with those protecting the Haldane phase in spin-1 chains, which have already been found by a completely different approach using the matrix-product state (MPS). On the other hand, the last one is not known so far. To understand it, we explicitly construct a microscopic model that has two distinct disordered phases protected by the combined inversion symmetry. We examine this model and confirm the existence of those disordered phases by perturbation theory and numerical simulations. For completeness, we further give a more rigorous proof of their existence, based on the non-translation-invariant MPS. We also propose an extension of the Lieb-Schultz-Mattis theorem for the absence of a unique gapped ground state in half-odd-integer spin systems with site-centered inversion symmetry.

This thesis is based on the following papers:

- Yohei Fuji, Frank Pollmann, and Masaki Oshikawa,

  Distinct trivial phases protected by a point-group symmetry in quantum spin chains,

  arXiv:1409.8616.

- Yohei Fuji,

  Effective field theory for one-dimensional valence-bond solid phases and their symmetry protection,

  arXiv:1410.4211.

Acknowledgments

I would like to thank my supervisor, Masaki Oshikawa, for many helpful discussions, insightful advices, and encouragement during my doctoral study. It was a great pleasure for me to have an opportunity to join his group from the doctoral course. This thesis would not have been possible without his great help and deep discernment of physics.

I also appreciate Frank Pollmann for helpful discussions and many advices on the matrix-product state as both computational and mathematical tools. On finalizing the collaboration underlying this thesis, it was important to discuss with him at a workshop "Topology and Entanglement in Correlated Quantum Systems," held in Max-Plunck-Institute für Physik komplexer Systeme, which also gave me an exciting experience.

I especially thank Satoshi Nishimoto for valuable discussions and the collaboration at an early stage of this work. A study with him on four-leg spin tubes (cf. Sec. 4.3) eventually led me to the idea of a field-theoretical proof of the symmetry-protected nature of valence-bond-solid phases.

I am grateful to Philippe Lecheminant for helpful discussions and comments on my study. He kindly accepted me to visit his laboratory at Université de Cergy-Pontoise, and interactions with him were definitely important for me to have confidence in my results.

I appreciate Xavier Plat, Sylvain Capponi, and Pierre Pujol for valuable comments and a different collaboration on spin tube systems, and the hospitality of Laboratoire de Physique Théorique, IRSAMC, Université Paul Sabatier and CNRS, Toulouse, France.

I also appreciate Rex Lundgren and Shunsuke Furukawa for a different collaboration on the entanglement spectrum in spin ladder systems, which is helpful for me to understand the role of entanglement in condensed matter physics.

I thank the members and collaborators at my master's course in Chiba University, including Hitoshi Nakada and Yukinori Ohta for different collaborations, and especially Kazuhiro Seki for helpful discussions and advices.

I thank the members at Institute for Solid State Physics for creating an enjoyable environment during my doctoral course, including Hiroyuki Fujita, Yoshiki Fukusumi, Yuta Kumano, Miklós Lajkó, Soichiro Mohri, Yuya Nakagawa, Hidetaka Nishihara, Wenxing Nie, James Quach, Sakano Rui, Takafumi Suzuki, Yasuhiro Tada, Emika Takata, and Atsuko Tsuji. Especially, I thank Yuta Kumano, as a friend and a colleague at the same grade, for inspiring discussions and sharing sometimes hard but substantial moments, Soichiro Mohri for careful discussions and his deep insights on the matrix-product state, and Yasuhiro Tada for penetrating discussions and comments.

I am also indebted to Ignacio Cirac, Satoshi Ejima, Akira Furusaki, Shunsuke Furuya, Hosho Katsura, Masaaki Nakamura, Kiyomi Okamoto, Edmond Orignac, Didier Poilblanc, Masahiro Sato, Ken Shiozaki, Shintaro Takayoshi, Takashi Tonegawa, Keisuke Totsuka, Masahisa Tsuchiizu, Xiao-Gang Wen, and Tsuneya Yoshida for useful and inspiring discussions.

I acknowledge financial supports by the Global COE Program "the Physical Science Frontier" in part and the Program for Leading Graduate School for "Frontiers of Mathematical Science and Physics (FMSP)" and a travel support by the Institutional Program for Young Reseacher Overseas Visits.

Contents

Chapter 1

Introduction

The Landau theory exhaustively classifies all possible symmetry-breaking phases in classical and quantum systems. In this framework, distinct phases are fully characterized by local order parameters. It also tells us that all disordered states, which do not break any symmetry of the corresponding Hamiltonian, are classified into a single phase. However, recent understanding on topological phases, which cannot be characterized by any local quantity, signals that the Landau theory fails to completely classify *quantum* phases. Even among disordered phases, phase transitions are known to occur in quantum systems.

A perfect scheme classifying all the quantum phases beyond the Landau theory has not been known yet. However, a very general scheme based on the local unitary transformation (LUT) has been proposed for the classification of *gapped* quantum phases [1–3]. In this scheme, two gapped ground states of local Hamiltonians belong to the same phase if and only if they can be transformed each other by an LUT. Equivalently, two gapped ground states belong to the same phase if and only if the one is adiabatically connected to the other by a continuous change of the parameters in the Hamiltonian. Therefore, there must be a gap closing between different gapped quantum phases. From the point of view of many-body entanglement, which is a key ingredient to understand the topological phases, LUTs can only change short-range entanglement (SRE). Thus a ground state with long-range entanglement, such as fractional quantum Hall states, cannot be connected to a direct-product state by LUTs, as it contains long-range entanglement. On the other hand, any SRE state can be transformed into a single direct-product state by an LUT, and thus all SRE states belong to the same phase.

However, if we impose symmetries on the Hamiltonian, a rich variety of SRE phases appears. In this case, a certain SRE state cannot be connected to another SRE state by LUTs that respect the symmetry imposed to the Hamiltonian. These states belong to the class of either the symmetry-breaking phase or the *symmetry-protected topological* (SPT) phase [4]. States in the class of the SPT phase do not break any symmetry of the Hamiltonian, but they are still distinct from each other. The SPT phase now becomes a new frontier in condensed matter physics.

A notable example of SPT phases is the Haldane phase in the spin-1 Heisenberg chain [5,6]. Its properties are qualitatively understood in terms of the Affleck-Kennedy-Lieb-Tasaki (AKLT) state [7, 8]. Although there is no local order parameter due to the absence of symmetry breaking, the spin-1 Haldane phase has a nonlocal (string) order parameter associated with the hidden $Z_2 \times Z_2$ symmetry breaking [9–11]. Furthermore, spin-1/2 gapless excitations appear at the ends of an open chain [12]. These features are actually traced back to an entangled nature of the state. Indeed, the spin-1 Haldane phase is composed of entangled pairs

(spin singlets), which cannot be resolved as long as we keep one of three symmetries [13]: time reversal, bond-centered inversion, and dihedral group of π rotations around two orthogonal spin axes. These entangled pairs are directly observed by examining two-fold degeneracy of the entanglement spectrum [13].

The general notion of the SPT phase was first proposed in 2009 [4]. Following that, many systematic results on SPT phases in one dimension, such as classification of 1D SPT phases, have been obtained primarily based on the matrix-product state (MPS) representation [13–16]. The MPS representation gives a faithful description of general gapped ground states in one dimension and is thus a powerful tool to classify 1D SPT phases. However, it should be recalled that many properties of the Haldane phase had been known earlier, even before the notion of the SPT phase was established. In particular, a field-theoretical approach based on Abelian bosonization successfully describes many universal features of a wide range of quantum many-body systems in one dimension.

A notable application of the bosonization approach on the Haldane phase was done by Schulz in 1986 [17]. He showed that the Haldane phase is separated from another disordered phase, the so-called large-D phase, by a phase transition. However, at that time, it was not clearly recognized that the Haldane phase is an SPT phase. A main purpose of this thesis is to revisit his approach from the modern point of view, in order to elucidate the mechanism of symmetry protection in the framework of bosonization. As a result, we find that his effective field theory perfectly captures all the three symmetries protecting the Haldane phase, which are mentioned above.

This effective field theory provides us with a different point of view on the Haldane phase; so far the symmetry-protected nature of the Haldane phase is characterized by its nontrivial entanglement structure, while we focus on whether the Haldane phase is separated from another disordered phase by a gap closing. In this regard, our approach is rather close to the original spirit of the classification of SPT phases—based on the LUT. From this point, we also find that the Haldane phase is still protected by site-centered inversion symmetry combined with a π spin rotation, even in the absence of the above three symmetries. Indeed, the Haldane phase loses its entangled nature in this case, but it is still separated from the large-D phase under this symmetry.

We further argue that the effective field theory describes various phase transition between valence-bond-solid (VBS) phases realized in 1D spin systems. Such VBS phases include the spin-S Haldane phases in spin-S chains, the rung-singlet phase in spin ladders, and the dimer phases in dimerized spin chains and ladders. Based on perturbation theory in the parameters of microscopic models, the effective field theory provides which phase is separated from or connected to the other phase, as the odd-S Haldane phase is separated from the large-D phase while the even-S Haldane phase is not [18]. It tells us that the distinction among VBS phases is also protected by one of four symmetries: time reversal, bond-centered inversion, dihedral group of spin rotations, and site-centered inversion combined with a spin rotation.

Our study based on the effective field theory also feeds back importance of the inversion symmetry to the MPS approach. We show that the use of non-translation-invariant MPSs, in spite of the subtlety on their pureness as a physical requirement, leads to the same consequence as that predicted by the effective field theory. It indicates the existence of distinct trivial phases, in the sense that they can be transformed into direct-product states by LUTs, under the only site-centered inversion symmetry. We further support this fact by numerical simulations in an explicit 1D model. The MPS approach also confirms an extension of the Lieb-Schultz-Mattis theorem [19, 20], which states that half-odd-integer spin systems with site-centered inversion symmetry and either dihedral group or time reversal symmetries

cannot have a unique gapped ground state.

Organization of this thesis

In Chapter 2, we summarize three basic facts underlying this thesis. We first review the failure of the Landau symmetry-breaking theory on quantum systems and introduce a concept of the local unitary transformation for the classification of gapped quantum phases. After an intuitive argument based on many-body entanglement, we reach a definition of the SPT phase. Second, we give a short historical review on 1D quantum spin systems. In particular, we explain their field-theoretical descriptions using the non-linear sigma model and the physical properties of the Haldane phase from the VBS picture. Third, we give a short course on the MPS formalism. Starting from the definition of the MPS, we explain its pureness and symmetry on translation-invariant MPSs as physical requirements. Then we review the classification of 1D SPT phases and its application to the Affleck-Kennedy-Lieb-Tasaki state.

In Chapter 3, we revisit the field-theoretical description of spin ladder systems by Abelian bosonization, following Schulz [17]. We derive an effective Hamiltonian only with a single bosonic field, which captures essential low-energy properties of 1D spin systems. However, we not only follow his derivation based on perturbation theory but also provide a non-perturbative argument focusing on the compactification of a bosonic field and symmetries. We also mention an extension of the Lieb-Schultz-Mattis theorem for 1D spin systems with the site-centered inversion symmetry.

In Chapter 4, we clarify a physical meaning of the effective field theory on various 1D spin systems. Starting from a review on the two-leg ladder that has been extensively studied, we further consider spin-S XXZ chains, N-leg spin-1/2 ladders, and dimerized spin ladders. All these examples point out that the effective field theory faithfully describes phase transitions between VBS phases, which have already been known by several numerical studies.

Chapter 5 is the highlight of this thesis. Based on the effective field theory, we show that the phase transition between different VBS phases is protected by one of four symmetries: time reversal, bond-centered inversion, dihedral group of spin rotations, and site-centered inversion combined with a spin rotation. While the first three are already known, we do not know what the last one indicates. To investigate its consequence, we propose a microscopic model which breaks the first three symmetries but preserves the last one, that is, a spin-1 chain with a staggered magnetic field. By a simple perturbative argument and numerical simulations, we find that the site-centered inversion symmetry combined with a spin rotation preserves the distinction between two trivial phases. We further confirm this fact by the MPS formalism without assuming translational invariance. We also give a proof of the Lieb-Schultz-Mattis theorem under the site-centered inversion symmetry.

We finish this thesis by summarizing our results in Chapter 6. Some future prospects are also mentioned.

Chapter 2

Preliminaries

In this chapter, we summarize several basic facts used in this thesis. In Sec. 2.1, we explain an idea to classify quantum phases. We start from a review on the Landau theory for classical and quantum systems. Then we introduce the concepts of gapped quantum phases and the local unitary transformation. Combined with the notion of many-body entanglement, these ingredients naturally lead us to the idea of the symmetry-protected topological phase. Section 2.2 is devoted to a historical review on one-dimensional (1D) spin systems. Essential physical properties of spin chains and spin ladders are explained here. The latter part of this section is spent to introduce the notion of the valence-bond-solid state, which can be realized as unique gapped ground states of certain Hamiltonians of 1D spin systems. In Sec. 2.3, we define the matrix-product state (MPS) for 1D gapped states with translational invariance. Many important facts on 1D SPT phases are understood through the MPS formalism. The basic knowledge on the MPS results will be helpful to read Sec. 5.3.

2.1 Classification of quantum phases

A state of matter belongs to a *phase* that is a region in the parameter space spanned by temperature, interactions, external fields, and so on. Every state belonging to the same phase shares the same physical properties. When a system passes from one phase to another, it undergoes a *phase transition* at which macroscopic quantities, such as specific heat or susceptibility, exhibit some singular behavior. One of main goals in condensed matter physics is to classify all the phases and phase transitions, based on some general principle.

In the following, we review the Landau symmetry-breaking theory and its failure on quantum phases (see for example, Section I of Ref. [2]). Introducing the notion of *gapped* quantum phases, we explain an idea to classify them from the point of view of the many-body entanglement. In the end, the concept of the *symmetry-protected topological phase*, which is the most important object in this thesis, is clarified

2.1.1 Symmetry-breaking phases

Many phases known in condensed matter physics, such as ferromagnet, superfluid, and superconductor, are associated with *spontaneous symmetry breaking*. These phases can be understood (at least qualitatively) in terms of mean-field theory and have some classical analogue. In the following, we first review the case of a classical system and then move to a quantum system. In both cases, a distinction between different symmetry-breaking phases is well described by the Landau theory (see for example [21]).

Classical system

As an example, we consider a classical Heisenberg ferromagnet given by the Hamiltonian,

$$H = -\sum_{\langle ij \rangle} \vec{S}_i \cdot \vec{S}_j, \tag{2.1}$$

where $\vec{S}_i \equiv (S_i^x, S_i^y, S_i^z)$ and $\langle ij \rangle$ represents a pair of nearest-neighboring sites on a d-dimensional hypercubic lattice. In high temperature, each spin behaves randomly due to the thermal fluctuation, and the system is in a *disordered* (or *paramagnetic*) phase. In this phase, a correlation function decays exponentially in a large distance as

$$\langle S_i^z S_j^z \rangle \propto e^{-|i-j|/\xi}, \quad \langle \cdots \rangle = \frac{\sum_{\{\vec{S}_i\}} (\cdots) e^{-\beta H}}{\sum_{\{\vec{S}_i\}} e^{-\beta H}} \tag{2.2}$$

where the sum runs over all possible spin configurations $\{\vec{S}_i\}$ and β is the inverse temperature $\beta = 1/T$ (we set the Boltzmann constant to unity, $k_B = 1$). ξ determines a characteristic length scale depending on the microscopic model, over which spins are correlated, and is called the *correlation length*. In the hight-temperature limit $T \to \infty$, the correlation length goes zero, $\xi \to 0$.

In the zero temperature, spins are all aligned in a parallel way, and the system is in an *ordered* (*ferromagnetic*) phase. In the ordered phase, the O(3) spin-rotational symmetry is spontaneously broken, so that the expectation value of a local spin moment, say $\langle S_i^z \rangle$, takes a finite value and works as an *order parameter*. [1] In $d \leq 2$, this ordered phase only exists in the zero temperature because of the Mermin-Wagner theorem, which forbids any continuous symmetry breaking in a finite temperature. On the other hand, it can extend to finite temperatures T in $d > 2$. Below the critical temperature $T < T_c$, the system is in the ferromagnetic phase and there exists a long-range order detected by a correlation function,

$$\lim_{|i-j| \to \infty} \langle S_i^z S_j^z \rangle = \langle S_i^z \rangle^2. \tag{2.3}$$

On the other hand, a connected correlation function decays exponentially as

$$\langle (S_i^z - \langle S_i^z \rangle)(S_j^z - \langle S_j^z \rangle) \rangle \propto e^{-|i-j|/\xi'}, \tag{2.4}$$

with some correlation length ξ'.

At the critical temperature $T = T_c$, the system undergoes a phase transition at which the correlation function behaves as

$$\langle S_i^z S_j^z \rangle \propto \frac{1}{|i-j|^{d-2+\eta}}, \tag{2.5}$$

where η is a universal quantity called as the critical exponent. At this point, the correlation length diverges, $\xi \to \infty$. Thus, the paramagnetic and ferromagnetic phases are separated by the phase transition in the classical Heisenberg ferromagnet.

[1] More precisely, for a quantity to work as a proper order parameter detecting spontaneous symmetry breaking, we need to proceed as follows. We choose a local quantity $\mathcal{O}_i$ as an order parameter when $\mathcal{O}_i$ is *non*-invariant under a symmetry operation g that is supposed to be spontaneously broken: $g\mathcal{O}_i g^{-1} \neq \mathcal{O}_i$. Here "local" means that a region in which $\mathcal{O}_i$ is defined does not extend as the system size is increased. Then we add a small *conjugate field* $h_{\mathcal{O}}\mathcal{O}_i$ to the Hamiltonian. On calculating the expectation value of $\mathcal{O}_i$ with respect to $H + h_{\mathcal{O}} \sum_i \mathcal{O}_i$ as in Eq. (2.2), we *first* take the thermodynamic limit $V \to \infty$ (V is the volume of the system) and *then* turn off the conjugate field $h_{\mathcal{O}} \to 0$. If the system spontaneously breaks the symmetry, we will obtain a finite value of $\langle \mathcal{O}_i \rangle$ in this procedure. We also require the same procedure in quantum systems, while $\mathcal{O}_i$ are read off as a local operator and the expectation value is taken with respect to the ground state of $H + h_{\mathcal{O}} \sum_i \mathcal{O}_i$.

Quantum system

In the quantum-mechanical case, we consider the transverse Ising model on a d-dimensional hypercubic lattice,

$$H = -\sum_{\langle ij \rangle} s_i^z s_j^z - h \sum_i s_i^x, \tag{2.6}$$

where s^α, $\alpha = x, y, z$ is a spin-1/2 operator obeying the SU(2) algebra, $[s^\alpha, s^\beta] = i\epsilon^{\alpha\beta\gamma} s^\gamma$. At the zero temperature, the low-energy physics is governed by the *ground state* of the Hamiltonian, $|\Phi_0\rangle$, which satisfies $H|\Phi_0\rangle = E_0|\Phi_0\rangle$ with the lowest energy eigenvalue E_0. In this case, we can consider *quantum phases* in a space spanned by parameters of the Hamiltonian. A phase transition driven by a change of the parameters is called the *quantum phase transition.* As in the classical case, spontaneous symmetry breaking is a guiding principle to classify the ground state into some quantum phase.

For $h \gg 1$, the ground state $|\Phi_0\rangle$ is in a paramagnetic phase where spins are all polarized along the magnetic field. In this phase, the ground state is unique and has a finite excitation gap below the first-excited state. Then, a correlation function decays exponentially:

$$\langle s_i^z s_j^z \rangle \propto e^{-|i-j|/\xi}, \quad \langle \cdots \rangle = \langle \Phi_0 | \cdots | \Phi_0 \rangle. \tag{2.7}$$

For $h \ll 1$, spins are aligned in the z direction. In this case, the ground state is two-fold *degenerate* in the thermodynamic limit, due to spontaneous breaking of the spin reversal symmetry $s_i^z \to -s_i^z$. As in the classical ferromagnet, we can detect this symmetry breaking by the long-range order in a correlation function $\langle s_i^z s_j^z \rangle$ or the finite expectation value of an order parameter $\langle s_i^z \rangle$. If the ground state is in a *cat state*, which is a superposition of degenerate ground states belonging to different superselection sectors, such as $|\tilde{\Phi}_0\rangle = (|\uparrow\uparrow\uparrow\uparrow \cdots\rangle \pm |\downarrow\downarrow\downarrow\downarrow \cdots\rangle)/\sqrt{2}$, the order parameter $\langle s_i^z \rangle$ vanishes but the connected correlation function $\langle (s_i^z - \langle s_i^z \rangle)(s_j^z - \langle s_j^z \rangle) \rangle$ remains finite.

In this example, at $d = 1$, the model can be mapped onto a two-dimensional Ising model and the exact solution exists [22]. There is a continuous phase transition between the ferromagnetic and disordered phases, at a critical point $h = 1/2$. At this point, a finite excitation gap above the ground state vanishes. This is a simplest example of the quantum phase transition.

Landau theory

Given a Hamiltonian, there naturally exist some symmetries, such as spin rotation, time reversal, lattice translation, reflection, inversion, particle conservation (gauge symmetry), and so on. Regardless of whether we consider classical or quantum systems, states with spontaneous symmetry breaking are all classified by the *Landau theory.* Indeed, the states with different symmetries belong to different phases. As seen in the previous examples, a symmetry-breaking state is detected by an appropriate order parameter. Since the symmetry forms a group, with the help of group theory, we can in principle classify all possible subgroups of the full symmetry group and construct a full set of order parameters, each of which is only invariant under the symmetry operation associated with such a subgroup. By examining which order parameter takes a finite expectation value, we can identify the pattern of symmetry breaking and classify the states with different symmetries into different phases.

By the use of these order parameters, we can draw the complete phase diagram for classical systems. Indeed, all the classical phases are classified by the Landau theory. In an example

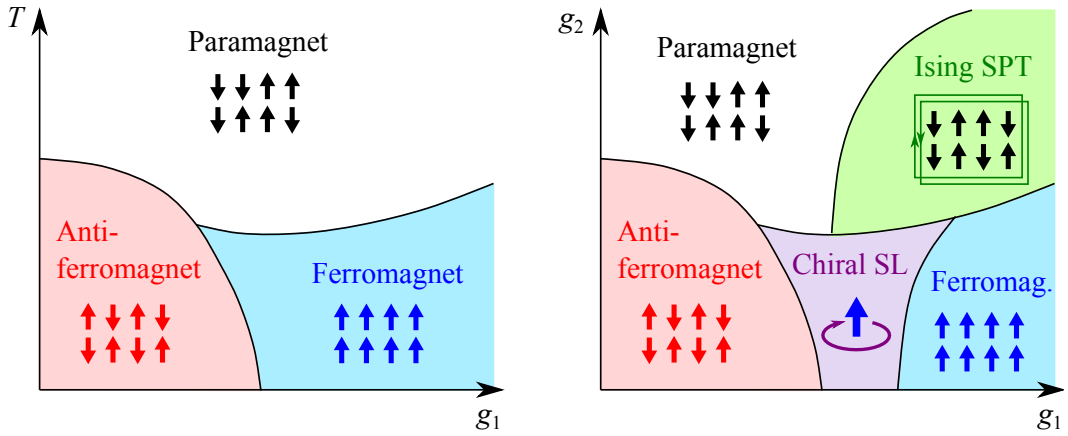

Figure 2.1: Conceptual phase diagrams for (a) classical and (b) quantum spin systems. In the classical phase diagram, the parameter space is spanned by temperature T and a parameter g_1 of the Hamiltonian. There only exist one symmetric phase (paramagnet) and other symmetry-breaking phases (ferromagnet and antiferromagnet). In the quantum phase diagram, the parameter space is spanned by two parameters g_1 and g_2 of the Hamiltonian. In addition to the phases that also appear in the classical case, there is also another kind of the paramagnets, namely a symmetry-protected topological phase with a Z_2 symmetry. Even among phases sharing the same symmetry breaking, there could be more phases. An example is the chiral spin liquid, a lattice realization of the fractional quantum Hall state, which can be accompanied by spontaneously breaking of time reversal symmetry.

of Fig. 2.1 (a), a ferromagnetic phase breaks a spin-reversal symmetry and is detected by a local magnetization $\langle s^z_{i,j}\rangle$. [We consider a square lattice whose coordinates are specified by integers (i,j).] An antiferromagnetic phase breaks not only the spin-reversal symmetry but also a lattice symmetry and is detected by a staggered magnetization $\langle(-1)^{i+j}s^z_{i,j}\rangle$. If no order parameter takes a finite value, we will find a paramagnetic phase.

Can we classify all the quantum phases by the Landau theory based on the symmetry breaking? While this was believed so, recent understanding on the quantum phases clearly answers no. A prominent exception is the fractional quantum Hall states. They have some characteristic feature that cannot be captured by any local operator; it is often called topological order. Recently, a different notion of topological order only meaningful under the symmetry, symmetry-protected topological order, has also been proposed. This is a main target in this thesis. An example of quantum phase diagrams is drawn in Fig. 2.1 on a space spanned by two parameters of the Hamiltonian.

2.1.2 Beyond Landau theory: Entanglement point of view

Quantum systems can have richer phase structures than classical systems. Even if we focus on the quantum "paramagnets," in which no symmetry breaking occurs, there are infinitely many possible quantum phases. One will naturally ask how to characterize different quantum phases. However, at the present stage, there is no clue for the general case. Nevertheless, if we only focus on *gapped* quantum phases, we can characterize different quantum phases.

Let us consider the ground state $|\Phi(g)\rangle$ of a local Hamiltonian $H(g)$, which is written as a sum of local operators depending on a parameter g, $H(g) = \sum_i \mathcal{O}_i(g)$. The ground state $|\Phi(g)\rangle$ could have finite degeneracy. We suppose that it has a *uniform gap*, that is, an

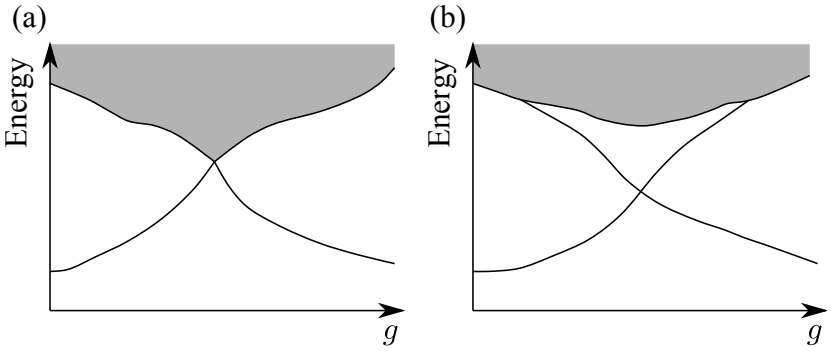

Figure 2.2: Two types of gap closing between two gapped quantum phases. (a) Continuous phase transition: two levels corresponding to the ground states are merged into the gapless continuum at the transition point. (b) First-order phase transition: two levels cross each other at the transition point.

energy gap below the first excited state, which is independent of the system size. Thus, for a sufficiently large system, the gap becomes a constant of order of unity. Then we consider two gapped states $|\Phi(0)\rangle$ and $|\Phi(1)\rangle$ as the ground states of respective Hamiltonians $H(0)$ and $H(1)$. They belong to the same phase, if and only if there exists a finite-time evolution operator satisfying [2]

$$|\Phi(0)\rangle = U\,|\Phi(1)\rangle\,, \quad U = T\left[e^{-i\int_0^1 d\tilde{g}\tilde{H}(\tilde{g})}\right], \tag{2.8}$$

where T is a "time-ordering" operator. $\tilde{H}(\tilde{g})$ is also a sum of local operators but can be different from $H(g)$. U is called the *local unitary transformation* (LUT) [2]. Roughly speaking, if we can find a finite continuous path connecting two gapped states without gap closing, they belong to the same phase. Conversely, between two gapped phases belonging to different phases, there must be a gap closing or an infinite-time evolution connecting them. Here the "gap closing" can mean either a gapless critical point corresponding to a continuous phase transition, or a first-order transition caused by a level crossing. This is depicted in Fig. 2.2.

Topologically ordered phases and long-range entanglement

Here we focus on gapped quantum phases in two dimensions. A notion of *topological order* [23] was originally introduced to represent the ground-state degeneracy of the chiral spin liquid, which is a lattice generalization of the fractional quantum Hall state, on torus or nontrivial closed manifolds. The origin of the ground-state degeneracy is emergent excitations, called the *fractionalized quasiparticles*. These quasiparticles obey a nontrivial particle statistics of neither boson nor fermion, generally referred to braiding statistics. Since a braiding statistics is characterized by a set of discrete parameters,[2] two states with fractionalized quasiparticles with different statistics cannot be adiabatically connected.

The ground-state degeneracy on torus basically counts the number of different fractionalized quasiparticles. However, a practical computation of the ground-state degeneracy is difficult. Instead, we can use the *entanglement entropy* that also captures the same information but is relatively easy to calculate. Given the ground state $|\psi\rangle$, let us consider a bipartition of the system into subsystems A and B. We define the *reduced density matrix* of

[2]This property is known as Ocneanu rigidity.

the subsystem A as

$$\rho_A = \mathrm{Tr}_B \left|\psi\right\rangle \left\langle\psi\right| , \tag{2.9}$$

which is obtained by tracing out the degrees of freedom in the subsystem B from the density matrix of the whole system $|\psi\rangle\langle\psi|$. Then, the von Neumann entanglement entropy is defined by

$$S = -\mathrm{Tr}_A \left[\rho_A \log \rho_A\right] . \tag{2.10}$$

In *topologically ordered phases*, such as the fractional quantum Hall state, the entanglement entropy takes the form [24, 25],

$$S = \alpha L - \log \mathcal{D}, \tag{2.11}$$

where L is the length of the boundary between the subsystems, α is a nonuniversal constant, and $\mathcal{D}^2$ is the ground-state degeneracy on torus. The first term comes from the *short-range entanglement* only living near the boundary. On the other hand, the last term encapsulates a nonlocal information, the so-called *long-range entanglement*.

The LUT defined in Eq. (2.8) is composed of local operators. It will manipulate the short-range entanglement but will not change the long-range entanglement. If we consider states that do not contain the long-range entanglement, by using U, we can completely remove the short-range entanglement and every state will reach to a single direct-product state. This class of the state is called the short-range entanglement (SRE) state, and every SRE state belongs to a single SRE phase, since they can be connected to a direct-product state by U. Otherwise, the state belongs to some long-range entanglement (LRE) phase [see Fig. 2.3 (a)].[3]

Short-range entangled phases

The SRE phase seems much boring because there is only one phase. However, this situation is drastically changed when we impose the symmetry on the Hamiltonian. In this case, there are multiple SRE phases, which cannot be connected each other by any LUT respecting the imposed symmetry. One class of SRE phases is the symmetry-breaking phase, which we reviewed in the previous section. Another class is the *symmetry-protected topological phase*[4] [4], which has no symmetry breaking. States belonging to different symmetry-protected topological phases preserve the full symmetry of the Hamiltonian but cannot be connected each other.

[3]The term "LRE phase" is defined in this negative way. States belonging to the LRE phase cannot be transformed into a direct-product state by any LUT. It naturally includes states characterized by the ground-state degeneracy on torus, such as fractional quantum Hall states, toric code states, and string-net condensate states. All these states also have fractionalized quasiparticles obeying braiding statistics. On the other hand, states that have neither fractionalized quasiparticles nor ground-state degeneracy, such as the integer quantum Hall state and its bosonic analogue (Kitaev E_8 state), also belong to the LRE phase in the above sense [26, 27]. These phases are said to have an invertible topological order. Moreover, three-dimensional self-correcting quantum code states are also considered to belong to the other kind of LRE phases. The notion of topological order is still under development. It could be changed if some other "strange" phase is found.

[4]The symmetry-protected topological phase is also called the symmetry-protected *trivial* phase, in the sense that it can be transformed into a direct-product state by an LUT. This terminology is often used by one of its inventors.

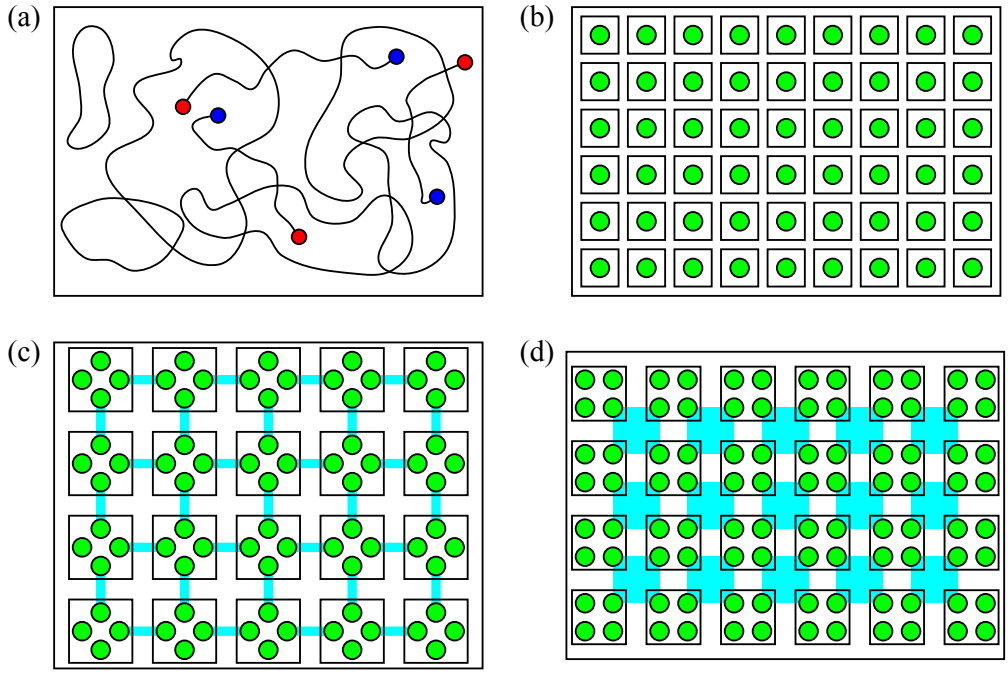

Figure 2.3: Schematic pictures of LRE and SRE states. (a) A LRE state is filled with objects like closed strings. Its excitation is an open string that has fractionalized quasiparticles at its ends. SRE states are transformed into a direct-product state of (b) site local states, (c) entangled pairs where two spins are connected by a blue solid line, and (d) entangled plaquettes where four spins are connected by a blue square. The symmetry acts on each square enclosing one or four spins.

2.1.3 Symmetry-protected topological phases

Let us summarize the definition of the symmetry-protected topological (SPT) phase.

> *The SPT phase is a class of gapped quantum phases that have no symmetry breaking. States belonging to different SPT phases cannot be connected each other by any LUT respecting the symmetry. But they can be transformed into a single direct-product state by an LUT that does not respect the symmetry.*

This also says that the SPT phase has a unique ground state. There are many systematic studies on the SPT phase [14–16, 28–33]. For the 1D case, we summarize the known classification of SPT phases in Sec. 2.3.3. Although the definition of the SPT phase is exhausted in the above one, here we try to provide one way to think what is the SPT phase.

Intuitive picture

The idea of the renormalization group is still useful on the understanding of gapped quantum phases. States belonging to the same phase flow to the same fixed point, while states belonging to different phases flow to different fixed points. What is the fixed point of a gapped quantum state? The existence of a finite gap immediately indicates a finite or zero correlation length [34], which gives a certain length scale to the system. But any fixed point must be invariant under the scale transformation, so that the correlation length should be zero. Since we are

considering the short-range entanglement phase, the zero correlation length is only achieved in direct-product states.

Even if we impose some symmetry on the Hamiltonian and consider states belonging to the SPT phase, their fixed points must be some direct-product states. A simple way to achieve such state is to form a direct product of states on each site, as in Fig. 2.3 (b). We can also consider another direct-product state composed of entangled pairs, such as spin singlets [Fig. 2.3 (c)]. But we can always resolve these entangled pairs by applying a proper LUT. However, if we impose some symmetry among these entangled pairs, there is the case that we cannot remove the entanglement of the pair by any symmetric LUT. This becomes an SPT phase different from the simple direct-product state. We can further consider a direct-product state formed by extended objects, such as entangled plaquettes [see Fig. 2.3 (d)], and achieve another SPT phase if those plaquettes cannot be resolved under any symmetric LUT.

Edge states and entanglement spectrum

As we can expect, if we consider the system with a boundary, these nontrivial SPT phases could reveal unpaired objects at the boundary. This is an intuitive explanation of the existence of edge states in several SPT phases. In one dimension, the Haldane phase in spin-1 chains is of this type; it has gapless spin-1/2 edge states (see Sec. 2.2.3). The Haldane phase is in fact protected by time reversal, spin rotation, and bond-centered inversion symmetries [13]. As long as one of these symmetries exists, we cannot resolve entangled pairs of spin-1/2's, namely spin singlets. In two dimensions, there are also SPT phases that support edge states: the quantum spin Hall state [35, 36], Z_2 SPT phase [37, 38], and bosonic integer quantum Hall state protected by a U(1) symmetry [28, 39–41]. In three dimensions, the topological insulator protected by time reversal symmetry also supports a gapless Dirac fermion on its surface [42, 43].

These nontrivial entanglement structures are not captured by the entanglement entropy (2.10); it only detects the signature of the long-range entanglement, and the term proportional to the length of the boundary does not serve as a universal probe. However, entries of the reduced density matrix itself may capture the formation of the short-range entangled objects. In fact, the entanglement spectrum [44] [defined in Eq. (2.77)], which is the eigenvalue spectrum of the reduced density matrix, captures these entanglement structure as a nontrivial degeneracy or a gapless dispersion relation [13, 45–48].

We want to stress that, although the presence of edge states and/or a nontrivial structure in the entanglement spectrum are clear signatures for some kinds of SPT phases, these are not a defining property of all the SPT phases. There still exist SPT phases that cannot be characterized by their nontrivial entanglement structure. Let us consider an SPT phase in *zero dimension*, that is just a few-body problem. We can still define the phases according to the presence or absence of a gap closing between two states. First, states belonging to an SPT phase must form a 1D representation of the imposed symmetry; otherwise multi-dimensional representations lead to some symmetry breaking. Second, there should be a level crossing between states forming different 1D representations, since they are orthogonal each other. Thus different SPT phases in zero dimension are distinguished by different 1D representations of the symmetry. Even in higher dimension, there are the cases where different SPT phases are characterized by different 1D representations in the presence of certain lattice symmetries [14] (see also Refs. [49, 50]). In such cases, there are distinct SPT phases in which the short-range entanglement is completely removable by an LUT. This becomes one of main

issues in Chapter 5.

2.2 One-dimensional spin systems

In one dimension, the allowed structure of many-body entanglement is quite limited. It has been proven that there is no long-range entanglement in one dimension [14]. However, besides symmetry-breaking phases, we can still have SPT phases under the symmetry.

In this thesis, we will focus on one-dimensional SPT phases. A prototypical example of the SPT phase is the Haldane phase realized in spin-1 chains and its generalization, the valence-bond-solid phases. We here briefly review the physics in one-dimensional spin systems. In particular, we explain the Haldane's conjecture on 1D antiferromagnets and physical properties of the Haldane phase and its representative, the Affleck-Kennedy-Lieb-Tasaki state.

2.2.1 Spin chain

We first consider the Heisenberg chain with an antiferromagnetic exchange coupling ($J > 0$),

$$H = J \sum_i \vec{S}_i \cdot \vec{S}_{i+1}. \tag{2.12}$$

As opposed to higher-dimensional cases where some magnetic order appears, in 1D, antiferromagnetic long-range order is forbidden by the Mermin-Wagner theorem. In fact, the $S = 1/2$ case is exactly solved by the Bethe ansatz, and its ground state is known to be gapless and critical. If we introduce an uniaxial anisotropy as

$$H = J \sum_i \left[S_i^x S_{i+1}^x + S_i^y S_{i+1}^y + \Delta S_i^z S_{i+1}^z \right], \tag{2.13}$$

the model is called the XXZ chain. This model is again solved by the Bethe ansatz for $S = 1/2$. For $\Delta \leq -1$, spins are aligned along the z axis in the parallel way and lead to the ferromagnetic long-range order with Z_2 symmetry breaking. For $\Delta > 1$, spins are aligned in the antiparallel way and lead to the antiferromagnetic long-range order with Z_2 symmetry breaking. For $-1 < \Delta \leq 1$, including the Heisenberg point, this model is in a critical phase. Its low-energy effective theory is described by a massless free boson or the Tomonaga-Luttinger model,

$$H = \frac{v}{2\pi} \int dx \left[K(\partial_x \theta)^2 + \frac{1}{K}(\partial_x \phi)^2 \right], \tag{2.14}$$

where $\phi(x)$ and $\theta(x)$ are dual bosonic fields, and v and K are the velocity and stiffness depending on J and Δ. This relationship enables us to describe the low-energy effective theory of many one-dimensional spin systems in terms of bosonic fields. Such an approach is called *Abelian bosonization* and extensively used in this thesis. A derivation of Eq. (2.14) from the Heisenberg model (2.12) will be reviewed in Appendix 3.A.

For $S > 1/2$, no exact solution is known for Eq. (2.12). However, in 1982, Haldane conjectured that the ground state of the antiferromagnetic Heisenberg model is in a gapless critical phase for half-odd-integer S while in a gapped disordered phase for integer S [5, 6]. He used the nonlinear sigma model with a topological term, whose Euclidean action is given by (we refer to Ref. [51])

$$S = \int d^2x \left[\frac{1}{2g} \left(\frac{1}{v}(\partial_0 \vec{m})^2 + v(\partial_1 \vec{m})^2 \right) + i \frac{\theta}{8\pi} \epsilon_{ij} \vec{m} \cdot (\partial_i \vec{m} \times \partial_j \vec{m}) \right], \tag{2.15}$$

where $\vec{m}(\vec{x})$ is a three-component vector field and

$$g = \frac{2}{S}, \quad v = 2a_0 JS, \quad \theta = 2\pi S. \tag{2.16}$$

The nonlinearity comes from that the vector field $\vec{m}(\vec{x})$ is constrained to take its value on two-sphere S_2 such that $\vec{m}^2(\vec{x}) = 1$. The last term in Eq. (2.15) is called the topological term, and it takes integral values,

$$W = \frac{1}{8\pi} \int d^2x \; \epsilon_{ij} \vec{m} \cdot (\partial_i \vec{m} \times \partial_j \vec{m}) \in \mathbb{Z}. \tag{2.17}$$

W classifies a smooth configuration $\vec{m}(x)$, which is a mapping from the two-dimensional Euclidean space-time S_2 to the target space S_2, according to the homotopy group $\pi_2(S_2) = \mathbb{Z}$. This topological terms contributes to the partition function as a phase factor factor $e^{i2\pi SW} = (-1)^{2SW}$.

If S is integer, this factor is just unity and the resulting action is the usual nonlinear sigma model. Under the renormalization group, g goes to the strong-coupling limit, $g \to \infty$. Consequently, $\vec{m}(\vec{x})$ strongly fluctuates and acquires a mass, so that the Heisenberg chain with integer S has a disordered ground state with a finite excitation gap. On the other hand, if S is half-odd-integer, the phase factor cannot be neglected. Yet g also goes to the strong-coupling limit, we cannot forget the effect of S due to the topological term. From $g = 2/S$, the low-energy physics of Eq. (2.15) will be governed by that for $S = 1/2$. According to the result of the Bethe ansatz for $S = 1/2$, we expect that the ground state of the Heisenberg chain with half-odd-integer S is gapless and critical.

After the Haldane's conjecture, several numerical studies confirmed the existence of a finite gap [52–55]. Some of studies also investigated a related model [53, 54, 56], the XXZ chain with an on-site uniaxial anisotropy,

$$H = \sum_i \left[J(S_i^x S_{i+1}^x + S_i^y S_{i+1}^y + \Delta S_i^z S_{i+1}^z) + D(S_i^z)^2 \right]. \tag{2.18}$$

This model has an obvious disordered phase in the limit $D \to \infty$, which is connected to a direct-product state $|0000\cdots\rangle$. However, this phase (*large-D phase*) seemed to be separated from the other disordered phase (*Haldane phase*) around the Heisenberg point, predicted by Haldane (see Fig. 2.4). The physical picture of the ground state for the $S = 1$ Heisenberg model had not been clear yet. This point was first addressed by Affleck, Kennedy, Lieb, and Tasaki, as we will see in Sec. 2.2.3.

2.2.2 Spin ladder

In 1986, Schulz considered a one-dimensional model [17], which would share the same low-energy properties with those of Eq. (2.18), namely

$$\begin{aligned} H = \sum_i \Bigg[& J \sum_{j=1}^{2S} (s_{i,j}^x s_{i+1,j}^x + s_{i,j}^y s_{i+1,j}^y + \Delta s_{i,j}^z s_{i+1,j}^z) \\ & + J \sum_{j=1}^{2S} \sum_{j' \neq j} \left(s_{i,j}^x s_{i+1,j'}^x + s_{i,j}^y s_{i+1,j'}^y + \Delta s_{i,j}^z s_{i+1,j'}^z \right) + D \sum_{j=1}^{2S} \sum_{j' \neq j} s_{i,j}^z s_{i,j'}^z \Bigg], \end{aligned} \tag{2.19}$$

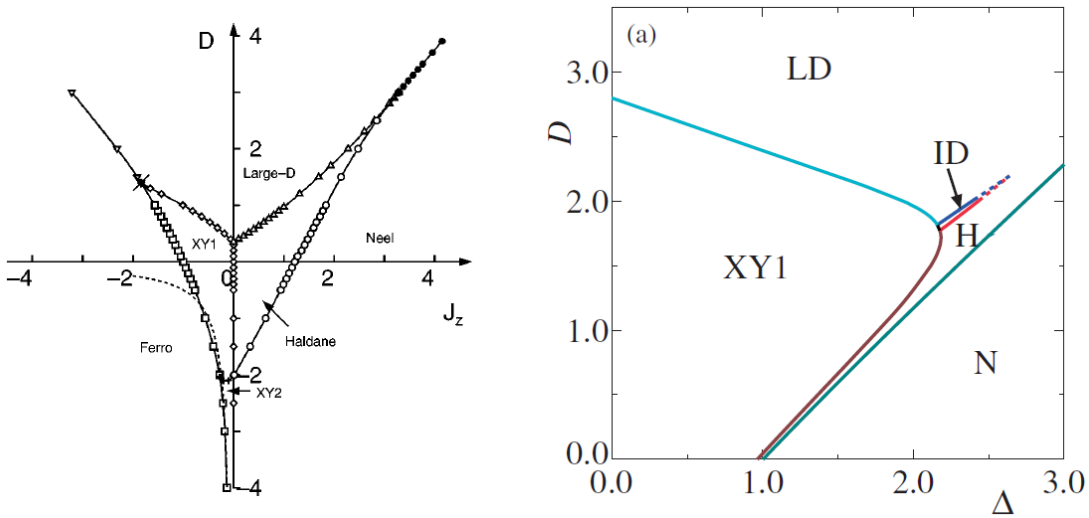

Figure 2.4: Phase diagrams of Eq. (2.18) for (left panel) $S = 1$ [57] and (right panel) $S = 2$ [58]. In the right panel, J_z corresponds to Δ. For $S = 1$, the Haldane (H) and large-D (LD) phase are separated by a continuous phase transition, but for $S = 2$, they can be connected without gap closing.

where $\vec{s}_{i,j}$ is the spin-1/2 operator. This is obtained by replacing $\vec{S}_i \to \sum_{j=1}^{2S} \vec{s}_{i,j}$ in Eq. (2.18). He regarded this model as a $2S$-leg ladder and applied Abelian bosonization technique. Then he proposed an effective sine-Gordon Hamiltonian (see Chapter 3),

$$H = \frac{v}{2\pi} \int dx \left[K(\partial_x \theta)^2 + \frac{1}{K}(\partial_x \phi)^2 \right] + g_{\text{eff}} \int dx \cos(\mu\sqrt{4S}\phi), \tag{2.20}$$

where $\mu = 1$ for integer S while $\mu = 2$ for half-odd-integer S. He reached a similar conclusion to that by Haldane, namely the ground state of this model can be disordered for integer S while not for half-odd-integer S. He also predicted a phase transition between the Haldane and large-D phases for integer S. Although this would turn out to be not true for *even* S (see Fig. 2.4), his effective theory itself is very suggestive. A large part of this thesis is spent to show the usefulness of this effective theory on the phase transitions between various disordered phases (Chapter 4) and their symmetry-protected feature (Sec. 5.1).

We can also consider a more conventional ladder system given by

$$H = \sum_i \sum_{j=1}^{N-1} \left[J\vec{S}_{i,j} \cdot \vec{S}_{i+1,j} + J_\perp \vec{S}_{i,j} \cdot \vec{S}_{i,j+1} \right]. \tag{2.21}$$

For $J > 0$ and $J_\perp > 0$, as in the case of Eq. (2.12), this can be mapped on to the nonlinear sigma model (2.15) with $\theta = 2\pi SN$ [59, 60]. Thus, for integer S, the ground state is always disordered. This can be naively understand that integer spins can form a singlet on each rung. On the other hand, for half-odd-integer S, the ground state is disordered for even N while gapless for odd N. This will follow that only an even number of half-odd-integer spins can form a singlet. This model is also treated by the Schulz's effective field theory (2.20) by decomposition of the spin-S into spin-1/2's.

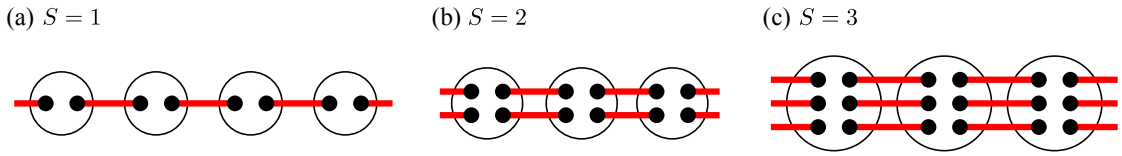

Figure 2.5: VBS states for (a) $S = 1$, (b) $S = 2$, and (c) $S = 3$. Each black filled circle and red solid line represent the spin-1/2 and the singlet pair, respectively. The black circle enclosing spins means a symmetrization to the largest total-spin sector.

2.2.3 VBS phase

In 1987, Affleck, Kennedy, Lieb, and Tasaki (AKLT) proposed a toy model [7, 8], known as the *AKLT model*,

$$H = \sum_i \left[\vec{S}_i \cdot \vec{S}_{i+1} + \frac{1}{3} (\vec{S}_i \cdot \vec{S}_{i+1})^2 \right], \tag{2.22}$$

to explain the nature of the disordered ground state for the $S = 1$ Heisenberg model. This model can be rewritten as a sum of projection operators $P^{S=2}_{j,j+1}$, which project two neighboring spins onto the $S = 2$ sector. Thus if we can form a state in which each neighboring spins have the total spin $S = 0$ or 1, it becomes the exact ground state. Such a ground state is constructed as follows. First, we decompose a spin-1 into two spin-1/2's. Then we form a singlet between two spin-1/2's on neighboring sites. Finally, we symmetrize two spin-1/2's on each site back to a single spin-1. A state constructed in this way [see Fig. 2.5 (a)], called the *valence-bond-solid (VBS) state* or *AKLT state*, has the total spin $S = 0$ or 1 on each neighboring spins and thus becomes a ground state of Eq. (2.22). This state is unique and gapped, and any correlation function decays exponentially. Thus, it fully satisfies the desired ground-state properties for the $S = 1$ Heisenberg chain, predicted by Haldane.

The AKLT state has some exotic properties, which are also shared in the Haldane phase. One is the appearance of spin-1/2 edge states on an open chain, which causes four-fold degeneracy of the ground state [12]. The other is the existence of hidden $Z_2 \times Z_2$ symmetry breaking and associated string order parameters [9–11]. Specifically, by a nonlocal unitary transformation [61],

$$V = \prod_{j<k} \exp\left(i\pi S^z_j S^z_k\right), \tag{2.23}$$

the Hamiltonian (2.18) under the open boundary condition is transformed into

$$VHV^{-1} = \sum_i \left[J \left(S^x_i e^{i\pi S^x_{i+1}} S^x_{i+1} + S^y_i e^{i\pi (S^z_i + S^x_{i+1})} S^y_{i+1} + \Delta S^z_i e^{i\pi S^z_{i+1}} S^z_{i+1} \right) + D (S^z_i)^2 \right], \tag{2.24}$$

This Hamiltonian is still local and has a $\mathcal{D}_2 = Z_2 \times Z_2$ symmetry corresponding to π rotations around two orthogonal spin axes. Thus we expect $\mathcal{D}_2$ symmetry breaking around the Heisenberg point ($\Delta = 1$ and $D = 0$), which leads to four-fold degenerate ground state. This degeneracy is consistent with that caused by the edge states. Correspondingly, the string order parameters [9],

$$O^\alpha = \lim_{|j-k| \to \infty} \left\langle S^\alpha_j \exp\left(i\pi \sum_{l=j}^{k-1} S^\alpha_l \right) S^\alpha_k \right\rangle, \quad \alpha = z, x, \tag{2.25}$$

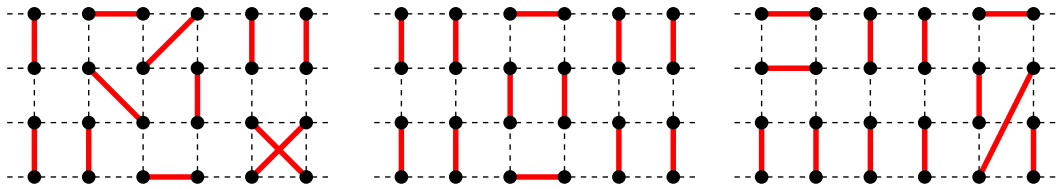

Figure 2.6: Examples of singlet configurations forming a VBS state on the four-leg ladder. These configurations can be transformed each other by a local flip of he singlets.

take a finite expectation values in the Haldane phase. They become just usual ferromagnetic order parameters after the transformation (2.23).

These remarkable features, that is the edge states and the string order parameters, do not appear in the large-D phase realized in Eq. (2.18), which is also disordered. One might think that the hidden $\mathcal{D}_2$ symmetry breaking perfectly describes the distinction between the Haldane and large-D phases in the conventional framework of the Landau theory. If this is true, applying a magnetic field, say hS_i^z, must wash out the distinction, since it adds the $\mathcal{D}_2$ symmetry-breaking nonlocal term to Eq. (2.24). Then, one could find a way to connect the two phases without gap closing. In fact, this naive thought is not quite correct. We cannot eliminate the phase transition between them as long as certain symmetries are preserved. To reach this fact, we had to wait the foundation of a concept of the *symmetry-protected topological phase* in 2009 [4]. The Haldane phase is protected by not only the $\mathcal{D}_2$ symmetry but also time reversal and bond-centered inversion symmetries [13]. We will review this fact based on the matrix-product state formalism in Sec. 2.3.4. We further claim that the Haldane phase is also protected by site-centered inversion symmetry combined with a π-rotation around the z axis, in the sense that it is still separated from the large-D phase. This is a main issue in Chapter 5.

The idea of the VBS state is also applied to higher-S cases. Even for these cases, we can still construct VBS states as follows. We first decompose a spin-S into $2S$ spin-1/2's, then form singlets between neighboring sites, and finally project $2S$ spin-1/2's on each site onto the fully symmetric sector. The ground state of the Heisenberg model (2.12) for $S > 1$ is also understood in this way [see Fig. 2.5 (a) and (b)]. However, for half-odd-integer S, we have no way to construct the VBS states without translational symmetry breaking. If we wish to obtain a unique VBS state in this case, we have to initially break translational invariance in the Hamiltonian.

We can also construct unique gapped states in a similar way for spin-1/2 ladder systems. We distribute short-range singlet pairs on the whole system and superpose them such that the resulting state does not break the lattice symmetry, as in a manner of the short-range resonating valence-bond state [62, 63]. We further require that the constituent states can transform each other by a local flip of the singlets (see Fig. 2.6). Throughout this thesis, we also call the state formed by the singlet coverings in this way as the *VBS state*. We say that a state belongs to the *VBS phase* if and only if the state can be smoothly connected to a VBS state. We discuss that the distinction between various VBS phases is faithfully captured by the effective field theory (2.20) in Chapter 4. Within this theory, it turns out that such distinction is also protected by the set of symmetries, as in the $S = 1$ Haldane phase (Sec. 5.1).

2.3 Matrix-product state and SPT phase

The *matrix-product state* [5] (MPS) [64–66] gives a faithful description of the gapped ground state of one-dimensional quantum systems. We here review its definition and several physical requirements. It is used to prove the existence of the symmetry-protected topological phases in one dimension. Its application to the AKLT state is also reviewed. Basic facts discussed here will be required when we deal with the non-translational-invariant MPS in Sec. 5.3.

2.3.1 Definition of matrix-product state

We consider a quantum state $|\psi\rangle$ defined on a one-dimensional lattice with L sites each of which is associated with the d-dimensional Hilbert space. We impose the periodic boundary condition on the lattice. The state $|\psi\rangle$ is written in terms of the MPS as

$$|\psi\rangle = \sum_{\{m_n\}} \mathrm{Tr}\left[A^{[1]}_{m_1} A^{[2]}_{m_2} \cdots A^{[L]}_{m_L}\right] |m_1 m_2 \cdots m_L\rangle\,, \tag{2.26}$$

where the sum is taken over all possible configurations of $\{m_1, m_2, \cdots, m_L\}$ with $m_n = 1, \cdots, d$, and $A^{[n]}_{m_n}$ is a $\chi_{n-1/2} \times \chi_{n+1/2}$ matrix. χ_a is called as the *bond dimension*. Without loss of generality, the MPS (2.26) is also described in the form proposed by Vidal [67],

$$|\psi\rangle = \sum_{\{m_n\}} \mathrm{Tr}\left[\Gamma^{[1]}_{m_1} \Lambda^{[1+1/2]} \Gamma^{[2]}_{m_2} \Lambda^{[2+1/2]} \cdots \Gamma^{[L]}_{m_L} \Lambda^{[L+1/2]}\right] |m_1 m_2 \cdots m_L\rangle\,, \tag{2.27}$$

where $\Lambda^{[a]}$ is a $\chi_a \times \chi_a$ positive diagonal matrix and $\Gamma^{[n]}_{m_n}$ is a $\chi_{n-1/2} \times \chi_{n+1/2}$ matrix. This representation is certainly convenient to see its entanglement structure. In the following, for simplicity, we assume translational invariance of the system. It is proven that there exists a translation-invariant MPS with a site-independent matrices $\Gamma^{[n]}_{m_n} \equiv \Gamma_{m_n}$ and $\Lambda^{[a]} \equiv \Lambda$ [68],

$$|\psi\rangle = \sum_{\{m_n\}} \mathrm{Tr}\left[\Gamma_{m_1} \Lambda \Gamma_{m_2} \Lambda \cdots \Gamma_{m_L} \Lambda\right] |m_1 m_2 \cdots m_L\rangle\,. \tag{2.28}$$

Thus $\chi_a \equiv \chi$ and Γ_{m_n} becomes a square matrix. If we consider the system *only* with inversion symmetry, it is essential to consider the non-translation-invariant MPS. But this is more technical and separately discussed in Sec. 5.3.

For a given state $|\psi\rangle$, there are several different ways (the gauge degrees of freedom) to write down the MPS. Assuming that $|\psi\rangle$ is normalized, this freedom is uniquely fixed by imposing the *canonical condition* [67, 68],

$$\sum_m \Gamma_m \Lambda^2 \Gamma^\dagger_m = \sum_m \Gamma^\dagger_m \Lambda^2 \Gamma_m = \mathbb{I}_\chi \tag{2.29}$$

where $\mathbb{I}_\chi$ is the χ-dimensional identity matrix. This condition is interpreted as that the transfer matrix,

$$R_{\alpha\alpha';\beta\beta'} = \sum_m \Gamma_{m,\alpha\beta} \Gamma^*_{m,\alpha'\beta'} \Lambda_\beta \Lambda_{\beta'}, \tag{2.30}$$

[5] The "matrix-product state" is also called as the "finitely correlated state" in the literature, as first introduced in Ref. [64].

has a right eigenvector $\delta_{\beta\beta'}$ with the eigenvalue 1 [69]. Similarly, another transfer matrix,

$$L_{\alpha\alpha';\beta\beta'} = \sum_m \Gamma^*_{m\alpha'\beta'}\Gamma_{m,\alpha\beta}\Lambda_\alpha\Lambda_{\alpha'}, \tag{2.31}$$

has a left eigenvector $\delta_{\alpha\alpha'}$ with the eigenvalue 1.

We also require the condition of a *pure* MPS, that is, the eigenvalue 1 is the largest one of the left/right transfer matrix and is nondegenerate [67,68]. This condition guarantees that the state $|\psi\rangle$ is the unique ground state of the corresponding Hamiltonian, and any connected correlation function decays exponentially with a finite correlation length. The latter can be seen as follows. Let us introduce two local operators P and Q and consider a connected correlation function $\langle P(0)Q(r)\rangle - \langle P(0)\rangle\langle Q(r)\rangle$. As in the usual transfer-matrix method, the correlation function is written as

$$\langle P(0)Q(r)\rangle - \langle P(0)\rangle\langle Q(r)\rangle = \frac{\mathrm{Tr}\left[R_P R^r R_Q R^{L-r-2}\right]}{\mathrm{Tr}\left[R^L\right]} - \frac{\mathrm{Tr}\left[R_P R^{L-1}\right]}{\mathrm{Tr}\left[R^L\right]}\frac{\mathrm{Tr}\left[R_Q R^{L-1}\right]}{\mathrm{Tr}\left[R^L\right]}, \tag{2.32}$$

where

$$(R_P)_{\alpha\alpha';\beta\beta'} = \sum_{m,m'} \Gamma_{m,\alpha\beta}P_{mm'}\Gamma^*_{m',\alpha'\beta'}\Lambda_\beta\Lambda_{\beta'}, \tag{2.33}$$

$$(R_Q)_{\alpha\alpha';\beta\beta'} = \sum_{m,m'} \Gamma_{m,\alpha\beta}Q_{mm'}\Gamma^*_{m',\alpha'\beta'}\Lambda_\beta\Lambda_{\beta'}. \tag{2.34}$$

We expand the transfer matrix R as

$$R = \sum_{j=1}^{\chi^2} \lambda_j |r_j\rangle\langle l_j| \tag{2.35}$$

where λ_j's are the eigenvalues of R in non-increasing order, and $|r_j\rangle$ and $\langle l_j|$ are the corresponding right and left eigenvectors, respectively. Then, we obtain

$$\begin{aligned}
&\langle P(0)Q(r)\rangle - \langle P(0)\rangle\langle Q(r)\rangle \\
&= \frac{\mathrm{Tr}\left[R_P\left(\sum_j \lambda_j^r |r_j\rangle\langle l_j|\right)R_Q\left(\sum_j \lambda_j^{L-r-2}|r_j\rangle\langle l_j|\right)\right]}{\mathrm{Tr}\left[\sum_j \lambda_j^L |r_j\rangle\langle l_j|\right]} \\
&\quad - \frac{\mathrm{Tr}\left[R_P\left(\sum_j \lambda_j^{L-1}|r_j\rangle\langle l_j|\right)\right]}{\mathrm{Tr}\left[\sum_j \lambda_j^L |r_j\rangle\langle l_j|\right]}\frac{\mathrm{Tr}\left[R_Q\left(\sum_j \lambda_j^{L-1}|r_j\rangle\langle l_j|\right)\right]}{\mathrm{Tr}\left[\sum_j \lambda_j^L |r_j\rangle\langle l_j|\right]}
\end{aligned} \tag{2.36}$$

If $\lambda_1 = 1$ and $\lambda_j < 1$ for all $2 \le j \le \chi^2$, for a large system size L, this becomes

$$\langle P(0)Q(r)\rangle - \langle P(0)\rangle\langle Q(r)\rangle \approx \langle l_1|R_P\left(\sum_j \lambda_j^r |r_j\rangle\langle l_j|\right)R_Q|r_1\rangle - \langle l_1|R_P|r_1\rangle\langle l_1|R_Q|r_1\rangle. \tag{2.37}$$

For a large distance r, this can be evaluated as

$$\langle P(0)Q(r)\rangle - \langle P(0)\rangle\langle Q(r)\rangle \approx \lambda_2^r\langle l_1|R_P|r_2\rangle\langle l_2|R_Q|r_1\rangle + \mathcal{O}(\lambda_3^r). \tag{2.38}$$

Thus the correlation function decays exponentially with a finite correlation length,

$$\xi = -\frac{1}{\log \lambda_2}. \tag{2.39}$$

On the other hand, if the largest eigenvalue of R is q-fold degenerate, that is, $\lambda_1 = \cdots = \lambda_q = 1$ and $\lambda_j < 1$ for $q < j \leq \chi^2$, Eq. (2.36) becomes

$$\begin{aligned} &\langle P(0)Q(r)\rangle - \langle P(0)\rangle \langle Q(r)\rangle \\ &\approx \sum_{j,k=1}^{q} \left(\frac{1}{q} \langle l_j|R_P|r_k\rangle \langle l_k|R_Q|r_j\rangle - \frac{1}{q^2} \langle l_j|R_P|r_j\rangle \langle l_k|R_Q|r_k\rangle \right) + \mathcal{O}(\lambda_{q+1}^r). \end{aligned} \tag{2.40}$$

Therefore, nonvanishing contributions independent of r remain and the correlation length diverges. This indicates that the ground state is in a "cat state" and has some long-range order associated with spontaneous symmetry breaking. To avoid this, in the following, we assume pureness of the MPS, i.e. nondegeneracy of the largest eigenvalue of R and similarly of L.

2.3.2 Symmetries on MPS

To investigate the symmetry-protected topological phases, we need to implement *symmetry* on the MPS. We here consider the three types of symmetries: on-site global symmetry, inversion symmetry, and time reversal symmetry.

On-site symmetry

The quantum Ising model (2.6) has a Z_2 symmetry generated by $\prod_i \sigma_i^x$, and the AKLT model (2.22) has an SO(3) symmetry corresponding to spin rotations. Such on-site global symmetries are generated by

$$\mathcal{G}(g) \equiv u^{[1]}(g) \otimes u^{[2]}(g) \otimes \cdots \otimes u^{[L]}(g), \tag{2.41}$$

where $u^{[n]}(g)$ is a unitary representation of a symmetry group G for a group element $g \in G$ on site n. We consider a state $|\psi\rangle$ that transforms under this symmetry as

$$\mathcal{G}(g)\,|\psi\rangle = e^{i\theta_L(g)}\,|\psi\rangle\,, \tag{2.42}$$

where $e^{i\theta_L(g)}$ is a 1D representation of G.

We want to know the transformations of the matrices in Eq. (2.28) when the symmetry (2.41) is applied on $|\psi\rangle$. From Refs. [13, 70], the transformation of the matrix Γ is given by

$$\sum_{m'} u_{mm'}(g)\Gamma_{m'} = e^{i\theta(g)} U^\dagger(g)\Gamma_m U(g), \tag{2.43}$$

where $e^{i\theta(g)}$ is a 1D representation of G and $U(g)$ is a unitary operator acting on the χ-dimensional virtual space. $U(g)$ satisfies $[\Lambda, U(g)] = 0$. In fact, $U(g)$ is generally a *projective representation* of G [13, 14] satisfying the multiplication rule,

$$U(g_1)U(g_2) = e^{i\rho(g_1,g_2)} U(g_1 g_2), \tag{2.44}$$

where $g_1, g_2 \in G$ and $e^{i\rho(g_1,g_2)}$ is a phase factor called the factor system. If $\rho(g_1, g_2) = 0$, Eq. (2.44) means $U(g)$ forms a linear representation, such as the integer-spin representation of

SO(3). On the other hand, the half-odd-integer-spin representation of SO(3) gives a nontrivial phase, $\rho(g_1, g_2) \neq 0$.

Following Ref. [13], let us see the case of the $Z_2 \times Z_2$ symmetry, which is a subgroup of SO(3). The $Z_2 \times Z_2$ symmetry is formed by spin rotations by π around two orthogonal axes, say $\mathcal{R}_x = e^{i\pi S_x}$ and $\mathcal{R}_z = e^{i\pi S_z}$. A combined operation, $\mathcal{R}_x\mathcal{R}_z$ or $\mathcal{R}_z\mathcal{R}_x$, gives the rotation around the y axis, $\mathcal{R}_y = e^{i\pi S^y}$. We assume that the $Z_2 \times Z_2$ symmetry takes a linear representation on the physical Hilbert space as in integer-spin systems. Acting $\mathcal{R}_x$ on the matrix Γ, we obtain

$$\sum_{m'} (\mathcal{R}_x)_{mm'} \Gamma_m = e^{i\theta(\mathcal{R}_x)} U^\dagger(\mathcal{R}_x) \Gamma_m U(\mathcal{R}_x). \tag{2.45}$$

Using this relation twice, we have

$$\Gamma_m = e^{2i\theta(\mathcal{R}_x)} (U^\dagger(\mathcal{R}_x))^2 \Gamma_m (U(\mathcal{R}_x))^2. \tag{2.46}$$

Substituting this into the canonical condition (2.29),

$$\sum_m \Gamma_m^\dagger \Lambda (U(\mathcal{R}_x))^2 \Lambda \Gamma_m = e^{2i\theta(\mathcal{R}_x)} (U(\mathcal{R}_x))^2. \tag{2.47}$$

Thus we find $e^{2i\theta(\mathcal{R}_x)} = 1$ and $(U(\mathcal{R}_x))^2 = e^{i\phi(\mathcal{R}_x)}\mathbb{I}$ with some phase $\phi(\mathcal{R}_x)$. The latter phase can be absorbed in a redefinition of the unitary matrix, $U(\mathcal{R}_x) \to e^{i\phi(\mathcal{R}_x)/2} U(\mathcal{R}_x)$ and thus has no effect on the MPS. Similarly for $\mathcal{R}_z$, we obtain $e^{2i\theta(\mathcal{R}_z)} = 1$ and $U(\mathcal{R}_z) = e^{i\phi(\mathcal{R}_z)}\mathbb{I}$, and again $\phi(\mathcal{R}_z)$ affects nothing. However, if we consider a combination of the two operations $\mathcal{R}_x$ and $\mathcal{R}_z$, the situation will be changed. Applying first $\mathcal{R}_z$ and then $\mathcal{R}_x$ on Γ, we obtain

$$\sum_{m'} (\mathcal{R}_x\mathcal{R}_z)_{mm'} \Gamma_{m'} = e^{i(\theta(\mathcal{R}_z)+\theta(\mathcal{R}_x))} U^\dagger(\mathcal{R}_z) U^\dagger(\mathcal{R}_x) \Gamma_m U(\mathcal{R}_x) U(\mathcal{R}_z). \tag{2.48}$$

Conversely, applying first $\mathcal{R}_x$ and then $\mathcal{R}_z$, we obtain

$$\sum_{m'} (\mathcal{R}_z\mathcal{R}_x)_{mm'} \Gamma_{m'} = e^{i(\theta(\mathcal{R}_x)+\theta(\mathcal{R}_z))} U^\dagger(\mathcal{R}_x) U^\dagger(\mathcal{R}_z) \Gamma_m U(\mathcal{R}_z) U(\mathcal{R}_x). \tag{2.49}$$

Since $\mathcal{R}_x\mathcal{R}_z = \mathcal{R}_z\mathcal{R}_x$, equating the left-hand sides of Eqs. (2.48) and (2.49), we have

$$\Gamma_m = U(\mathcal{R}_x) U(\mathcal{R}_z) U^\dagger(\mathcal{R}_x) U^\dagger(\mathcal{R}_z) \Gamma_m U(\mathcal{R}_z) U(\mathcal{R}_x) U^\dagger(\mathcal{R}_z) U^\dagger(\mathcal{R}_x). \tag{2.50}$$

Substituting this into the canonical condition (2.29), we find

$$\sum_m \Gamma_m^\dagger \Lambda U(\mathcal{R}_z) U(\mathcal{R}_x) U^\dagger(\mathcal{R}_z) U^\dagger(\mathcal{R}_x) \Lambda \Gamma_m = U(\mathcal{R}_z) U(\mathcal{R}_x) U^\dagger(\mathcal{R}_z) U^\dagger(\mathcal{R}_x). \tag{2.51}$$

This indicates that

$$U(\mathcal{R}_z) U(\mathcal{R}_x) = e^{i\phi_{xz}} U(\mathcal{R}_x) U(\mathcal{R}_z). \tag{2.52}$$

The phase ϕ_{xz} cannot be absorbed into the redefinitions of $U(\mathcal{R}_x)$ and $U(\mathcal{R}_z)$. Since we can fix $(U(\mathcal{R}_x))^2 = \mathbb{I}$, we obtain $e^{2i\phi_{xz}} = 1$, i.e. $\phi_{xz} = 0, \pi$. We expect that different states are classified by $\theta(\mathcal{R}_x)$ and $\theta(\mathcal{R}_z)$, both of which take the values 0 or π, and $\phi_{xz} = 0, \pi$. The former two phases are associated with four 1D representations of the $Z_2 \times Z_2$ symmetry, while the last one corresponds to two projective representations.

Inversion symmetry

An inversion symmetry operation $n \to -n$ acts on the matrix Γ as transposition with some unitary [13, 14] (see also Ref. [71]):

$$\sum_{m'} u_{mm'}(\mathcal{I})\Gamma^T_{m'} = e^{i\theta(\mathcal{I})}U^\dagger(\mathcal{I})\Gamma_m U(\mathcal{I}). \tag{2.53}$$

Here $e^{i\theta(\mathcal{I})}$ is a 1D representation of $\mathcal{I}$, namely ± 1, and $U(\mathcal{I})$ is a projective representation. To see this, applying (2.53) twice, we obtain

$$\Gamma_m = e^{2i\theta(\mathcal{I})}U^T(\mathcal{I})U^\dagger(\mathcal{I})\Gamma_m U(\mathcal{I})U^*(\mathcal{I}). \tag{2.54}$$

Substituting this into the canonical condition (2.29), we have

$$\sum_m \Gamma^\dagger_m \Lambda U(\mathcal{I})U^*(\mathcal{I})\Lambda\Gamma_m = e^{2i\theta(\mathcal{I})}U(\mathcal{I})U^*(\mathcal{I}). \tag{2.55}$$

Thus, we find $e^{2i\theta(\mathcal{I})} = 1$ and

$$U(\mathcal{I})U^*(\mathcal{I}) = e^{i\rho(\mathcal{I})}\mathbb{I}. \tag{2.56}$$

These relations lead to $\theta(\mathcal{I}) = 0, \pi$ and $\rho(\mathcal{I}) = 0, \pi$. Equation (2.56) is corresponding to the multiplication rule (2.44) for group elements involving an odd number of transposition or complex conjugation (see Appendix B of Ref. [29]). Therefore, $\rho(\mathcal{I})$ is associated with the projective representations of $\mathcal{I}$.

Time reversal symmetry

Here, we assume that time reversal symmetry satisfies $\mathcal{T}^2 = 1$ as it acts on integer spin. It acts on the matrix Γ as complex conjugation with some unitary [13, 14],

$$\sum_{m'} u_{mm'}(\mathcal{T})\Gamma^*_{m'} = e^{i\theta(\mathcal{T})}U^\dagger(\mathcal{T})\Gamma_m U(\mathcal{T}). \tag{2.57}$$

Again, $e^{i\theta(\mathcal{T})}$ is a 1D representation and $U(\mathcal{T})$ is a projective representation that satisfies the multiplication rule of the form (2.56). However, $\theta(\mathcal{T})$ does not provide any information in this case. Using the relation (2.57) twice, we have

$$\Gamma_m = U^T(\mathcal{T})U^\dagger(\mathcal{T})\Gamma_m U(\mathcal{T})U^*(\mathcal{T}). \tag{2.58}$$

Thus the phase $\theta(\mathcal{T})$ is canceled. Substituting this into the canonical condition (2.29), we obtain

$$\sum_m \Gamma^\dagger_m \Lambda U(\mathcal{T})U^*(\mathcal{T})\Lambda\Gamma_m = U(\mathcal{T})U^*(\mathcal{T}). \tag{2.59}$$

Thus, this gives

$$U(\mathcal{T})U^*(\mathcal{T}) = e^{i\rho(\mathcal{T})}\mathbb{I}, \tag{2.60}$$

and then $\rho(\mathcal{T}) = 0, \pi$.

2.3.3 General result on 1D SPT phase

As seen in above, the projective representation of an on-site symmetry is associated with the phase $\rho(g_1, g_2)$ from Eq. (2.44). For the inversion and time reversal symmetries, their projective representations are also related to $\rho(\mathcal{I})$ and $\rho(\mathcal{T})$ through Eqs. (2.56) and (2.60). Since the change of ρ between different projective representations is discontinuous, we cannot change ρ by a continuous deformation of the matrix Γ. Thus we have to violate the pureness condition when ρ is changed, which leads to a phase transition with a divergent correlation length. As long as the MPS representation is valid, even for a *finite* system, there must be a gap closing along any path interpolating two gapped states with different projective representations [3]. Thus, two states with different projective representations belong to different quantum phases. A similar discussion also holds for the 1D representation θ.

We so far assumed translational invariance. We here summarize known results [13, 14] for the *bosonic* 1D SPT phase on both translational-invariant and non-translational-invariant systems. For a *non-translation-invariant* system with

- an on-site symmetry G, distinct SPT phases are classified by different projective representations of G.
- time reversal symmetry $\mathcal{T}$, there are two distinct phases characterized by $\rho(\mathcal{T}) = 0, \pi$.

For a *translational-invariant* system with

- an on-site symmetry G with a *linear* representation, distinct SPT phase are classified by different projective representations and different 1D representations of G.
- an on-site symmetry G with a *projective* representation, there is no SPT phase; the ground state is gapless or degenerate.
- time reversal symmetry with $\mathcal{T}^2 = 1$, there are two SPT phases characterized by $\rho(\mathcal{T}) = 0, \pi$.
- time reversal symmetry with $\mathcal{T}^2 = -1$, there is no SPT phase; the ground state is gapless or degenerate.
- inversion symmetry $\mathcal{I}$, there are four SPT phases characterized by $\theta(\mathcal{I}) = 0, \pi$ and $\rho(\mathcal{I}) = 0, \pi$.

The reason why the translation-invariant system with either an on-site symmetry G with a projective representation or time reversal symmetry with $\mathcal{T}^2 = -1$ cannot have a unique gapped ground state is explained later in Sec. 5.3.5. This is like the Lieb-Schultz-Mattis theorem [19, 20] from the point of view of symmetries. For non-translational-invariant systems, such a difference between the projective and linear representations of G does not appear, since we can always group several sites into a supersite such that a projective representation of G takes a linear representation on each supersite. Similarly, we can group two sites into a supersite such that time reversal symmetry satisfies $\mathcal{T}^2 = 1$ on each supersite. An SPT phase with a nontrivial projective representation of G or $\rho = \pi$ must form entangled pairs, which appear as stable edge states and/or degeneracy in the entanglement spectrum.

For translational invariant systems, different 1D representations of G also give distinct SPT phases. If we consider the case in which a projective representation of G is trivial (linear representation), different 1D representations correspond to distinct trivial phases in the sense

that they can be smoothly connected to direct-product states. A simple example is given by [14]

$$H = \sum_i \left[\sigma_{i-1}^x \sigma_i^y \sigma_{i+1}^z - h\sigma_i^z\right]. \tag{2.61}$$

This model has a Z_2 spin reversal symmetry generated by σ^z, which has two 1D representations ± 1. Accordingly, one state $|\uparrow\uparrow\uparrow\uparrow\cdots\rangle$ realized in $h \to \infty$ and the other state $|\downarrow\downarrow\downarrow\downarrow\cdots\rangle$ realized in $h \to -\infty$ belong to different SPT phases. There is obviously neither an edge state nor a particular entanglement structure in both phases. In the case of a U(1) symmetry, states with different particle numbers on each site belong to distinct SPT phases. The fact that different 1D representations give distinct phases seems somewhat trivial. If there is no translational invariance, we can glue several sites into a supersite such that any 1D representation takes 1 on each supersite. Thus the 1D representation loses its role.

If the system has both translational invariance and inversion symmetry, we have four SPT phases. But in this case, there is no distinction between the bond-centered and site-centered inversions. In principle, we can consider the non-translation-invariant system with either of the two inversion symmetries. We will carefully discuss this point in Sec. 5.3.

2.3.4 AKLT state as an SPT phase

Following Ref. [13], we review that the AKLT state takes nontrivial projective representations for the $\mathcal{T}$, $\mathcal{I}_b$, and $\mathcal{D}_2$ ($Z_2 \times Z_2$) symmetries. To represent the AKLT state in the MPS form, it is convenient to introduce the time-reversal-invariant basis,

$$|x\rangle = \frac{1}{\sqrt{2}}(|+\rangle - |-\rangle), \quad |y\rangle = \frac{i}{\sqrt{2}}(|+\rangle + |-\rangle), \quad |z\rangle = |0\rangle. \tag{2.62}$$

In this basis, the matrices Γ_a ($a = x, y, z$) and Λ are given by 2×2 matrices,

$$\Gamma_a = \sigma_a, \quad \Lambda = \frac{1}{\sqrt{2}}\mathbb{I}_2, \tag{2.63}$$

where σ_a is the Pauli matrices and $\mathbb{I}$ is the 2×2 identity matrix. We also note that the spin operators and the generators of π rotations, $\mathcal{R}_a = e^{i\pi S^a}$, are written as

$$S^x = \begin{pmatrix} 0 & 0 & 0 \\ 0 & 0 & -i \\ 0 & i & 0 \end{pmatrix}, \quad S^y = \begin{pmatrix} 0 & 0 & i \\ 0 & 0 & 0 \\ -i & 0 & 0 \end{pmatrix}, \quad S^z = \begin{pmatrix} 0 & -i & 0 \\ i & 0 & 0 \\ 0 & 0 & 0 \end{pmatrix}, \tag{2.64}$$

and

$$\mathcal{R}_x = \begin{pmatrix} 1 & 0 & 0 \\ 0 & -1 & 0 \\ 0 & 0 & -1 \end{pmatrix}, \quad \mathcal{R}_y = \begin{pmatrix} -1 & 0 & 0 \\ 0 & 1 & 0 \\ 0 & 0 & -1 \end{pmatrix}, \quad \mathcal{R}_z = \begin{pmatrix} -1 & 0 & 0 \\ 0 & -1 & 0 \\ 0 & 0 & 1 \end{pmatrix}. \tag{2.65}$$

First we consider the dihedral symmetry $\mathcal{D}_2$ formed by two spin rotations, say $\mathcal{R}_x$ and $\mathcal{R}_z$. Under $\mathcal{R}_x$, the matrix Γ transforms as

$$\Gamma_x \to \sigma_x, \quad \Gamma_y \to -\sigma_y, \quad \Gamma_z \to -\sigma_z. \tag{2.66}$$

Bring these together in a single expression, we find

$$\Gamma_a \to \sum_{a'} (\mathcal{R}_x)_{aa'} \Gamma_{a'} = \sigma_x \Gamma_a \sigma_x. \tag{2.67}$$

Similarly, under $\mathcal{R}_z$, we have

$$\Gamma_a \to \sum_{a'} (\mathcal{R}_z)_{aa'} \Gamma_{a'} = \sigma_z \Gamma_a \sigma_z. \tag{2.68}$$

Compared with Eq. (2.52), we can read $U(\mathcal{R}_x) = \sigma_x$ and $U(\mathcal{R}_z) = \sigma_z$. Since the Pauli matrices anticommute each other, we find

$$U(\mathcal{R}_x)U(\mathcal{R}_z) = -U(\mathcal{R}_z)U(\mathcal{R}_x). \tag{2.69}$$

Thus, $\phi_{xz} = \pi$ and $U(\mathcal{R}_a)$ forms a projective representation (half-odd-integer-spin representation).

Next, we consider the inversion symmetry. Since the AKLT state is translational invariant, it has both site-centered and bond-centered inversion symmetries. In both cases, the matrix Γ is transformed under the inversion symmetry as $\Gamma \to \Gamma^T$, and for the AKLT state, we find

$$\Gamma_x \to \sigma_x, \quad \Gamma_y \to -\sigma_y, \quad \Gamma_z \to \sigma_z. \tag{2.70}$$

These are rewritten as

$$\Gamma_a \to \Gamma_a^T = -\sigma_y \Gamma_a \sigma_y. \tag{2.71}$$

Compared with Eq. (2.53), we can read $\theta(\mathcal{I}) = \pi$ and $U(\mathcal{I}) = \sigma_y$. From Eq. (2.56), $U(\mathcal{I})$ forms a projective representation,

$$U(\mathcal{I})U^*(\mathcal{I}) = -\mathbb{I}_2, \tag{2.72}$$

and thus $\phi(\mathcal{I}) = \pi$. As seen from a careful study on the non-translation-invariant MPS in Sec. 5.3.2, the phase $\phi(\mathcal{I})$ is actually associated with the bond-centered inversion $\mathcal{I}_b$, while $\theta(\mathcal{I}) + \phi(\mathcal{I})$ is associated with the site-centered inversion $\mathcal{I}_s$.

Finally we consider time reversal symmetry $\mathcal{T}$. In the S^z basis, a time reversal operation is given by $\mathcal{R}_y\mathcal{K}$ where $\mathcal{K}$ is complex conjugation. However, in the time-reversal-invariant basis, the time reversal operation is given by $\mathcal{T} = -\mathcal{K}$. Thus, the matrix Γ transforms as $\Gamma \to -\Gamma^*$. Then we find

$$\Gamma_x \to -\sigma_x, \quad \Gamma_y \to \sigma_y, \quad \Gamma_z \to -\sigma_z. \tag{2.73}$$

They can be brought together into

$$\Gamma_a \to -\Gamma_a^* = \sigma_y \Gamma_a \sigma_y. \tag{2.74}$$

Since $U(\mathcal{T}) = \sigma_y$, compared with Eq. (2.60), we find that $\phi(\mathcal{T}) = \pi$ and $U(\mathcal{T})$ forms a projective representation as it acts on half-odd-integer spin.

All the three symmetries, $\mathcal{D}_2$, $\mathcal{I}_b$, and $\mathcal{T}$, form nontrivial projective representations on the virtual space living on the bond. As pointed out in Ref. [13], since $U(g)$ commutes with Λ, all the eigenvalues of Λ must have at least two-fold degeneracy in the Haldane phase, in the presence of one of these symmetries. In fact, the element of Λ is directly related to the *entanglement spectrum* [44]. The entanglement spectrum is the eigenvalue of the entanglement Hamiltonian H_A defined from the reduced density matrix (2.9) as

$$\rho_A \equiv e^{-H_A}. \tag{2.75}$$

We denote the eigenvalue spectrum of H_A as $\{\xi_\alpha\}$. On the other hand, the elements of the matrix Λ, $\{\lambda_\alpha\}$, appear in the Schimdt decomposition of $|\psi\rangle$,

$$|\psi\rangle = \sum_\alpha \lambda_\alpha |\alpha A\rangle |\alpha B\rangle , \tag{2.76}$$

where $|\alpha A\rangle$ and $|\alpha B\rangle$ are orthogonal basis vectors of the subsystems A and B, respectively. Since $\{\lambda_\alpha^2\}$ is the eigenvalue of the reduced density matrix ρ_A in the subsystem A, it is related to the entanglement spectrum by

$$\xi_\alpha = -2 \log \lambda_\alpha. \tag{2.77}$$

Chapter 3

Bosonization and effective field theory

In this chapter, we derive an effective field theory for various spin ladder models, based on the Abelian bosonization approach. In Sec. 3.1, we introduce a general spin-1/2 ladder model with N legs, considered in this thesis. In Sec. 3.2, following the argument by Schulz [17], we bosonize the ladder model and deduce an effective Hamiltonian only with a single bosonic field. Although the derivation of the effective Hamiltonian was originally based on perturbation theory, in Sec. 3.3, we reconsider it from the consistency with the compactification of the bosonic field and the symmetry of the microscopic Hamiltonian. These conditions in fact uniquely determine the allowed form of the effective Hamiltonian beyond the perturbative regime. In Sec. 3.4, we predict an extension of the Lieb-Schulz-Mattis theorem, which is not only applied to translational-invariant systems but also site-centered-inversion-symmetric systems.

A short course to the Abelian bosonization method is given in Appendix 3.A. Appendix 3.B supplements the perturbative derivation of the effective Hamiltonian, which will be also important in Chapter 4.

3.1 Model

In this section, we introduce a general form of the spin ladder Hamiltonian for a unified description of various one-dimensional spin systems. Several limiting cases are also shown.

3.1.1 General form

In this study, we consider the Hamiltonian given by

$$H = H_{\parallel} + H_{\perp} + H'. \tag{3.1}$$

The first term represents N decoupled spin-1/2 chains,

$$H_{\parallel} = J \sum_{i} \sum_{j=1}^{N} \left(s_{i,j}^{x} s_{i+1,j}^{x} + s_{i,j}^{y} s_{i+1,j}^{y} + \Delta s_{i,j}^{z} s_{i+1,j}^{z} \right), \tag{3.2}$$

where $\vec{s}_{i,j}$ is a spin-1/2 operator on the rung i and leg j. J is an intrachain exchange coupling and supposed to be positive (antiferromagnetic) throughout this thesis. Δ controls a uniaxial

anisotropy of the exchange coupling. As interchain couplings, we consider the quadratic forms in spin operators,

$$H_\perp = \sum_i \sum_\alpha \sum_{j=1}^{N} \sum_{j' \neq j} \left[J^{xy}_{\perp,(\alpha,j,j')} \left(s^x_{i,j} s^x_{i+\alpha,j'} + s^y_{i,j} s^y_{i+\alpha,j'} \right) + J^z_{\perp,(\alpha,j,j')} s^z_{i,j} s^z_{i+\alpha,j'} \right]. \tag{3.3}$$

α is taken to be a small integer such that the couplings are short-ranged. $J^{xy}_{\perp,(\alpha,j,j')}$ and $J^z_{\perp,(\alpha,j,j')}$ can be either positive or negative, i.e. antiferromagnetic or ferromagnetic. We have implicitly assumed that the spin ladder Hamiltonian $H_\parallel + H_\perp$ is invariant under several symmetry operations, that is,

- one-site translation: $\vec{s}_{i,j} \to \vec{s}_{i+1,j}$,
- reflection (or *inversion* since we are in one dimension): $\vec{s}_{i,j} \to \vec{s}_{-i,j}$,
- time reversal: $\vec{s}_{i,j} \to -\vec{s}_{i,j}$,
- rotation about z axis by an arbitrary angle: $s^\pm_{i,j} \to e^{\pm i\beta} s^\pm_{i,j}$, $\beta \in [0, 2\pi]$,
- rotation about x axis by π: $s^{y,z}_{i,j} \to -s^{y,z}_{i,j}$.

These symmetries can be fully or partially broken by a perturbation H' in Eq. (3.1). On the other hand, we do not assume any point-group symmetry associated with a permutation of the chains, which has less important roles in this study.

Our strategy in this thesis is as follows: (i) we first deduce an effective Hamiltonian description of gapped disordered phases realized in the ladder Hamiltonian $H_\parallel + H_\perp$, and then (ii) examine the stability of phase transitions between those phases when a symmetry-breaking perturbation H' is added. For a moment, we suppose $H' = 0$.

3.1.2 Examples of spin ladder

We here show examples of simple limiting cases of the general spin ladder model (3.1) and briefly summarize their ground-state properties. The simplest case is given by choosing $\alpha = 0$ and $j' = j + 1$. This provides a conventional spin ladder, which is a portion of the square lattice, only with perpendicular interchain couplings,

$$H_\perp = \sum_i \sum_{j=1}^{N} \left[J^{xy}_\perp \left(s^x_{i,j} s^x_{i,j+1} + s^y_{i,j} s^y_{i,j+1} \right) + J^z_\perp s^z_{i,j} s^z_{i,j+1} \right]. \tag{3.4}$$

Depending on the boundary condition along the rung, we refer to this model as the spin *tube* if the periodic boundary condition $\vec{s}_{i,N+1} \equiv \vec{s}_{i,1}$ is imposed, while as the *open* spin ladder if the open one $\vec{s}_{i,N+1} \equiv 0$ is imposed. These models are depicted in Fig. 3.1 (a) and (b) for $N = 4$.

The $N = 2$ case has been extensively studies [72–83]. There are also several systematic studies on the N-leg spin ladders and tubes [59, 60, 63, 84–90]. If the interchain couplings are ferromagnetic, the ground-state property is essentially the same as that of the spin-$N/2$ XXZ chain. In particular, at the $SU(2)$ symmetric point $\Delta = 1$ and $J^{xy}_\perp = J^z_\perp$, we have the spin-$N/2$ Haldane phase for even N while a gapless critical phase for odd N. If the interchain couplings are antiferromagnetic, for even N, the ground state is in a rung-singlet phase, which is adiabatically connected to a direct product of singlet states formed on each rung, and thus

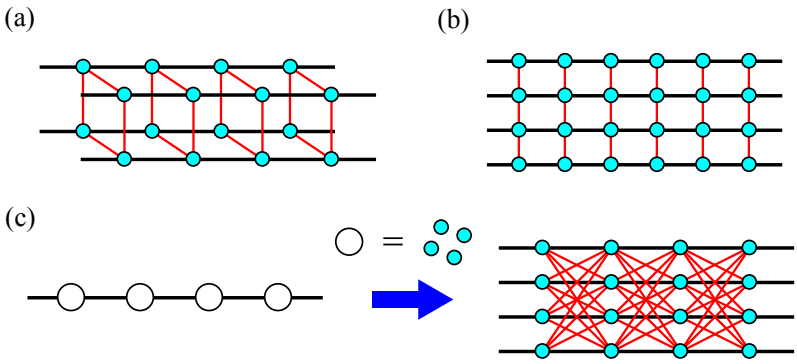

Figure 3.1: Various spin ladders considered in this thesis for $N = 4$. (a) Spin tube and (b) open spin ladder with perpendicular interchain couplings. (c) Decomposing a spin-2 into four spin-1/2's, a spin-2 chain can be mapped onto a four-leg spin-1/2 ladder with diagonal interchain couplings.

disordered with a finite excitation gap. For odd N, a dependence on the boundary condition appears: an open spin ladder has a gapless ground state, while a spin tube can have a gapped ground state with spontaneous breaking of translational invariance. These results imply that, unless the system has geometrical frustration such as the spin tube with odd N, qualitative properties of the ground state are well understood in the strong-coupling limit $J_\perp^{xy}, J_\perp^z \gg J$.

Another interesting example is a ladder mapping of the antiferromagnetic spin-S XXZ chain [17,56,91–98]. The corresponding ladder model is obtained by setting $\alpha = 1$ in Eq. (3.3),

$$H_\perp = \sum_i \sum_{j=1}^{2S} \sum_{j' \neq j} \left[J_\times^{xy} \left(s_{i,j}^x s_{i+1,j'}^x + s_{i,j}^y s_{i+1,j'}^y \right) + J_\times^z s_{i,j}^z s_{i+1,j'}^z \right], \tag{3.5}$$

where the number of legs is $N = 2S$. The relation with the XXZ chain can be seen as follows. The Hamiltonian of the spin-S XXZ chain is given by

$$H_{\mathrm{XXZ}} = J \sum_i (S_i^x S_{i+1}^x + S_i^y S_{i+1}^y + \Delta S_i^z S_{i+1}^z), \tag{3.6}$$

where $\vec{S}$ is a spin-S operator on the site i. If we decompose a spin-S into $2S$ spin-1/2's as

$$\vec{S}_i = \sum_{j=1}^{2S} \vec{s}_{i,j}, \tag{3.7}$$

we can express the chain Hamiltonian (3.6) as a sort of spin ladders with diagonal coupling,

$$H_{\mathrm{XXZ}} = H_\parallel + \sum_i \sum_{j=1}^{2S} \sum_{j \neq j'} \left[J \left(s_{i,j}^x s_{i+1,j'}^x + s_{i,j}^y s_{i+1,j'}^y \right) + J\Delta s_{i,j}^z s_{i+1,j'}^z \right]. \tag{3.8}$$

Equation (3.5) is identified as the second term in Eq. (3.8) by setting $J_\times^{xy} = J$ and $J_\times^z = J\Delta$. If the composite spins on each rung (3.7) are perfectly projected onto the fully symmetric sector with total spin S, we will recover the physics of the single spin-S XXZ chain (3.6). Nevertheless, low-energy properties of the XXZ chain are qualitatively captured by Eq. (3.5), even if we choose smaller couplings $|J_\times^{xy}|, |J_\times^z| < J$ with $J_\times^z / J_\times^{xy} = \Delta$ [17, 56, 91–98].

We can also introduce an on-site uniaxial anisotropy in the XXZ chain (3.6), which is expressed as additional perpendicular couplings through the ladder mapping,

$$D_z \sum_i (S_i^z)^2 = 2D_z \sum_i \sum_{j=1}^{2S} \sum_{j' \neq j} s_{i,j}^z s_{i,j'}^z + \frac{S}{2}. \tag{3.9}$$

For integer S and $D_z \gg J$, this term aligns every site in the $S^z = 0$ state. A phase smoothly connected to a direct product of the $S^z = 0$ states is called the "large-D" phase and has a finite excitation gap. A phase diagram of the spin-S XXZ chain with the on-site uniaxial anisotropy has been investigated through the ladder mapping in Ref. [17].

3.2 Bosonization and effective Hamiltonian

In this section, we apply the standard Abelian bosonization approach [99–101] to the spin ladder Hamiltonian (3.1) with $H' = 0$. We here follow the perturbative derivation first discussed by Schulz [17] to reproduce an effective low-energy theory only with a single bosonic field.

3.2.1 Bosonization

For the easy-plane anisotropic regime $-1 < \Delta \leq 1$, the decoupled chain part (3.2) consists of N critical spin-1/2 chains. In the continuum limit, each spin-1/2 chain is described by a massless free boson. Thus, $H_\parallel$ is written as

$$H_\parallel \approx \frac{v}{2\pi} \int dx \sum_{j=1}^{N} \left[K(\partial_x \theta_j)^2 + \frac{1}{K}(\partial_x \phi_j)^2 \right], \tag{3.10}$$

where we have introduced dual fields with respect to each chain, satisfying the commutation relation,

$$[\phi_j(x), \theta_{j'}(x')] = -\frac{i\pi}{2} \delta_{jj'} [\mathrm{sgn}(x - x') + 1], \tag{3.11}$$

v and K are the spin velocity and the Luttinger parameter determined by Bethe ansatz,

$$v = \frac{\pi J a_0 \sqrt{1 - \Delta^2}}{2 \cos^{-1} \Delta}, \quad K = \frac{\pi}{\pi - \cos^{-1} \Delta}, \tag{3.12}$$

and $x = i a_0$ with the lattice spacing a_0. In Eq. (3.10), we have neglected a marginally irrelevant term appearing at $\Delta = 1$ since it does not affect the following qualitative discussion. [1] Spin operators are expressed in terms of the bosonic fields as

$$\begin{aligned} s_{i,j}^z &\approx \frac{a_0}{\pi\sqrt{2}} \partial_x \phi_j - (-1)^i a_1 \sin(\sqrt{2}\phi_j), \\ s_{i,j}^+ &\approx e^{i\sqrt{2}\theta_j} \left[b_0 (-1)^i + b_1 \sin(\sqrt{2}\phi_j) \right], \end{aligned} \tag{3.14}$$

[1] In the continuum limit, a single Heisenberg chain is given by

$$H \approx \frac{v}{2\pi} \int dx \left[K(\partial_x \theta_j)^2 + \frac{1}{K}(\partial_x \phi_j)^2 \right] + \frac{v\lambda}{a_0^2} \int dx \cos(\sqrt{8}\phi), \tag{3.13}$$

with $v = \pi J a_0 / 2$ and $K = 1$ (see Appendix 3.A). The last term is marginally irrelevant and gives logarithmic corrections to various finite-size quantities. The coupling constant λ cannot be determined exactly from the microscopic theory at $\Delta = 1$ but has been estimated by numerical calculation [102].

where a_1, b_0, and b_1 are nonuniversal constants, which have been analytically evaluated [103–106] except for $\Delta = 1$. A derivation of those bosonization formulas is briefly reviewed in App. 3.A.

Substituting the above expressions into Eq. (3.3), we obtain

$$\begin{aligned} H_\perp \approx \int dx \sum_{j\neq j'} \Big[& g_{0,(j,j')}\partial_x\phi_j\partial_x\phi_{j'} + g_{1,(j,j')}\cos\sqrt{2}(\phi_j+\phi_{j'}) + g_{2,(j,j')}\cos\sqrt{2}(\phi_j-\phi_{j'}) \\ & + g_{3,(j,j')}\cos\sqrt{2}(\theta_j-\theta_{j'}) + g_{4,(j,j')}\cos\sqrt{2}(\phi_j+\phi_{j'})\cos\sqrt{2}(\theta_j-\theta_{j'}) \\ & + g_{5,(j,j')}\cos\sqrt{2}(\phi_j-\phi_{j'})\cos\sqrt{2}(\theta_j-\theta_{j'})\Big], \end{aligned} \tag{3.15}$$

where coupling constants are given by

$$\begin{aligned} g_{0,(j,j')} &= \frac{a_0}{2\pi^2}\sum_\alpha J^z_{\perp,(\alpha,j,j')}, \\ g_{1,(j,j')} &= -\frac{a_1^2}{2a_0}\sum_\alpha (-1)^\alpha J^z_{\perp,(\alpha,j,j')}, \\ g_{2,(j,j')} &= \frac{a_1^2}{2a_0}\sum_\alpha (-1)^\alpha J^z_{\perp,(\alpha,j,j')}, \\ g_{3,(j,j')} &= \frac{b_0^2}{a_0}\sum_\alpha (-1)^\alpha J^{xy}_{\perp,(\alpha,j,j')}, \\ g_{4,(j,j')} &= \frac{b_1^2}{2a_0}\sum_\alpha J^{xy}_{\perp,(\alpha,j,j')}, \\ g_{5,(j,j')} &= -\frac{b_1^2}{2a_0}\sum_\alpha J^{xy}_{\perp,(\alpha,j,j')}. \end{aligned} \tag{3.16}$$

For brevity, we collectively denote $g_{i,(j,j')}$ as g_i. For instance, when we say that g_i is relevant under renormalization group, it means that all $g_{i,(j,j')}$ are relevant. If we denote the scaling dimensions of g_i as x_i, they are given by

$$x_0 = 2, \quad x_1 = x_2 = K, \quad x_3 = \frac{1}{K}, \quad x_4 = x_5 = K + \frac{1}{K}. \tag{3.17}$$

In general, the bosonized expression (3.15) is only valid for perturbatively small $J_\perp$'s. However, as in many one-dimensional quantum systems, there is a continuity between the weak- and strong-coupling limits, so that we can investigate qualitative properties of the system beyond the perturbative regime.

3.2.2 Effective Hamiltonian

Since our model involves N bosons and they are not decoupled for $N > 2$ (the $N = 2$ case will reviewed in Sec. 4.1), the analysis of the Hamiltonian $H_\perp + H_\parallel$ seems a formidable task. However, Schulz noticed that low-energy physics of the spin-S chain is faithfully described by an effective Hamiltonian only with a *single* boson [17]. It turns out that this effective Hamiltonian also neatly describes various interesting properties of one-dimensional spin systems, such as the Lieb-Schulz-Mattis theorem (Sec. 3.4), phase transitions between VBS phases (Chapter 4), and the symmetry protection of VBS phases (Chapter 5).

To this end, we introduce a canonical transformation of the bosonic fields. A "center-of-mass" field is defined by

$$\Phi_0 = \frac{1}{\sqrt{N}} \sum_{j=1}^{N} \phi_j, \quad \Theta_0 = \frac{1}{\sqrt{N}} \sum_{j=1}^{N} \theta_j, \tag{3.18}$$

and $N-1$ "relative" fields are defined by

$$\Phi_\nu = \sum_{j=1}^{N} u_j^{(\nu)} \phi_j, \quad \Theta_\nu = \sum_{j=1}^{N} u_j^{(\nu)} \theta_j, \quad \nu = 1, \cdots, N-1. \tag{3.19}$$

If we add one extra dimension $u_j^{(\nu)}$ and set $u_j^{(0)} = 1/\sqrt{N}$, the coefficients $u_j^{(\mu)}$, $\mu = 0, \cdots, N$ form an $N \times N$ orthogonal matrix that satisfies

$$\sum_{j=1}^{N} u_j^{(\mu)} u_j^{(\mu')} = \delta_{\mu\mu'}, \quad \sum_{\mu=1}^{N} u_j^{(\mu)} u_{j'}^{(\mu)} = \delta_{jj'}. \tag{3.20}$$

Thanks to this orthogonality, commutation relations of those new fields are still independent with respect to the index μ, namely,

$$[\Phi_\mu(x), \Theta_{\mu'}(x')] = \frac{i\pi}{2} \delta_{\mu\mu'} [\mathrm{sgn}(x - x') + 1]. \tag{3.21}$$

Then, the original chain fields are expressed as

$$\phi_j = \frac{1}{\sqrt{N}} \Phi_0 + \sum_{\nu=1}^{N-1} u_j^{(\nu)} \Phi_\nu, \quad \theta_j = \frac{1}{\sqrt{N}} \Theta_0 + \sum_{\nu=1}^{N-1} u_j^{(\nu)} \Theta_\nu. \tag{3.22}$$

In terms of these new fields, $H_\parallel$ in Eq. (3.23) is rewritten as

$$H_\parallel \approx \frac{v}{2\pi} \int dx \left[K(\partial_x \Theta_0)^2 + \frac{1}{K} (\partial_x \Phi_0)^2 \right] + \frac{v}{2\pi} \int dx \sum_{\nu=1}^{N-1} \left[K(\partial_x \Theta_\nu)^2 + \frac{1}{K} (\partial_x \Phi_\nu)^2 \right]. \tag{3.23}$$

We note that a canonical transformation of the bosonic fields is usually chosen to diagonalize the marginal interactions $g_{0,(j,j')} \partial_x \phi_j \partial_x \phi_{j'}$ and generally not restrictive in the form (3.18) and (3.19). For that purpose, a particular combination corresponding to the center-of-mass field Φ_0 appears only when the Hamiltonian has an additional symmetry associated with the permutation of chains, such as the S_N symmetry in Eq. (3.5) or the C_N symmetry in Eq. (3.4). However, as we will discuss below, in order to derive the effective Hamiltonian only with a single bosonic field, it is essential to consider the above set of linear combinations in Eqs. (3.18) and (3.19). For general Hamiltonians, this choice of linear combinations leaves some marginal interactions. g_5 is also marginal at $K = 1$. These marginal interactions g_0 and g_5 have nonzero conformal spins and in fact renormalize the spin velocity and Luttinger parameter from their initial values, but we assume that which coupling in Eq. (3.16) is most relevant is not affected by the marginal interactions. In the following discussion, we thus neglect the effect of the marginal coupling g_0 and g_5.

As seen from Eq. (3.22), a linear combination of the fields $\phi_j - \phi_{j'}$ never involves the center-of-mass field Φ_0. Thus, from Eq. (3.15), the terms with g_2 and g_3 do not contain Φ_0 or Θ_0 but would involve all the relative fields Φ_ν or Θ_ν. Our key assumption is to consider

that g_3 is the most relevant coupling constant and reaches the strong-coupling limit faster than the other g_i's under renormalization group. This assumption is obviously justified when considering easy-plane anisotropic case with $|\Delta| < 1$; since $K > 1$, we easily find $x_3 > x_1, x_2$. At the SU(2) symmetric point $\Delta = 1$, the three coupling constants have the same scaling dimension $x = 1$. Nevertheless, in most cases, the initial coupling of g_3 is still largest among them. For instance, if we take the spin ladder given by Eq. (3.4) with $|J_\perp^z| \leq |J_\perp^{xy}|$, the initial value of g_3 is at least twice larger than those of g_1 and g_2 [see Eq. (3.16)] [2]. This is also true for the spin-S chain (3.6) with $-1 < \Delta \leq 1$ through the ladder mapping (3.5). The above assumption is natural, in the sense that we must suppress any antiferromagnetic long-range order governed by g_1 and g_2, to favor gapped disordered ground states like VBS states.

Once g_3 goes the strong-coupling limit, all the relative fields Θ_ν are pinned and acquire masses. Correspondingly, their dual fields Φ_ν strongly fluctuate due to the uncertainty relation (3.21). Thus we can integrate out the relative fields (Φ_ν, Θ_ν) and derive an effective Hamiltonian only with the center-of-mass field (Φ_0, Θ_0). As first shown by Schulz [17], we obtain the effective Hamiltonian,

$$H_{\text{eff}} = \frac{v_0}{2\pi} \int dx \left[K_0 (\partial_x \Theta_0)^2 + \frac{1}{K_0} (\partial_x \Phi_0)^2 \right] + g_{\text{eff}} \int dx \cos(\sqrt{2N} \Phi_0), \tag{3.24}$$

for *even* N, while

$$H_{\text{eff}} = \frac{v_0}{2\pi} \int dx \left[K_0 (\partial_x \Theta_0)^2 + \frac{1}{K_0} (\partial_x \Phi_0)^2 \right] + g'_{\text{eff}} \int dx \cos(\sqrt{8N} \Phi_0), \tag{3.25}$$

for *odd* N, where v_0 and K_0 are a renormalized velocity and Luttinger parameter depending on the actual integration procedure.[3] The vertex operator of Φ_0 is generated by $N/2$-th (N-th) order perturbation theory in g_1 for even (odd) N. Even if g_1 vanishes by some circumstance, this vertex operator is also generated by the same mechanism for g_4, by replacing $\cos \sqrt{2}(\theta_j - \theta_{j'})$ with its expectation value $\langle \cos \sqrt{2}(\theta_j - \theta_{j'}) \rangle$ [97, 98].

In Appendix 3.B, we demonstrate a derivation of the above effective Hamiltonians, based on the perturbation theory. This effective Hamiltonian has also been obtained directly from the spin-$N/2$ Heisenberg chain without using the ladder mapping [107, 108]. A low-energy effective field theory of the Heisenberg chain is described by a perturbed level-N SU(2) Wess-Zumino-Witten model [109]. Using a coset structure of conformal field theory $SU(2)_N = U(1) \times Z_N$, this theory is also described by a free boson and Z_N parafermions. Integrating out massive Z_N parafermions, one reached the same effective theories only with a single boson as Eqs. (3.24) and (3.25).

In Chapter 4, we show that the effective Hamiltonian (3.24) describes gapped disordered phases, such as the Haldane phase, when g_{eff} is relevant. Moreover, phase transitions between VBS phases known to occur in several spin models are also described within this effective Hamiltonian. In the following sections, we consider the effective Hamiltonians (3.24) and (3.25) from the point of view of the symmetry, apart from details of the corresponding microscopic Hamiltonian.

[2] As seen in Appendix 3.A, at $\Delta = 1$, the SU(2) symmetry of the spin chain forces a constraint on the nonuniversal coefficients appearing in Eq. (3.14): $a_1 = b_0$, $b_1 = 1/\pi$.

[3] In practice, we can perturbatively estimate the renormalized values of v_0 and K_0 in two steps. We first solve renormalization group equations for the coupling constants appearing in Eq. (3.15) until g_3 grows order of unity. The resulting value of g_0 renormalizes the initial values of v and K for the center-of-mass field in Eq. (3.13). Second, when integrating out the relative fields, the resulting couplings g_1 and g_4 also contribute to v and K at the $N/2$-th (N-th) order perturbation theory for even (odd) N.

3.3 Consistency with compactification of field and symmetry

In the effective Hamiltonians (3.24) and (3.25), in fact, the vertex operators of Φ_0 are those compatible with the compactification of the center-of-mass field Φ_0 and the symmetries listed in Sec. 3.1.1, with the lowest scaling dimensions for each parity of N. In this section, we first elucidate the compactifications of the bosonic fields, which have been implicitly assumed in the previous discussions. We also provide bosonic representations of the symmetry transformations. These conditions restrict the allowed form of vertex operators beyond the perturbative argument.

3.3.1 Compactification of field

The free boson Hamiltonian (3.10) itself is invariant under any arbitrary translation of the bosonic fields. However, upon the identification with a physical operator (fermion, boson, or spin operator), the Hamiltonian is only invariant under the shifts by *compactification radii*,

$$\phi_j \sim \phi_j + 2\pi r, \quad \theta_j \sim \theta_j + 2\pi \tilde{r}. \tag{3.26}$$

This implies the following identification,

$$\phi_j \sim \phi_j + 2\pi n_j r, \quad \theta_j \sim \theta_j + 2\pi m_j \tilde{r}, \tag{3.27}$$

where $n_j, m_j \in \mathbb{Z}$. The two radii r and $\tilde{r}$ are not freely chosen and constrained by [4]

$$r\tilde{r} = 1/2. \tag{3.28}$$

In the present convention, r and $\tilde{r}$ are chosen as

$$r = \tilde{r} = \frac{1}{\sqrt{2}}. \tag{3.29}$$

One can easily see that the bosonized expression of the spin operator (3.14) is invariant under the substitution of Eq. (3.27).

After the canonical transformation in Eqs. (3.18) and (3.19), we have identifications for the new fields,

$$\begin{aligned} \Phi_0 &\sim \Phi_0 + \frac{2\pi r}{\sqrt{N}} \sum_{j=1}^{N} n_j, & \Theta_0 &\sim \Theta_0 + \frac{2\pi \tilde{r}}{\sqrt{N}} \sum_{j=1}^{N} m_j, \\ \Phi_\nu &\sim \Phi_\nu + 2\pi r \sum_{j=1}^{N} u_j^{(\nu)} n_j, & \Theta_\nu &\sim \Theta_\nu + 2\pi \tilde{r} \sum_{j=1}^{N} u_j^{(\nu)} m_j. \end{aligned} \tag{3.30}$$

However, in Sec. 3.2.2, we supposed that g_3 is the most relevant perturbation and the relative fields Θ_ν are pinned at fixed values corresponding to one of the potential minima. Then the fluctuations of Θ_ν are strongly suppressed. From Eq. (3.30), this gives a set of constraints on m_j,

$$\sum_{j=1}^{N} u_j^{(\nu)} m_j = 0. \tag{3.31}$$

[4] This is provided by a left-right (or holomorphic-antiholomorphic) connection of conformal field theory, associated with a physical system.

Using the orthogonality of the matrix $u_j^{(\nu)}$ in Eq. (3.20), these $N-1$ N-dimensional linear equations are easily solved as

$$m_j = M_0, \tag{3.32}$$

where M_0 is an arbitrary integer. On the other hand, n_j is not constrained and thus we can set $\sum_j n_j = N_0$ with a single arbitrary integer N_0. Hence, we obtain an identification for the center-of-mass field,

$$\Phi_0 \sim \Phi_0 + 2\pi R N_0, \quad \Theta_0 \sim \Theta_0 + 2\pi \tilde{R} M_0, \tag{3.33}$$

where we set

$$R = \frac{1}{\sqrt{2N}}, \quad \tilde{R} = \sqrt{\frac{N}{2}}. \tag{3.34}$$

These new compactification radii again satisfy $R\tilde{R} = 1/2$. As a consequence, this compactification forces vertex operators that can be added to the effective Hamiltonian to be in the form,

$$V = \sum_{p,q\in\mathbb{Z}} g(p,q) \int dx \cos\left(p\sqrt{2N}\Phi_0 + q\sqrt{\frac{2}{N}}\Theta_0 + \alpha(p,q)\right), \tag{3.35}$$

where $\alpha(p,q)$ is a real constant. Here we implicitly assume that the vertex operators are spatially homogeneous (invariant under a translation $x \to x+\alpha$). This will promise that the system acquires a finite excitation gap independent of the system size, i.e. stable in the thermodynamic limit, when a vertex operator is relevant. Scaling dimensions of the couplings $g(p,q)$ are given by

$$x(p,q) = \frac{p^2 N K_0}{2} + \frac{q^2}{2NK_0}, \tag{3.36}$$

3.3.2 Symmetry

Further restrictions on the vertex operators come from the symmetry of the ladder Hamiltonian $H_\parallel + H_\perp$. All the symmetry operations considered in this thesis are defined through individual operations on each spin-1/2 operator, $\vec{s}_{i,j} \to \mathcal{G}\vec{s}_{i,j}\mathcal{G}^{-1}$, where $\mathcal{G}$ is an element of a symmetry group G, that is, $\mathcal{G} \in G$. From the bosonized form of the spin operator (3.14), we can identify the corresponding symmetry transformation on the bosonic fields. For example, time reversal operation transforms the spin operator as [5]

$$\begin{aligned} s^z_{i,j} &\to -s^z_{i,j} \approx -\frac{a_0}{\pi\sqrt{2}}\partial_x\phi_j + (-1)^i a_1 \sin(\sqrt{2}\phi_j), \\ s^+_{i,j} &\to -s^-_{i,j} \approx -e^{-i\sqrt{2}\theta_j}\left[b_0(-1)^i - b_1\sin(\sqrt{2}\phi_j)\right]. \end{aligned} \tag{3.37}$$

[5] Since ϕ_j and θ_j do not commute each other [see Eq. (3.11)], one should deal with their vertex operators as matrices. Indeed, Hermite conjugation on the staggered part of $s^+_{i,j}$ becomes

$$\left(e^{i\sqrt{2}\theta_j(x)}\sin(\sqrt{2}\phi_j(x))\right)^\dagger = \sin(\sqrt{2}\phi_j(x))e^{-i\sqrt{2}\theta_j(x)} = -e^{-i\sqrt{2}\theta_j(x)}\sin(\sqrt{2}\phi_j(x)).$$

Table 3.1: Symmetry transformations on the spin operators and the center-of-mass field (Φ_0, Θ_0).

Symmetry operation	Symbol	Transformation on spins	Transformation on field (Φ_0, Θ_0)
Odd-site translation	trs	$\vec{s}_{i,j} \to \vec{s}_{i+q,j}$ [1]	$\begin{cases} \Phi_0 \to \Phi_0 + \pi\sqrt{N/2} \\ \Theta_0 \to \Theta_0 + \pi\sqrt{N/2} \end{cases}$
Time reversal	$\mathcal{T}$	$\vec{s}_{i,j} \to -\vec{s}_{i,j}$ [2]	$\begin{cases} \Phi_0 \to -\Phi_0 \\ \Theta_0 \to \Theta_0 + \pi\sqrt{N/2} \end{cases}$
Bond-centered inversion	$\mathcal{I}_b$	$\vec{s}_{i,j} \to \vec{s}_{1-i,j}$	$\begin{cases} \Phi_0(x) \to -\Phi_0(-x) \\ \Theta_0(x) \to \Theta_0(-x) + \pi\sqrt{N/2} \end{cases}$
Site-centered inversion	$\mathcal{I}_s$	$\vec{s}_{i,j} \to \vec{s}_{-i,j}$	$\begin{cases} \Phi_0(x) \to -\Phi_0(-x) + \pi\sqrt{N/2} \\ \Theta_0(x) \to \Theta_0(-x) \end{cases}$
π rotation around x axis	$\mathcal{R}_x$	$\begin{cases} s^x_{i,j} \to s^x_{i,j} \\ s^{y,z}_{i,j} \to -s^{y,z}_{i,j} \end{cases}$	$\begin{cases} \Phi_0 \to -\Phi_0 \\ \Theta_0 \to -\Theta_0 \end{cases}$
π rotation around y axis	$\mathcal{R}_y$	$\begin{cases} s^y_{i,j} \to s^y_{i,j} \\ s^{x,z}_{i,j} \to -s^{x,z}_{i,j} \end{cases}$	$\begin{cases} \Phi_0 \to -\Phi_0 \\ \Theta_0 \to -\Theta_0 + \pi\sqrt{N/2} \end{cases}$
π rotation around z axis	$\mathcal{R}_z$	$\begin{cases} s^z_{i,j} \to s^z_{i,j} \\ s^{x,y}_{i,j} \to -s^{x,y}_{i,j} \end{cases}$	$\begin{cases} \Phi_0 \to \Phi_0 \\ \Theta_0 \to \Theta_0 + \pi\sqrt{N/2} \end{cases}$

[1] q is an arbitrary odd integer.
[2] With complex conjugation.

One can easily confirm that the transformation on the field $\phi_j \to -\phi_j$ and $\theta_j \to \theta_j + \pi/\sqrt{2}$ in Eq. (3.14) recovers the right-hand side of Eq. (3.37), together with complex conjugation. Then, substituting this transformation into the definition of the center-of-mass field (3.18), we obtain $\Phi_0 \to -\Phi_0$ and $\Theta_0 \to \Theta_0 + \pi\sqrt{N/2}$. Symmetries of the Hamiltonian (3.1) with $H' = 0$ and their transformations on the spin operators and the center-of-mass field are listed in Table 3.1. [6] Symmetry operations on each chain field (ϕ_j, θ_j) are also recovered by setting $N = 1$.

We note that some symmetry transformations in Table 3.1 form a set in which a symmetry operation is related to successive operations of the other two symmetries. One such set is composed of π rotations around three spin axes. For example, $\mathcal{R}_x\mathcal{R}_y = \mathcal{R}_z$. This means that the π rotations around spin axes are elements of a dihedral group $\mathcal{D}_2 = \{1, \mathcal{R}_x, \mathcal{R}_y, \mathcal{R}_z\}$. Another set is formed by an odd-site translation trs, bond-centered inversions $\mathcal{I}_b$, and site-centered inversion $\mathcal{I}_s$. This can be understood as follows (see also Fig. 3.2): if we impose both the site-centered inversion symmetry with respect to a site $i = 0$ and the bond-centered inversion symmetry with respect to a bond between $i = r$ and $r + 1$ to a system, those two inversions automatically enforce the system to be invariant under the $(2r+1)$-site translation,

[6] Even-site translation does not affect Eq. (3.14) in the *zero magnetic field*, up to higher-order derivative terms.

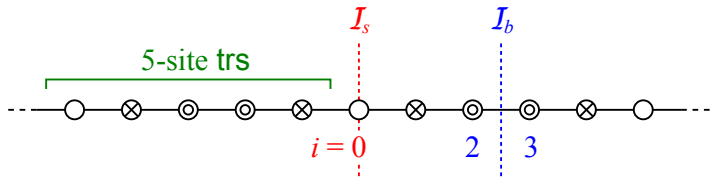

Figure 3.2: Schematic picture of an infinite chain with the site-centered inversion symmetry ($\mathcal{I}_s$) at $i = 0$ and bond-centered inversion symmetry ($\mathcal{I}_b$) between $i = 2$ and 3. Those inversion symmetries enforce the system to have 5-site translational invariance (trs).

i.e. $\mathcal{I}_s\mathcal{I}_b = \mathsf{trs}$ (the r dependence does not enter in the transformations on the bosonic field). As seen from Table 3.1, those transformation properties among the sets of symmetries are also reflected on the bosonic field, up to ambiguity from its compactification (3.33).

Although only π rotations around spin axes are shown in Table 3.1, we have assumed a larger symmetry in the Hamiltonian $H_\parallel + H_\perp$, that is, a U(1) symmetry under the spin rotation around z axis by an arbitrary angle γ: $s^\pm_{i,j} \to e^{\pm i\gamma} s^\pm_{i,j}$. In the bosonic language, this makes the effective Hamiltonian invariant under the shift $\Theta_0 \to \Theta_0 + \gamma\sqrt{N/2}$. Setting $\gamma = \pi$, we obtain the transformation law for $\mathcal{R}_z$ in Table. 3.1. Thus any vertex operator of Θ_0 is forbidden by the U(1) symmetry, and we have to choose $q = 0$ in Eq. (3.35).

A symmetry constraint on the vertex operators of Φ_0 comes from the symmetries under $\Phi_0 \to -\Phi_0$. This constraint restricts the vertex operators to even functions in Φ_0, namely $\cos(p\sqrt{2N}\Phi_0)$, $p > 0$. Another constraint would arise from odd-site translation invariance trs or site-centered inversion symmetry $\mathcal{I}_s$. These symmetries leave the effective Hamiltonian invariant under a constant shift of Φ_0 by $\pi\sqrt{N/2}$. For even N, this shift is just a multiple of $2\pi R$ and can be absorbed in Eq. (3.33). Then $\cos(p\sqrt{2N}\Phi_0)$ for any positive integer p is allowed in the Hamiltonian. On the other hand, the invariance of the Hamiltonian under this shift is relevant for odd N and only $\cos(p\sqrt{2N}\Phi_0)$ with $p \geq 2$ is possible. The above symmetry analysis is consistent with the effective Hamiltonians (3.24) and (3.25) derived by lowest-order perturbation theory in Sec. 3.B, which only keep vertex operators with the lowest scaling dimensions, i.e. the lowest values of p. The compatibility of the effective Hamiltonians with one-site translational invariance has been already pointed out in Ref. [98].

3.4 An extension of the Lieb-Schultz-Mattis theorem

For half-odd-integer antiferromagnetic spin chains with one-site translational invariance and the U(1) spin-rotational symmetry in the zero magnetic field, the Lieb-Schultz-Mattis theorem [19, 20] states that the ground state either has a gapless excitation or spontaneously breaks translational invariance in the thermodynamic limit. This theorem can also be understood by means of the bosonization approach [110]. If one of vertex operators $\cos(p\sqrt{2N}\Phi_0 + \alpha)$ with $p \geq 2$ and some real number α is relevant, the ground state is degenerate and gapped. This follows that the potential minima,

$$\Phi_0 = \frac{n}{p}\sqrt{\frac{2}{N}}\pi - \frac{\beta}{p\sqrt{2N}}, \quad n \in \mathbb{Z}, \quad \beta = \alpha \text{ or } \alpha + \pi, \tag{3.38}$$

are identical within the compactification radius $2\pi R = \pi\sqrt{2/N}$ for $p = 1$ while p-fold degenerate for $p \geq 2$. On the other hand, if all the vertex operators are irrelevant, the ground state behaves as a massless free boson and thus is gapless. Therefore, if the effective Hamiltonian

with translational invariance only allows the vertex operators $\cos(p\sqrt{2N}\Phi_0 + \alpha)$ with $p \geq 2$, the ground state only has two possibilities: one is gapless and the other is gapped and degenerate. This is indeed the case of the effective Hamiltonian (3.25) for half-odd-integer spin chains, or equivalently (in our approach), odd-N spin-1/2 ladders.

From our bosonization approach, the ground state is either gapless or degenerate, when the effective Hamiltonian only allows vertex operators with multiple potential minima corresponding to degenerate ground states associated with spontaneous symmetry breaking. For this condition to be satisfied, the U(1) symmetry is not necessarily required. As a consequence, we find that, for half-odd-integer spin chains or odd-N spin-1/2 ladders, the ground state is either gapless or degenerate by spontaneous symmetry breaking, when either of the following two conditions is satisfied:

(i) the system has odd-site translational invariance and either $\mathcal{T}$ or $\mathcal{D}_2$ symmetry,

(ii) the system has site-centered inversion symmetry and either $\mathcal{T}$ or $\mathcal{D}_2$ symmetry.

Both of those conditions leave the effective Hamiltonian invariant under

$$\begin{aligned} \Phi_0 &\to \Phi_0 + \pi\sqrt{N/2}, \\ \Theta_0 &\to \Theta_0 + \pi\sqrt{N/2}, \end{aligned} \tag{3.39}$$

so that vertex operators lead to some degenerate ground state. More precisely, for odd-site translational invariance to give the above transformation property on the field, we must ensure that there is no magnetization. For example, a finite magnetization in z axis modifies the transformation on Φ_0 and can lead to a unique gapped ground state [110]. The absence of the magnetization is ensured by the symmetry under either time reversal $\mathcal{T}$ or dihedral group $\mathcal{D}_2$.

Although the present discussion based on the effective Hamiltonian is far from a mathematically rigorous proof, the same restriction on the ground state under the condition (i) has been obtained in terms of the matrix-product state formalism [14] (see also Sec. 2.3.3). Along with the discussion in Ref. [14], in Sec. 5.3.5, we also prove that the condition (ii) also leads to a gapless or degenerate ground state. While we do not know the other proof like the original discussion using a twist operator [20], a related discussion is found in Ref. [111] from the point of view of a Berry phase associated with a local gauge twist. A similarity between one-site translational invariance and site-centered inversion symmetry in time-reversal-invariant spin systems has been indicated.

3.A Review of bosonization

To obtain the bosonized expression of the spin-1/2 XXZ chain,

$$H = J\sum_i \left[s_i^x s_{i+1}^x + s_i^y s_{i+1}^y + \Delta s_i^z s_{i+1}^z\right], \tag{3.40}$$

we have mainly two approaches:

1. Using the Jordan-Wigner transformation, we map the spin-1/2 chain onto a spinless fermion chain with a nearest-neighbor interaction. Taking a continuum limit, the dispersion relation is linearized around the Fermi points, and thus we obtain a Dirac fermion. Then we bosonize the Dirac fermion and take into account the interaction perturbatively.

2. We start from the one-dimensional Hubbard model. Taking a continuum limit, we obtain two Dirac fermions with different spins. We bosonize those Dirac fermions and consider the on-site repulsive interaction. The interaction opens up an excitation gap in the charge sector but the spin sector remains free. Integrating out the charge degree of freedom, we obtain the bosonized expression of the Heisenberg model ($\Delta = 1$).

The first approach is well explained in Refs. [51, 99]. We here adopt the second approach that allows us to maintain the SU(2) symmetry. We refer to Refs. [79, 109, 112, 113] in the following argument.

3.A.1 Non-Abelian bosonization of Hubbard model

We consider the Hubbard model,

$$H = -t \sum_j \sum_{\alpha=\uparrow,\downarrow} \left[c^\dagger_{j,\alpha} c_{j+1,\alpha} + \text{h.c.} \right] + U \sum_j n_{j\uparrow} n_{j\downarrow}, \tag{3.41}$$

where $c^\dagger_{j,\alpha}$ ($c_{j,\alpha}$) is a fermion creation (annihilation) operator with spin α on site j, $n_{j,\alpha} = c^\dagger_{j,\alpha} c_{j,\alpha}$, t is a hopping, and U is a positive (repulsive) on-site interaction. At half-filling $\langle n_{j,\alpha} \rangle = 1/2$ and for any finite value of U, this model is in a Mott-insulating phase and has a finite charge-excitation gap. If we are interested only in low-energy physics, empty and doubly-occupied sites are suppressed, so that properties of this model would be essentially described by the Heisenberg model, which is usually obtained in the limit $U/t \gg 1$.

Free-fermion

We start from the free-fermion Hamiltonian,

$$H_0 = -t \sum_j \sum_{\alpha=\uparrow,\downarrow} \left[c^\dagger_{j,\alpha} c_{j+1,\alpha} + \text{h.c.} \right]. \tag{3.42}$$

Since only excitations around the Fermi points contribute to the low-energy properties, we can linearize the free-fermion dispersion relation around two Fermi points $\pm k_F$, $k_F = \pi/(2a_0)$ (a_0 is the lattice spacing). Taking the continuum limit, the free-fermion Hamiltonian is expressed by the massless Dirac fermion (the Luttinger model),

$$H_0 \approx -v_F \int dx \sum_{\alpha=\uparrow,\downarrow} \left[\psi^\dagger_{R,\alpha}(x) i\partial_x \psi_{R,\alpha}(x) - \psi^\dagger_{L,\alpha}(x) i\partial_x \psi_{L,\alpha}(x) \right], \tag{3.43}$$

where the Fermi velocity is given by $v_F = 2ta_0 \sin(k_F a_0) = 2ta_0$ and $x = ja_0$. Here we introduced fermionic fields,

$$c_{j,\alpha} \approx \sqrt{a_0} \psi_\alpha(x), \tag{3.44}$$

and they have the right-going (R) and left-going (L) chiral components corresponding to each Fermi point,

$$\psi_\alpha(x) = e^{-ik_F x} \psi_{R\alpha}(x) + e^{ik_F x} \psi_{L\alpha}(x). \tag{3.45}$$

We then introduce the U(1) and SU(2) current,

$$J_r(x) = :\psi^\dagger_{r,\alpha}(x) \psi_{r,\alpha}(x):, \quad \vec{\mathcal{J}}_r(x) = :\psi^\dagger_{r,\alpha}(x) \frac{\vec{\sigma}_{\alpha\beta}}{2} \psi_{r,\beta}(x):, \quad r = R, L, \tag{3.46}$$

where $\vec{\sigma}$ stands for the Pauli matrices. These currents respectively correspond to the charge and spin densities and satisfy the U(1) and SU(2) Kac-Moody algebras (or the current algebras) [114],

$$\begin{aligned}[J_R(x), J_R(x')] &= -\frac{i}{\pi}\partial_x\delta(x-x'),\\ [J_L(x), J_L(x')] &= \frac{i}{\pi}\partial_x\delta(x-x'),\end{aligned} \tag{3.47}$$

and

$$\begin{aligned}[\mathcal{J}_R^a(x), \mathcal{J}_R^b(x')] &= i\epsilon^{abc}\mathcal{J}_R^c(x)\delta(x-x') - \frac{i}{4\pi}\delta^{ab}\partial_x\delta(x-x'),\\ [\mathcal{J}_L^a(x), \mathcal{J}_L^b(x')] &= i\epsilon^{abc}\mathcal{J}_L^c(x)\delta(x-x') + \frac{i}{4\pi}\delta^{ab}\partial_x\delta(x-x').\end{aligned} \tag{3.48}$$

A meaning of the "anomalous" commutators $\partial_x\delta(x-x')$ is nicely explained in Ref. [51]. In terms of these current algebras, the Dirac Hamiltonian (3.43) is expressed in the Sugawara form,

$$H_0 = H_{\mathrm{U}(1)} + H_{\mathrm{SU}(2)}, \tag{3.49}$$

$$H_{\mathrm{U}(1)} = \frac{\pi v_F}{2}\int dx\,(:J_R(x)J_R(x):+:J_L(x)J_L(x):), \tag{3.50}$$

$$H_{\mathrm{SU}(2)} = \frac{2\pi v_F}{3}\int dx\left(:\vec{\mathcal{J}}_R(x)\cdot\vec{\mathcal{J}}_R(x):+:\vec{\mathcal{J}}_L(x)\cdot\vec{\mathcal{J}}_L(x):\right). \tag{3.51}$$

Bosonic description

The charge part $H_{\mathrm{U}(1)}$ is represented as a free bosonic theory,

$$H_{\mathrm{U}(1)} = \frac{v_F}{2}\int dx\left[(\partial_x\theta_c(x))^2 + (\partial_x\phi_c(x))^2\right] \tag{3.52}$$

through identifications

$$J_R(x) + J_L(x) = \sqrt{\frac{2}{\pi}}\partial_x\phi_c(x), \quad J_R(x) - J_L(x) = -\sqrt{\frac{2}{\pi}}\partial_x\theta_c(x). \tag{3.53}$$

The two fields $\phi_c(x)$ and $\partial_x\theta_c(x)$ form canonically conjugate variables,

$$[\phi_c(x), \partial_x\theta_c(x')] = i\delta(x-x'). \tag{3.54}$$

The spin part $H_{\mathrm{SU}(2)}$ represent the level-1 SU(2) Wess-Zumino-Witten model. It is also expressed by a free bosonic theory,

$$H_{\mathrm{SU}(2)} = \frac{v_F}{2}\int dx\left[(\partial_x\phi_s(x))^2 + (\partial_x\theta_s(x))^2\right], \tag{3.55}$$

through $\vec{\mathcal{J}}_r(x)\cdot\vec{\mathcal{J}}_r(x) = 3\mathcal{J}_r^z(x)\mathcal{J}_r^z(x)$ and identifications

$$\mathcal{J}_R^z(x) + \mathcal{J}_L^z(x) = \frac{1}{\sqrt{2\pi}}\partial_x\phi_s(x), \quad \mathcal{J}_R^z(x) - \mathcal{J}_L^z(x) = -\frac{1}{\sqrt{2\pi}}\partial_x\theta_s(x). \tag{3.56}$$

The two fields $\phi_s(x)$ and $\partial_x\theta_s(x)$ again satisfy a canonical commutation relation,

$$[\phi_s(x), \partial_x\theta_s(x')] = i\delta(x-x'). \tag{3.57}$$

The fermionic fields (3.45) are also related to the bosonic fields through the Mandelstam formula,

$$\psi_{R,\alpha}(x) = \frac{\eta_\alpha}{\sqrt{2\pi a_0}} e^{-i\sqrt{\pi}(\phi_\alpha(x)-\theta_\alpha(x))}, \quad \psi_{L,\alpha}(x) = \frac{\eta_\alpha}{\sqrt{2\pi a_0}} e^{i\sqrt{\pi}(\phi_\alpha(x)+\theta_\alpha(x))}. \tag{3.58}$$

Here we have introduced the Klein factors η_α to ensure the anticommutation relation between the fermions with different spins, and it satisfies

$$\{\eta_\alpha, \eta_{\alpha'}\} = 2\delta_{\alpha\alpha'}. \tag{3.59}$$

Other anticommutation relations of the fermionic fields are supplemented by the commutation relation of the bosonic fields,

$$\left[\phi_\alpha(x), \theta_{\alpha'}(x')\right] = \frac{i}{2}\delta_{\alpha\alpha'}\left[\mathrm{sgn}(x-x')+1\right]. \tag{3.60}$$

The bosonic fields associated with charge and spin in Eqs. (3.53) and (3.56) are given by a canonical transformation,

$$\begin{aligned} \phi_c(x) &= \frac{1}{\sqrt{2}}(\phi_\uparrow(x)+\phi_\downarrow(x)), \quad \theta_c(x) = \frac{1}{\sqrt{2}}(\theta_\uparrow(x)+\theta_\downarrow(x)), \\ \phi_s(x) &= \frac{1}{\sqrt{2}}(\phi_\uparrow(x)-\phi_\downarrow(x)), \quad \theta_s(x) = \frac{1}{\sqrt{2}}(\theta_\uparrow(x)+\theta_\downarrow(x)). \end{aligned} \tag{3.61}$$

In terms of $\phi_s(x)$ and $\theta_s(x)$, one can represent other components of the SU(2) current as

$$\mathcal{J}_R^\pm(x) = \frac{1}{2\pi a_0} e^{\pm i\sqrt{2\pi}(\phi_s(x)-\theta_s(x))}, \quad \mathcal{J}_L^\pm(x) = \frac{1}{2\pi a_0} e^{\mp i\sqrt{2\pi}(\phi_s(x)+\theta_s(x))}. \tag{3.62}$$

The commutation relations of the SU(2) current algebra (3.48) is equivalent to the following operator product expansions,

$$\begin{aligned} \mathcal{J}^a(z)\mathcal{J}^b(w) &\sim \frac{\delta^{ab}}{8\pi^2(z-w)^2} + \sum_c i\epsilon^{abc}\frac{\mathcal{J}^c(w)}{2\pi(z-w)}, \\ \bar{\mathcal{J}}^a(\bar{z})\bar{\mathcal{J}}^b(\bar{w}) &\sim \frac{\delta^{ab}}{8\pi^2(\bar{z}-\bar{w})^2} + \sum_c i\epsilon^{abc}\frac{\bar{\mathcal{J}}^c(\bar{w})}{2\pi(\bar{z}-\bar{w})}, \end{aligned} \tag{3.63}$$

where we used complex coordinates $z = v_F\tau + ix$, $\bar{z} = v_F\tau - ix$ [7] and identified as $\mathcal{J}_R^a(x) \equiv \mathcal{J}^a(z)$, $\mathcal{J}_L^a(x) \equiv \bar{\mathcal{J}}^a(\bar{z})$. Introducing chiral bosons,

$$\phi_s(z,\bar{z}) = \varphi_s(z) + \bar{\varphi}_s(\bar{z}), \quad \theta_s(z,\bar{z}) = -\varphi_s(z) + \bar{\varphi}_s(\bar{z}), \tag{3.64}$$

the SU(2) current is reexpressed as

$$\begin{aligned} \mathcal{J}^x(z) &= \frac{1}{2\pi a_0}\cos(\sqrt{8\pi}\varphi_s(z)), \quad \mathcal{J}^y(z) = \frac{1}{2\pi a_0}\sin(\sqrt{8\pi}\varphi_s(z)), \quad \mathcal{J}^z(z) = \frac{i}{\sqrt{2\pi}}\partial_z\varphi_s(z), \\ \bar{\mathcal{J}}^x(\bar{z}) &= \frac{1}{2\pi a_0}\cos(\sqrt{8\pi}\bar{\varphi}_s(\bar{z})), \quad \bar{\mathcal{J}}^y(z) = \frac{-1}{2\pi a_0}\sin(\sqrt{8\pi}\bar{\varphi}_s(\bar{z})), \quad \bar{\mathcal{J}}^z(\bar{z}) = \frac{-i}{\sqrt{2\pi}}\partial_{\bar{z}}\bar{\varphi}_s(\bar{z}). \end{aligned} \tag{3.65}$$

[7] We consider the two-dimensional Euclidean space-time $(x_0, x_1) = (v_F\tau, x)$ with the metric $g_{\mu\nu} = \mathrm{diag}(1,1)$.

Using operator product expansions of a free boson,

$$\partial_z\varphi(z)\partial_w\varphi(w) \sim -\frac{1}{4\pi}\frac{1}{(z-w)^2}, \tag{3.66}$$

$$\partial_z\varphi(z)e^{i\alpha\varphi(w)} \sim \frac{-i\alpha}{4\pi}\frac{1}{z-w}e^{i\alpha\varphi(w)}, \tag{3.67}$$

$$e^{i\alpha\varphi(z)}e^{-i\alpha\varphi(w)} \sim \left(\frac{a_0}{z-w}\right)^{\alpha^2/(4\pi)}\left[1+i\alpha(z-w)\partial_w\varphi(w)+\mathcal{O}((z-w)^2)\right]. \tag{3.68}$$

one can easily check that the bosonic representation of the SU(2) current (3.65) satisfies the Kac-Moody algebra (3.63).

Hubbard interaction

Next we consider effects of the Hubbard interaction,

$$H_U = U\sum_j n_{j\uparrow}n_{j\downarrow}. \tag{3.69}$$

Taking the continuum limit, we obtain

$$\begin{aligned} H_U &\approx Ua_0\int dx\ \psi_\uparrow^\dagger(x)\psi_\uparrow(x)\psi_\downarrow^\dagger(x)\psi_\downarrow(x) \\ &\approx Ua_0\int dx\ \Big[\left(\psi_{R\uparrow}^\dagger\psi_{R\uparrow}+\psi_{L\uparrow}^\dagger\psi_{L\uparrow}\right)\left(\psi_{R\downarrow}^\dagger\psi_{R\downarrow}+\psi_{L\downarrow}^\dagger\psi_{L\downarrow}\right) \\ &\qquad + \psi_{R\uparrow}^\dagger\psi_{L\uparrow}\psi_{L\downarrow}^\dagger\psi_{R\uparrow}+\psi_{L\uparrow}^\dagger\psi_{R\uparrow}\psi_{R\downarrow}^\dagger\psi_{L\downarrow} \\ &\qquad + e^{i4k_Fx}\psi_{R\uparrow}^\dagger\psi_{L\uparrow}\psi_{R\downarrow}^\dagger\psi_{L\downarrow}+e^{-i4k_Fx}\psi_{L\uparrow}^\dagger\psi_{R\uparrow}\psi_{L\downarrow}^\dagger\psi_{R\downarrow}\Big]. \end{aligned} \tag{3.70}$$

The last term represents an umklapp process and gives a nonvanishing contribution only at half-filling since $k_F = \pi/(2a_0)$. We have dropped oscillating terms with $e^{\pm i2k_Fx}$ because they vanish after the integration over the spatial coordinate. In terms of the current operators and bosonic fields, this expression is rewritten as

$$\begin{aligned} H_U \approx Ua_0\int dx\ \Big[&\frac{1}{4}\left(J_RJ_R+J_LJ_L\right)+\frac{1}{2}J_RJ_L-\frac{1}{3}\left(\vec{\mathcal{J}}_R\cdot\vec{\mathcal{J}}_R+\vec{\mathcal{J}}_L\cdot\vec{\mathcal{J}}_L\right) \\ &-2\vec{\mathcal{J}}_R\cdot\vec{\mathcal{J}}_L-\frac{2}{(2\pi a_0)^2}\cos(\sqrt{8\pi}\phi_c)\Big]. \end{aligned} \tag{3.71}$$

For the charge sector, the forward- and back-scattering terms $J_RJ_R+J_LJ_L$ and J_RJ_L can be absorbed into Eq. (3.52) and only change the velocity and the Luttinger parameter. The resulting Hamiltonian is given by

$$H_{\text{charge}} = \frac{v_c}{2}\int dx\left[K_c(\partial_x\theta_c(x))^2+\frac{1}{K_c}(\partial_x\phi_c(x))^2\right]-\frac{U}{2\pi^2a_0}\int dx\cos(\sqrt{8\pi}\phi_c(x)), \tag{3.72}$$

where v_c and K_c are an effective velocity and stiffness (usually called the *Luttinger parameter*),

$$v_c = v_F\left(1+\frac{Ua_0}{\pi v_F}\right)^{1/2}, \quad K_c = \left(1+\frac{Ua_0}{\pi v_F}\right)^{-1/2}. \tag{3.73}$$

The Luttinger parameter K_c now deviates from its free-fermion value $K_c = 1$ and changes the scaling dimension of the last term to $2K_c$. Since $2K_c < 2$ for $U > 0$, it is relevant and generates a Mott-Hubbard gap. Thus ϕ_c is pinned at one of potential minima $n\sqrt{\pi/2}$ with integer n. For the spin sector, the forward-scattering term $\vec{\mathcal{J}}_R \cdot \vec{\mathcal{J}}_R + \vec{\mathcal{J}}_L \cdot \vec{\mathcal{J}}_L$ can be incorporated into Eq. (3.55) and only makes a change of the velocity. Keeping the manifestly SU(2)-invariant form, we obtain

$$H_{\text{spin}} = \frac{2\pi v_s}{3} \int dx \left(: \vec{\mathcal{J}}_R(x) \cdot \vec{\mathcal{J}}_R(x) : + : \vec{\mathcal{J}}_L(x) \cdot \vec{\mathcal{J}}_L(x) : \right) - 2Ua_0 \int dx \; \vec{\mathcal{J}}_R(x) \cdot \vec{\mathcal{J}}_L(x), \tag{3.74}$$

where the spin velocity v_s is defined by

$$v_s = v_F - \frac{Ua_0}{2\pi}. \tag{3.75}$$

Since the back-scattering term $\vec{\mathcal{J}}_R \cdot \vec{\mathcal{J}}_L$ is marginally irrelevant, universal properties of Eq. (3.74) are still described by the level-1 SU(2) Wess-Zumino-Witten model. When the SU(2) symmetry is broken, the back-scattering term $\mathcal{J}_R^x \mathcal{J}_L^x + \mathcal{J}_R^y \mathcal{J}_L^y$ can be relevant, as we will see later for the spin-1/2 XXZ model.

Spin operator

Now we turn to derive bosonized expressions of the spin operators. Using fermionic operators, we can write

$$\vec{s}_j = c_{j,\alpha}^\dagger \frac{\vec{\sigma}_{\alpha\beta}}{2} c_{j,\beta}. \tag{3.76}$$

Taking the continuum limit, we find

$$\vec{s}_j \approx a_0 \left[\vec{\mathcal{J}}_R(x) + \vec{\mathcal{J}}_L(x) + (-1)^j \vec{\mathcal{N}}(x) \right]. \tag{3.77}$$

The uniform parts $\vec{\mathcal{J}}_{R,L}(x)$ have been defined in Eq. (3.46), while the staggered part $\vec{\mathcal{N}}(x)$ is defined as

$$\vec{\mathcal{N}}(x) = \psi_{R\alpha}^\dagger(x) \frac{\vec{\sigma}_{\alpha\beta}}{2} \psi_{L\beta}(x) + \psi_{L\alpha}^\dagger(x) \frac{\vec{\sigma}_{\alpha\beta}}{2} \psi_{R\beta}(x). \tag{3.78}$$

In terms of the bosonic fields, this can be represented as

$$\mathcal{N}^z(x) = \frac{1}{\pi a_0} \cos(\sqrt{2\pi}\phi_c(x)) \sin(\sqrt{2\pi}\phi_s(x)), \tag{3.79}$$

$$\mathcal{N}^\pm(x) = \frac{1}{\pi a_0} \cos(\sqrt{2\pi}\phi_c(x)) e^{\mp i\sqrt{2\pi}\theta_s(x)}. \tag{3.80}$$

Since ϕ_c is pinned, we can replace $\cos(\sqrt{2\pi}\phi_c(x))$ by its expectation value $C \equiv \langle \cos(\sqrt{2\pi}\phi_c(x)) \rangle$. Therefore, we end up with

$$\begin{aligned} s_j^z &\approx \frac{a_0}{\sqrt{2\pi}} \partial_x \phi_s(x) + \frac{C}{\pi} \sin(\sqrt{2\pi}\phi_s(x)), \\ s_j^\pm &\approx e^{\mp i\sqrt{2\pi}\theta_s(x)} \left[\frac{C}{\pi}(-1)^j - \frac{1}{\pi} \sin(\sqrt{2\pi}\phi_s(x)) \right]. \end{aligned} \tag{3.81}$$

3.A.2 Bosonization formulas for XXZ chain

When the SU(2) symmetry is reduced to the U(1) symmetry, the back-scattering term in Eq. (3.74) is split into two parts, $\mathcal{J}_R^z\mathcal{J}_L^z$ and $\mathcal{J}_R^x\mathcal{J}_L^x + \mathcal{J}_R^y\mathcal{J}_L^y$. Then the Hamiltonian in the spin sector takes the form,

$$H_{\text{spin}} = \frac{v_s}{2}\int dx \left[K_s(\partial_x\theta_s(x))^2 + \frac{1}{K_s}(\partial_x\phi_s(x))^2\right] + \frac{v_s\lambda}{a_0^2}\int dx \cos(\sqrt{8\pi}\phi_s(x)), \tag{3.82}$$

where v_s and K_s are the velocity and Luttinger parameter for spin and λ is some coupling constant. This is in fact the low-energy effective Hamiltonian for the spin-1/2 XXZ chain (3.40). v_s and K_s are obtained by comparison with the exact solution by Bethe ansatz as

$$v_s = \frac{\pi J a_0\sqrt{1-\Delta^2}}{2\cos^{-1}\Delta}, \quad K_s = \frac{\pi}{\pi - \cos^{-1}\Delta}. \tag{3.83}$$

The last term in Eq. (3.74) has the scaling dimension $2K_s$. As expected from Eq. (3.74), at the Heisenberg point $\Delta = 1$, this term is marginally irrelevant since $\lambda > 0$. For $-1 < \Delta \leq 1$, λ is irrelevant and has been analytically evaluated in Ref. [104] as

$$\lambda = \frac{4\Gamma(K)}{\Gamma(1-K)}\left[\frac{\Gamma\left(1+\frac{1}{2K-2}\right)}{2\sqrt{\pi}\,\Gamma\left(1+\frac{K}{2K-2}\right)}\right]^{2K-2}. \tag{3.84}$$

The bosonized expressions of the spin operators take the same form as Eq. (3.81) but with different coefficients,

$$\begin{aligned} s_j^z &\approx \frac{a_0}{\sqrt{2\pi}}\partial_x\phi_s(x) + a_1\sin(\sqrt{2\pi}\phi_s(x)), \\ s_j^\pm &\approx e^{\mp i\sqrt{2\pi}\theta_s(x)}\left[b_0(-1)^j - b_1\sin(\sqrt{2\pi}\phi_s(x))\right]. \end{aligned} \tag{3.85}$$

The nonuniversal coefficients a_1, b_0, and b_1 have also been obtained as functions of Δ [103–106],

$$\begin{aligned} a_1^2 &= \frac{4}{\pi^2}\left[\frac{\Gamma\left(\frac{\eta}{2(1-\eta)}\right)}{2\sqrt{\pi}\,\Gamma\left(\frac{1}{2(1-\eta)}\right)}\right]^{1/\eta} \exp\left[\int_0^\infty \frac{dt}{t}\left(\frac{\sinh[(2\eta-1)t]}{\sinh(\eta t)\cosh[(1-\eta)t]} - \frac{2\eta-1}{\eta}e^{-2t}\right)\right], \\ b_0^2 &= \frac{1}{4(1-\eta)^2}\left[\frac{\Gamma\left(\frac{\eta}{2(1-\eta)}\right)}{2\sqrt{\pi}\,\Gamma\left(\frac{1}{2(1-\eta)}\right)}\right]^{\eta} \exp\left[-\int_0^\infty \frac{dt}{t}\left(\frac{\sinh(\eta t)}{\sinh(t)\cosh[(1-\eta)t]} - \eta e^{-2t}\right)\right], \\ b_1^2 &= \frac{2}{\eta(1-\eta)}\left[\frac{\Gamma\left(\frac{\eta}{2(1-\eta)}\right)}{2\sqrt{\pi}\,\Gamma\left(\frac{1}{2(1-\eta)}\right)}\right]^{\eta+1/\eta} \\ &\quad\times \exp\left[-\int_0^\infty \frac{dt}{t}\left(\frac{\cosh(2\eta t)e^{-2t}-1}{2\sinh(\eta t)\sinh(t)\cosh[(1-\eta)t]} + \frac{1}{\sinh(\eta t)} - \frac{\eta^2+1}{\eta}e^{-2t}\right)\right], \end{aligned} \tag{3.86}$$

where $\eta = 1 - \cos^{-1}\Delta/\pi$. Bosonization formulas used in Sec. 3.2.1 are obtained by replacements, [8]

$$\phi_s(x) \to \frac{1}{\sqrt{\pi}}\phi(x) + \sqrt{\frac{\pi}{2}}, \quad \theta_s(x) \to -\frac{1}{\sqrt{\pi}}\theta(x). \tag{3.87}$$

[8] As many papers, as many conventions.

3.B Perturbative derivation of effective Hamiltonian

In this appendix, based on the perturbation theory, we demonstrate a derivation of the effective Hamiltonian (3.24) and (3.25). A similar discussion was already given by Schulz [17] who looked at a correlation function of the center-of-mass field. But here we take a more direct approach focusing on the action. This appendix also provides an evidence to consider that a nonuniversal prefactor A of the effective coupling constant $g_{\rm eff} \sim A(-g_1)^N$ is positive. Similar discussions will be applied to show the positivity of other nonuniversal prefactors in the effective couplings appearing in Chapter 4.

In the bosonized expression of $H_0+H_\perp$ in Sec. 3.2.1, g_3 is supposed to be the most relevant coupling and then Θ_ν acquire masses. Since the g_1 and g_4 terms involve the center-of-mass field Φ_0, they would give nontrivial contributions to the effective Hamiltonian by integrating out the relative fields. In fact, by replacing $\cos\sqrt{2}(\theta_j-\theta_{j'})$ with its expectation value, g_4 can be absorbed into g_1 as

$$g_1 \to g_1 - g_4\langle\cos\sqrt{2}(\theta_j-\theta_{j'})\rangle. \tag{3.88}$$

Thus, in the following discussion, we only consider the perturbation in g_1.

We start from the partition function,

$$\mathcal{Z} = \int \mathcal{D}\Phi_0\mathcal{D}\Phi_1\cdots\mathcal{D}\Phi_{N-1}e^{-\mathcal{S}_c[\Phi_0]-\mathcal{S}_r[\Phi_\nu]-\mathcal{S}_{cr}[\Phi_0,\Phi_\nu]}, \tag{3.89}$$

where

$$\mathcal{S}_c[\Phi_0] = \frac{v}{2\pi K}\int d^2r\left[\frac{1}{v^2}(\partial_\tau\Phi_0)^2+(\partial_x\Phi_0)^2\right], \tag{3.90}$$

$$\mathcal{S}_r[\Phi_\nu] = \frac{v}{2\pi K}\int d^2r\sum_{\nu=1}^{N-1}\left[\frac{1}{v^2}(\partial_\tau\Phi_\nu)^2+(\partial_x\Phi_\nu)^2\right]+\int d^2r\sum_{j\neq j'}g_{3,(j,j')}\cos\sqrt{2}(\theta_j-\theta_{j'}), \tag{3.91}$$

$$\mathcal{S}_{cr}[\Phi_0,\Phi_\nu] = \int d^2r\sum_{j\neq j'}g_{1,(j,j')}\cos\sqrt{2}(\phi_j+\phi_{j'}), \tag{3.92}$$

and $\vec{r}\equiv(\tau,x)$. Since we now assume that g_1 is small, the partition function is expanded in $\mathcal{S}_{cr}[\Phi_0,\Phi_\nu]$ as

$$\mathcal{Z} = \mathcal{Z}_r\int\mathcal{D}\Phi_0 e^{-\mathcal{S}_c[\Phi_0]}\sum_{n=0}^{\infty}\frac{1}{n!}\left\langle(-\mathcal{S}_{cr}[\Phi_0,\Phi_\nu])^n\right\rangle_r, \tag{3.93}$$

where the expectation value $\langle\cdots\rangle_r$ is taken with respect to the ground state of $\mathcal{S}_r[\Phi_\nu]$:

$$\langle\cdots\rangle_r = \frac{1}{\mathcal{Z}_r}\int\mathcal{D}\Phi_1\cdots\mathcal{D}\Phi_{N-1}(\cdots)e^{-\mathcal{S}_r[\Phi_\nu]}, \tag{3.94}$$

$$\mathcal{Z}_r = \int\mathcal{D}\Phi_1\cdots\mathcal{D}\Phi_{N-1}e^{-\mathcal{S}_r[\Phi_\nu]}. \tag{3.95}$$

If N is even, the first nonvanishing contribution appears at the $N/2$-th order in $\mathcal{S}_{cr}[\Phi_0,\Phi_\nu]$. This is naively understood as follows. Since $\cos\sqrt{2}(\phi_j+\phi_{j'})$ involves the fluctuating fields Φ_ν, its M-point correlation functions

$$\left\langle\prod_{m=1}^{M}\cos\sqrt{2}(\phi_{j_m}(\vec{r}_m)+\phi_{j'_m}(\vec{r}_m))\right\rangle_r \tag{3.96}$$

decay exponentially. Thus, a possible nonvanishing contribution mainly comes from the correlation function *at the same point*, $\vec{r}_1 = \vec{r}_2 = \cdots = \vec{r}_M$. To eliminate Φ_ν, we have to sum up all ϕ_j with equal weights. Hence, $N/2$ is the lowest order in which correlation functions involving such a combination of ϕ_j is allowed. For example, we consider

$$I_{N/2} = \left\langle \prod_{n=1}^{N/2} (-g_{1,(2n-1,2n)}) \int d^2 r_n \cos\sqrt{2}\left(\phi_{2n-1}(\vec{r}_n) + \phi_{2n}(\vec{r}_n)\right) \right\rangle_r . \tag{3.97}$$

We can write

$$\begin{aligned} I_{N/2} &= \left\langle \prod_{n=1}^{N/2} \left(-\frac{g_{1,(2n-1,2n)}}{2}\right) \int d^2 r_n \left[e^{i\sqrt{2}(\phi_{2n-1}(\vec{r}_n)+\phi_{2n}(\vec{r}_n))} + e^{-i\sqrt{2}(\phi_{2n-1}(\vec{r}_n)+\phi_{2n}(\vec{r}_n))} \right] \right\rangle_r \\ &\approx \left(\prod_{n=1}^{N/2} \left(-\frac{g_{1,(2n-1,2n)}}{2}\right) \int d^2 r_n \right) \left\langle \exp\left(i\sqrt{2} \sum_{m=1}^{N/2} \left(\phi_{2m-1}(\vec{r}_m) + \phi_{2m}(\vec{r}_m)\right) \right) + \text{h.c.} \right\rangle_r , \end{aligned} \tag{3.98}$$

where we dropped all the cross terms in the second line. Since the relative fields Φ_ν are not canceled out in those cross terms, their expectation values vanish after integration over the coordinate. Using the canonical transformation in Eqs. (3.18) and (3.19), the exponent is rewritten as

$$\begin{aligned} &\sum_{m=1}^{N/2} \left(\phi_{2m-1}(\vec{r}_m) + \phi_{2m}(\vec{r}_m)\right) \\ &= \frac{2}{\sqrt{N}} \sum_{m=1}^{N/2} \Phi_0(\vec{r}_m) + \sum_{m=1}^{N/2} \sum_{\nu=1}^{N-1} \left(u_{2m-1}^{(\nu)} + u_{2m}^{(\nu)} \right) \Phi_\nu(\vec{r}_m) \\ &= \frac{2}{\sqrt{N}} \sum_{m=1}^{N/2} \Phi_0(\vec{r}_m) + \sum_{m=1}^{N/2-1} \sum_{\nu=1}^{N-1} \sum_{k=1}^{2m} u_k^{(\nu)} \left[\Phi_\nu(\vec{r}_m) - \Phi_\nu(\vec{r}_{m+1})\right] + \sum_{\nu=1}^{N-1} \sum_{k=1}^{N} u_k^{(\nu)} \Phi_\nu(\vec{r}_{N/2}). \end{aligned} \tag{3.99}$$

In the last line, the third term vanishes due to the orthogonality of $u_k^{(\nu)}$ in Eq. (3.20). The latter two terms do not appear for $N = 2$ and clearly vanish at the same point $\vec{r}_1 = \cdots = \vec{r}_{N/2}$. Substituting this expression into Eq. (3.98), we see that the second term gives a product of correlation functions,

$$\left\langle \prod_{m=1}^{N/2-1} e^{i\sqrt{2}\Psi_m(\vec{r}_m)} e^{-i\sqrt{2}\Psi_m(\vec{r}_{m+1})} \right\rangle_r , \tag{3.100}$$

where we defined

$$\Psi_m(\vec{r}) = \sum_{\nu=1}^{N-1} \sum_{k=1}^{2m} u_k^{(\nu)} \Phi_\nu(\vec{r}). \tag{3.101}$$

Since Ψ_m are sums of the disordered fields Φ_ν, their correlation functions exponentially decay. If the masses of Ψ_m are sufficiently large, the correlation functions rapidly decay and a leading

contribution to the integral (3.98) would only come from their amplitudes at $\vec{r}_m \sim \vec{r}_{m+1}$. Thus we approximate the correlation functions as delta functions and obtain

$$I_{N/2} \approx \left(\prod_{n=1}^{N/2} \left(-\frac{g_{1,(2n-1,2n)}}{2} \right) \int d^2 r_n \right) \times \left[\exp\left(2i\sqrt{\frac{2}{N}} \sum_{m=1}^{N/2} \Phi_0(\vec{r}_m) \right) \prod_{m=1}^{N/2-1} C_m \delta(\vec{r}_m - \vec{r}_{m+1}) + \text{h.c.} \right], \tag{3.102}$$

where the amplitudes C_m are nonuniversal constants and positive by its definition. After integration over the $N/2-1$ coordinate variables, we obtain a vertex operator only with Φ_0,

$$I_{N/2} \approx \frac{1}{2} \left(\prod_{m=1}^{N/2-1} C_m \right) \left(\prod_{n=1}^{N/2} \left(-\frac{g_{1,(2n-1,2n)}}{2} \right) \right) \int d^2 r \cos\left(\sqrt{2N} \Phi_0(\vec{r}) \right). \tag{3.103}$$

Similar contributions arise from any possible pairing of ϕ_j. Putting them back onto the action in Eq. (3.93), we obtain the effective action $\mathcal{S}_{\text{eff}}[\Phi_0]$ defined through $\mathcal{Z} \approx \int \mathcal{D}\Phi_0 e^{-\mathcal{S}_{\text{eff}}[\Phi_0]}$.

If the couplings among chains do not depend on j, namely $g_{1,(j,j')} \equiv g_1$, we can write the effective action as

$$\mathcal{S}_{\text{eff}}[\Phi_0] \approx \frac{v}{2\pi K} \int d^2 r \left[\frac{1}{v^2} (\partial_\tau \Phi_0)^2 + (\partial_x \Phi_0)^2 \right] - A'(-g_1)^{N/2} \int d^2 r \cos(\sqrt{2N}\Phi_0), \tag{3.104}$$

where the nonuniversal coefficient A' is positive since it is solely proportional to a sum of products of the positive amplitudes, $C_1 C_2 \cdots C_{N/2-1}$. For $N = 2$, this is simply read off as $A' = 1$. This positivity of the nonuniversal coefficient is also the key to discuss the phase transitions between different VBS phases in Chapter 4. Equation (3.104) corresponds to the effective Hamiltonian for even N in Eq. (3.24),

$$H_{\text{eff}} = \frac{v}{2\pi} \int dx \left[K(\partial_x \Theta_0)^2 + \frac{1}{K} (\partial_x \Phi_0)^2 \right] + A'(-g_1)^{N/2} \int dx \cos(\sqrt{2N}\Phi_0). \tag{3.105}$$

For odd N, the first nonvanishing contribution appears at the N-th order. For example, we consider

$$I_N = \left\langle \prod_{n=1}^{N} (-g_{1,(n,n+1)}) \int d^2 r_n \cos\sqrt{2}\left(\phi_n(\vec{r}_n) + \phi_{n+1}(\vec{r}_n) \right) \right\rangle_r, \tag{3.106}$$

where $\phi_{N+1} \equiv \phi_1$. Along with the same line as above, we can obtain the effective Hamiltonian (3.25).

Chapter 4

Effective Hamiltonian and VBS phases

In this chapter, we provide the connection between the effective Hamiltonian (3.24) derived in Sec. 3.2.2,

$$H_{\text{eff}} = \frac{v_0}{2\pi}\int dx \left[K_0(\partial_x\Theta_0)^2 + \frac{1}{K_0}(\partial_x\Phi_0)^2\right] + g_{\text{eff}}\int dx \cos(\sqrt{2N}\Phi_0), \tag{4.1}$$

and various VBS phases realized in one-dimensional spin systems. In particular, we focus on that different signs of the coupling constant g_{eff} are related to different VBS phases separated by a quantum phase transition. We first review the case of two-leg spin-1/2 ladders in Sec. 4.1, where the effective Hamiltonian description of the Haldane and rung-singlet phases is quite natural, thanks to a decoupling properties of the bosonized Hamiltonian with two bosonic fields. In the remaining sections, we provide examples of spin chains with integer spin (Sec. 4.2), spin-1/2 ladder with even legs (Sec. 4.3), and spin ladders with dimerization (Sec. 4.4). In those models, the effective Hamiltonian description of VBS phases is justified by simple perturbative arguments.

4.1 Review: Two-leg ladder

As a simplest example, we consider a two-leg spin-1/2 ladder,

$$\begin{aligned} H = J\sum_i\sum_{j=1,2}&\left(s^x_{i,j}s^x_{i+1,j} + s^y_{i,j}s^y_{i+1,j} + \Delta s^z_{i,j}s^z_{i+1,j}\right)\\ &+\sum_i\left[J^{xy}_\perp\left(s^x_{i,1}s^x_{i,2} + s^y_{i,1}s^y_{i,2}\right) + J^z_\perp s^z_{i,1}s^z_{i,2}\right]\\ &+\sum_i\left[J^{xy}_\times\left(s^x_{i,1}s^x_{i+1,2} + s^x_{i,2}s^x_{i+1,1} + s^y_{i,1}s^y_{i+1,2} + s^y_{i,2}s^y_{i+1,1}\right) + J^z_\times\left(s^z_{i,1}s^z_{i+1,2} + s^z_{i,2}s^z_{i+1,1}\right)\right], \end{aligned} \tag{4.2}$$

as depicted in Fig. 4.1. For $J^{xy}_\times = J^z_\times = 0$, the model is a conventional ladder and studied in Refs. [72–83]. In particular, if $\Delta = 1$ and $J^{xy}_\perp = J^z_\perp > 0$, the ground state is in the rung-singlet phase that is unique and has a finite excitation gap. On the other hand, as discussed in Sec. 3.1.2, if we set

$$J^{xy}_\perp = 0, \quad J^z_\perp = 2D_z, \quad J^{xy}_\times = J, \quad J^z_\times = J\Delta, \tag{4.3}$$

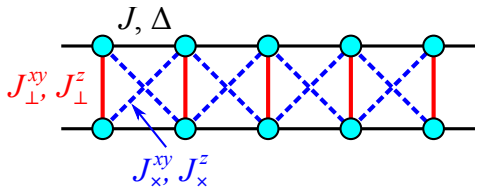

Figure 4.1: Two-leg spin-1/2 ladder given by Eq. (4.2).

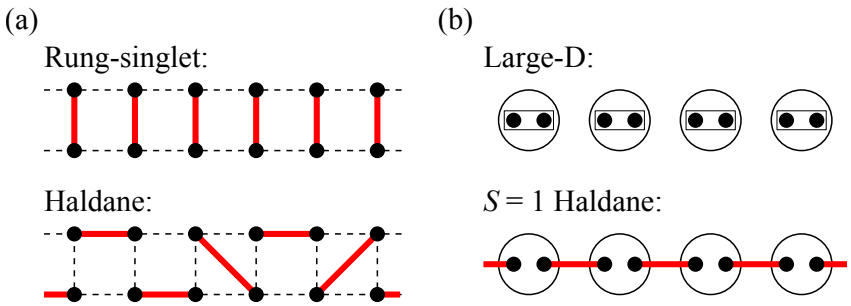

Figure 4.2: Schematic pictures of VBS phases in (a) the two-leg spin-1/2 ladder and (b) the spin-1 chain. The black dot represents a spin-1/2 and the black circle means the symmetrization of enclosed spin-1/2's. Two spin-1/2's linked by the red solid line form a singlet, while spin-1/2's enclosed by the black rectangle are frozen to the $S^z = 0$ state.

this model corresponds to the $S = 1$ XXZ chain with uniaxial anisotropy,

$$H = \sum_i \left[J(S_i^x S_{i+1}^x + S_i^y S_{i+1}^y + \Delta S_i^z S_{i+1}^z) + D_z (S_i^z)^2 \right], \tag{4.4}$$

through the ladder mapping. The model (4.4) has been extensively studied [9, 17, 53, 54, 56, 57, 91, 92, 115] and there are two VBS phases (see Fig. 2.4). One is the Haldane phase locating around the Heisenberg point ($\Delta = 1$ and $D_z = 0$), and the other is the large-D phase stabilized for sufficient for sufficiently large D_z. The large-D phase is corresponding to the rung-singlet phase in the two-leg ladder model (4.2). Those VBS phases are illustrated in Fig. 4.2.

A general principle to distinguish two different VBS phases is to count the number of singlet bonds N_b under a certain spatial cut. If we choose the cut perpendicular to the ladder or chain in Fig. 4.2, the rung-singlet or large-D phase has $N_b = 0$ while the Haldane phase has $N_b = 1$. Even if we consider some local move of singlets, this does not affect the parity of N_b unless unpaired spin-1/2's are created; in general, the former phase has even N_b while the latter has odd N_b. This parity of N_b is changed only when a phase transition occurs, so that the phase transition is necessary between two VBS phases with different parities of N_b. In the SU(2)-symmetric ladder model (4.2) with $\Delta = 1$, $J_\perp^{xy} = J_\perp^z$, and $J_\times^{xy} = J_\times^z$, a direct phase transition from the Haldane phase to the rung-singlet phase has been observed [116–121]. There is also a transition between the Haldane and large-D phases in the spin-1 XXZ chain (4.4) [17, 53, 54, 56, 91].

4.1.1 Bosonization of two-leg ladder

Here we demonstrate that those phase transitions between VBS phases are faithfully described by the bosonization approach [17, 72, 73, 77, 117]. Following the procedure in Sec. 3.2.1, the

Hamiltonian (4.2) is bosonized as

$$
\begin{aligned}
H \approx \frac{v}{2\pi}\int dx \sum_{j=1,2}\left[K(\partial_x\theta_j)^2 + \frac{1}{K}(\partial_x\phi_j)^2\right] \\
+\int dx \Big[g_0\partial_x\phi_1\partial_x\phi_2 + g_1\cos\sqrt{2}(\phi_1+\phi_2) + g_2\cos\sqrt{2}(\phi_1-\phi_2) + g_3\cos\sqrt{2}(\theta_1-\theta_2) \\
+g_4\cos\sqrt{2}(\phi_1+\phi_2)\cos\sqrt{2}(\theta_1-\theta_2) + g_5\cos\sqrt{2}(\phi_1-\phi_2)\cos\sqrt{2}(\theta_1-\theta_2)\Big],
\end{aligned}
\tag{4.5}
$$

where v and K are given in Eq. (3.12) and the coupling constants are given by

$$
\begin{aligned}
g_0 &= \frac{a_0}{2\pi^2}(J_\perp^z + 2J_\times^z), & g_1 &= -\frac{a_1^2}{2a_0}(J_\perp^z - 2J_\times^z), & g_2 &= \frac{a_1^2}{2a_0}(J_\perp^z - 2J_\times^z), \\
g_3 &= \frac{b_0^2}{a_0}(J_\perp^{xy} - 2J_\times^{xy}), & g_4 &= \frac{b_1^2}{2a_0}(J_\perp^{xy} + 2J_\times^{xy}), & g_5 &= -\frac{b_1^2}{2a_0}(J_\perp^{xy} + 2J_\times^{xu}).
\end{aligned}
\tag{4.6}
$$

As seen obviously, this Hamiltonian is simplified by introducing the center-of-mass and relative fields,

$$
\begin{aligned}
\Phi_0 &= \frac{1}{\sqrt{2}}(\phi_1+\phi_2), & \Theta_0 &= \frac{1}{\sqrt{2}}(\theta_1+\theta_2), \\
\Phi_1 &= \frac{1}{\sqrt{2}}(\phi_1-\phi_2), & \Theta_1 &= \frac{1}{\sqrt{2}}(\theta_1-\theta_2).
\end{aligned}
\tag{4.7}
$$

Then the Hamiltonian (4.5) is rewritten as

$$H \approx H_0 + H_1 + H_{01}, \tag{4.8}$$

$$H_0 = \frac{v_0}{2\pi}\int dx\left[K_0(\partial_x\Theta_0)^2 + \frac{1}{K_0}(\partial_x\Phi_0)^2\right] + g_1\int dx\cos(2\Phi_0), \tag{4.9}$$

$$H_1 = \frac{v_1}{2\pi}\int dx\left[K_1(\partial_x\Theta_1)^2 + \frac{1}{K_1}(\partial_x\Phi_1)^2\right] + g_2\int dx\cos(2\Phi_1) + g_3\int dx\cos(2\Theta_1), \tag{4.10}$$

$$H_{01} = g_4\int dx\cos(2\Phi_0)\cos(2\Theta_1). \tag{4.11}$$

Here the effect of g_0 is incorporated in the renormalizations of v and K as

$$
\begin{aligned}
v_0 &= v\left(1 + \frac{K(J_\perp^z + 2J_\times^z)a_0}{2\pi v}\right)^{1/2}, & K_0 &= \left(1 + \frac{K(J_\perp^z + 2J_\times^z)a_0}{2\pi v}\right)^{-1/2}, \\
v_1 &= v\left(1 - \frac{K(J_\perp^z + 2J_\times^z)a_0}{2\pi v}\right)^{1/2}, & K_1 &= \left(1 - \frac{K(J_\perp^z + 2J_\times^z)a_0}{2\pi v}\right)^{-1/2},
\end{aligned}
\tag{4.12}
$$

and we dropped the g_5 term since it is irrelevant. Unless some fine tuning of the parameters makes $g_1 = g_2 = g_3 = 0$, g_4 is always less relevant than these three couplings. Thus in general, we can neglect H_{01} and regard that the Hamiltonian H_0 and H_1 are decoupled. H_0 is nothing but what we refer to the effective Hamiltonian H_{eff} in the previous chapter.

4.1.2 Symmetry-breaking phases

Although, to describe VBS phases, we need to assume that g_1 and g_3 are relevant, we first consider the case when g_1 and g_2 are relevant. In this case, the ground state breaks some

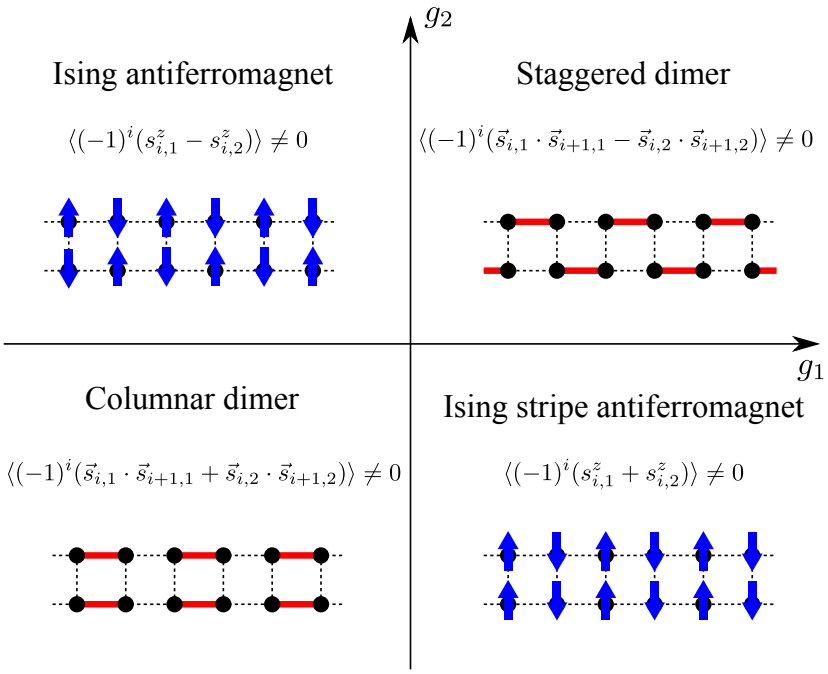

Figure 4.3: Phase diagram of the Hamiltonian (4.8) in the g_1-g_2 plane. Corresponding order parameters and schematic pictures of the ground state are also shown.

$\mathbb{Z}_2$ symmetry and becomes two-fold degenerate. If g_1 and g_2 reach the strong-coupling limits under the renormalization group, we can semiclassically evaluate the Hamiltonian (4.8) by minimizing the potential energies with respect to Φ_0 and Φ_1. Depending on the signs of g_1 and g_2, we will find the following four phases (see Fig. 4.3):

(i) $g_1 < 0$ and $g_2 > 0$ — *Ising antiferromagnetic phase*

In this phase, the potential energies are minimized by setting $\cos(2\Phi_0) = 1$ and $\cos(2\Phi_1) = -1$. Let us choose one of the potential minima $\Phi_1 = \pi(p_1 + 1/2)$, $p_1 \in \mathbb{Z}$. This fixes the compactification radius of Φ_0 defined through $\Phi_0 \sim \Phi_0 + 2\pi R$ to $R = 1$, as discussed in Sec. 3.3.1. Thus we find two independent solutions of $\cos(2\Phi_0) = 1$ within this radius: $\Phi_0 = 0$ or π mod 2π. This leads to the two-fold degeneracy of the ground state. Spontaneous symmetry breaking in the ground state is characterized by a staggered magnetization,

$$\langle(-1)^i(s^z_{i,1} - s^z_{i,2})\rangle \propto \langle\cos\Phi_0 \sin\Phi_1\rangle = \pm 1, \tag{4.13}$$

which takes a finite expectation value. This order parameter indicates an antiferromagnetic order in the z direction.

(ii) $g_1 > 0$ and $g_2 < 0$ — *Ising stripe antiferromagnetic phase*

The potential energies are minimized by setting $\cos(2\Phi_0) = -1$ and $\cos(2\Phi_1) = 1$. Then we find their solutions, $\Phi_0 = \pi(p_0 + 1/2)$ and $\Phi_1 = \pi p_1$ with $p_0, p_1 \in \mathbb{Z}$. However, as discussed above, two of them are independent and correspond to the two-fold degenerate ground state. The associated order parameter is given by another type of the staggered magnetization,

$$\langle(-1)^i(s^z_{i,1} + s^z_{i,2})\rangle \propto \langle\sin\Phi_0 \cos\Phi_1\rangle = \pm 1. \tag{4.14}$$

This also indicates an antiferromagnetic order in the z direction but with a stripe pattern along the leg. This phase can realize in the spin-1 XXZ chain (4.4).

(iii) $g_1 > 0$ and $g_2 > 0$ — *Staggered dimer phase*

The minimization of the potential energies is achieved by setting $\cos(2\Phi_0) = -1$ and $\cos(2\Phi_1) = -1$. The solutions are given by $\Phi_0 = \pi(p_0 + 1/2)$ and $\Phi_1 = \pi(p_1 + 1/2)$ with $p_0, p_1 \in \mathbb{Z}$. But two of them, say $\Phi_0 = \pi/2$ and $\Phi_1 = \pm\pi/2$, are independent. The corresponding order parameter is the staggered dimerization given by

$$\langle (-1)^i (\vec{s}_{i,1} \cdot \vec{s}_{i+1,1} - \vec{s}_{i,2} \cdot \vec{s}_{i+1,2}) \rangle \propto \langle \sin\Phi_0 \sin\Phi_1 \rangle = \pm 1. \tag{4.15}$$

(See Sec. 4.4 for the dimerization operator in the bosonic language.) This detects the dimer (singlet) formation on the legs and indicates that one-site translational invariance is spontaneously broken. Again, the ground state becomes two-fold degenerate.

(iv) $g_1 < 0$ and $g_2 < 0$ — *Columnar dimer phase*

The potential energies are minimized by choosing $\cos(2\Phi_0) = 1$ and $\cos(2\Phi_1) = 1$. This conditions are solved as $\Phi_0 = \pi p_0$ and $\Phi_1 = \pi p_1$ with $p_0, p_1 \in \mathbb{Z}$. Similarly, two independent solutions, say $\Phi_0 = 0$ and $\Phi_1 = 0, \pi$, lead to the two-fold degenerate ground state. The corresponding order parameter is the columnar dimerization,

$$\langle (-1)^i (\vec{s}_{i,1} \cdot \vec{s}_{i+1,1} + \vec{s}_{i,2} \cdot \vec{s}_{i+1,2}) \rangle \propto \langle \cos\Phi_0 \cos\Phi_1 \rangle = \pm 1, \tag{4.16}$$

which detects the one-site translational symmetry breaking. However, the pattern of singlets is different from the above case; here two singlets live on the same link.

Thus for the case of the two-leg ladder, the ground state breaks (at least) one-site translational invariance when both g_1 and g_2 are relevant. This will also be true for general N-leg ladders. If all the fields Φ_0 and Φ_ν are pinned, it generally implies that the ground state has some nonzero expectation values of the staggered magnetization and/or dimerization, since those operators are written as vertex operators of ϕ_j that is a linear combination of Φ_0 and Φ_ν. Thus one-site translational symmetry is spontaneously broken in the ground state. However, if g_3 is relevant, instead of g_2, such vertex operators involve fluctuating fields Φ_ν and cannot have nonzero expectation values. Therefore the assumption made in Sec. 3.2.2, that g_1 and g_3 are relevant, is justified to avoid the spontaneous symmetry breaking.

We note that, in the parameter space of Eq. (4.2), only the second and forth quadrants in Fig, 4.3 (i.e. the antiferromagnetic phases) are realized. However, we can also reproduce the dimer phases by careful consideration of an irrelevant term and higher-order perturbations [120–122] or by inclusion of a four-body interaction $(\vec{s}_{i,1} \cdot \vec{s}_{i+1,1})(\vec{s}_{i,2} \cdot \vec{s}_{i+1,2})$ [123–125].

4.1.3 VBS phases

Now we consider the case when g_1 and g_3 are relevant, as discussed in Sec. 3.2.2. In this phase, the ground state has no symmetry breaking and thus is unique. Again, the ground state properties can be understood by semiclassical treatments of the vertex operators as potential energies, that is, the minimization of $g_1 \cos(2\Phi_0)$ and $g_3 \cos(2\Theta_1)$. Depending on the signs of g_1 and g_3, we obtain the following four phases (see Fig. 4.4):

(i) $g_1 < 0$ and $g_3 > 0$ — *Rung-singlet phase*

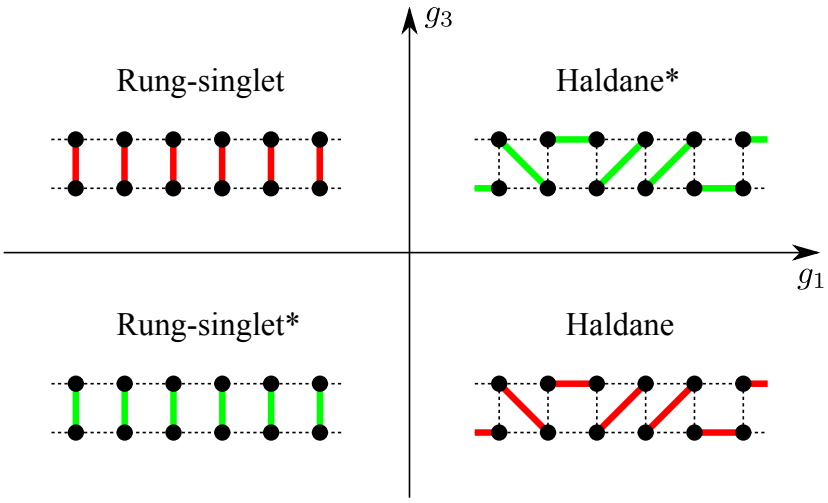

Figure 4.4: Phase diagram of the Hamiltonian (4.8) in the g_1-g_3 plane. The red solid line represents a usual singlet bond $(|\uparrow\downarrow\rangle - |\downarrow\uparrow\rangle)/\sqrt{2}$, while the green one represents a twisted singlet bond $(|\uparrow\downarrow\rangle + |\downarrow\uparrow\rangle)/\sqrt{2}$.

The potential energies are minimized by setting $\cos(2\Phi_0) = 1$ and $\cos(2\Theta_1) = -1$. Now the solution, say $\Phi_0 = 0$ and $\Theta_1 = \pi/2$, is unique within the compactification radii. Since there is no symmetry breaking, any local order parameter cannot characterize this phase. Instead, we can use a nonlocal (string) order parameter [117],

$$\mathcal{O}_{\text{even}} = -\lim_{|k-l|\to\infty} (s^z_{k,1} + s^z_{k+1,2}) \exp\left[i\pi \sum_{j=k+1}^{l-1} (s^z_{j,1} + s^z_{j+1,2}) \right] (s^z_{l,1} + s^z_{l+1,2}), \tag{4.17}$$

and a careful derivation shows that [126]

$$\langle \mathcal{O}_{\text{even}} \rangle \propto \lim_{|x-y|\to\infty} \langle \cos(\Phi_0(x)) \cos(\Phi_0(y)) \rangle = 1. \tag{4.18}$$

This order parameter takes a finite expectation value when the number of singlets N_b under a perpendicular cut is even [117]. A similar order parameter is also proposed in Ref. [127].

(ii) $g_1 > 0$ and $g_3 < 0$ — *Haldane phase*

The potential energies are minimized by setting $\cos(2\Phi_0) = -1$ and $\cos(2\Theta_1) = 1$. Here the solution, say $\Phi_0 = \pi/2$ and $\Theta_1 = 0$, is unique within the compactification radii. This phase is characterized by another type of string order parameters,

$$\mathcal{O}_{\text{odd}} = -\lim_{|k-l|\to\infty} (s^z_{k,1} + s^z_{k,2}) \exp\left[i\pi \sum_{j=k+1}^{l-1} (s^z_{j,1} + s^z_{j,2}) \right] (s^z_{l,1} + s^z_{l,2}), \tag{4.19}$$

and it is shown that [80, 126]

$$\langle \mathcal{O}_{\text{odd}} \rangle \propto \lim_{|x-y|\to\infty} \langle \sin(\Phi_0(x)) \sin(\Phi_0(y)) \rangle = 1. \tag{4.20}$$

This is a straightforward generalization of the conventional string order parameter in the spin-1 AKLT phase [9–11] to ladder systems. Thus a nonzero expectation value of $\mathcal{O}_{\rm odd}$ indicates a VBS phase whose number of singlets N_b under a perpendicular cut is odd. Furthermore, at the SU(2) symmetric point, it has been shown that a spin-1/2 state appears at the end of a semi-infinite chain through the Majorana fermion mapping [81]. This edge state is responsive to the uniform magnetic fined in any direction [81],

$$\left\langle s^\alpha_{i,1} + s^\alpha_{i,2} \right\rangle \approx \frac{2m_t}{v_t} e^{-2m_t x/v_t} \left\langle -\frac{i}{2}\epsilon^{\alpha\beta\gamma}\eta^\beta\eta^\gamma \right\rangle, \tag{4.21}$$

where m_t and v_t are the velocity and mass of the triplet excitation and η^α ($\alpha = x, y, z$) denotes a Majorana fermion operator. A quadratic operator in the parenthesis of the left-hand side is in fact a Majorana fermionic representation of the spin-1/2 operator [128]. This result tells us that the spin-1/2 moment localized at the chain end $x = 0$ appears in the spatial (uniform) magnetization profile, as known in the spin-1 AKLT state [12].

(iii) $g_1 < 0$ and $g_3 < 0$ — *Rung-singlet* phase*

The potential energies are minimized by setting $\cos(2\Phi_0) = 1$ and $\cos(2\Theta_1) = 1$. Thus, the string order parameter $\mathcal{O}_{\rm even}$ takes a finite expectation value, as in the rung-singlet phase. However, in this phase, a singlet wave function is not the usual one $(|\uparrow\downarrow\rangle - |\downarrow\uparrow\rangle)/\sqrt{2}$ but $(|\uparrow\downarrow\rangle + |\downarrow\uparrow\rangle)/\sqrt{2}$. If we go back to the original model (4.2), this is easily understood as follows. The usual rung-singlet phase is obtained by setting $J^{xy}_\perp = J^z_\perp \gg J$ and $J^{xy}_\times = J^z_\times = 0$. This phase (the rung-singlet* phase) is obtained by a canonical transformation only for spins on one leg, $s^{x,y}_{i,2} \to -s^{x,y}_{i,2}$. This flips the sign of $J^z_\perp$ and the singlet wave function on each rung should be interpreted as $(|\uparrow\downarrow\rangle + |\downarrow\uparrow\rangle)/\sqrt{2}$. The rung-singlet* phase corresponds to the large-D phase in the spin-1 chain, since the singlet wave function has $S = 1$ and $S^z = 0$.

(iv) $g_1 > 0$ and $g_3 > 0$ — *Haldane* phase*

The potential energies are minimized by setting $\cos(2\Phi_0) = -1$ and $\cos(2\Theta_1) = -1$. Thus, the string order parameter $\mathcal{O}_{\rm odd}$ takes a finite expectation value, as in the Haldane phase. But from the same reason as above, this phase is obtain by distributing the singlet $(|\uparrow\downarrow\rangle + |\downarrow\uparrow\rangle)/\sqrt{2}$ such that the number of singlets N_b under a perpendicular cut becomes odd. We call this phase as the Haldane* phase. A crucial difference from the Haldane phase appears in the response of edge states to the magnetic field. Here, the edge state only responds to the uniform magnetic field along the z axis,

$$\left\langle s^z_{i,1} + s^z_{i,2} \right\rangle \approx \frac{2m_t}{v_t} e^{-2m_t x/v_t} \left\langle -i\eta^x\eta^y \right\rangle. \tag{4.22}$$

But, it also responds to the antiparallel magnetic field along the x and y axes,

$$\left\langle s^\alpha_{i,1} - s^\alpha_{i,2} \right\rangle \approx \frac{2m_t}{v_t} e^{-2m_t x/v_t} \left\langle -\frac{i}{2}\epsilon^{\alpha\beta\gamma}\eta^\beta\eta^\gamma \right\rangle, \quad \alpha = x, y. \tag{4.23}$$

This is nothing but a consequence of the canonical transformation $s^{x,y}_{i,2} \to -s^{x,y}_{i,2}$ from the usual Haldane phase.

All the four phases have no symmetry breaking and no ground state degeneracy. Only ways to characterize those phases are nonzero expectation values of the nonlocal order parameter or the appearance of the edge states. This originates from the difference in the parity

of the number of singlets under a cut between the rung-singlet and Haldane phases. In fact, the distinction between the rung-singlet and Haldane (or the rung-singlet* and Haldane*) phases is hold only under some symmetries, as we will see in the next chapter. Once those symmetries are broken, those phases are smoothly connected without any phase transition. An obvious phase transition at $g_1 = 0$ is owing to those symmetries. We note that, even if g_1 vanishes, g_4 can be marginally relevant and lead to the first-order transition [117]. If g_4 is irrelevant at $g_1 = 0$, the phase transition between the two VBS phases becomes a continuous one.

Finally, we mention whether the rung-singlet and rung-singlet* phases or the Haldane and Haldane* phases are really distinguished. This is true at least when the Hamiltonian has a Z_2 symmetry corresponding to the interchange of two legs $j = 1$ and 2. [1] In the bosonic language, this symmetry operation transforms the relative bosonic field as $\Phi_1 \to -\Phi_1$ and $\Theta_1 \to -\Theta_1$. In Eq. (4.8), this Z_2 symmetry forbids the $\sin(2\Theta_1)$ term; if this term is allowed, two potential minima $\Theta_1 = 0$ and $\pi/2$ can be smoothly connected. (A similar discussion based on the bosonization will be given in Chapter 5.) If this additional Z_2 symmetry is absent, the two rung-singlet phases (or the two Haldane phases) are merged. But it does not affect the distinction between the rung-singlet and Haldane phases. On the effective Hamiltonian (3.24), this Z_2 symmetry does not appear and not affect the phase transition as g_{eff} varies.

4.2 XXZ chain with integer spin

We here consider an XXZ chain with integer spin S and an on-site uniaxial anisotropy,

$$H = \sum_i \left[J(S_i^x S_{i+1}^x + S_i^y S_{i+1}^y + \Delta S_i^z S_{i+1}^z) + D_z (S_i^z)^2 \right]. \tag{4.24}$$

We already discussed the $S = 1$ case in the previous section, where the effective Hamiltonian description by Eq. (3.24) is justified from the decoupling property of the bosonized Hamiltonian (4.8). A Gaussian phase transition between the large-D and Haldane phases is naturally expected in Eq. (4.9) at $g_1 = 0$. This transition has been numerically confirmed by several studies [53, 54, 56, 57].

For $S = 2$, the phase diagram of this model has also been studied [17, 58, 129–133]. The $S = 2$ Haldane phase exists for $\Delta = 1$ and $D_z = 0$ and is schematically understood as a VBS phase with two singlet bonds between neighboring sites [see Fig. 4.5 (b)]. For $D_z \gg J$, the ground state will be in the large-D phase that is adiabatically connected to a direct product of the $S^z = 0$ states. As opposed to the $S = 1$ case, recent careful numerical simulations have indicated that there is no phase transition between these phases [58, 133, 134]. Thus, for $S = 2$, the Haldane and large-D phases essentially belong to the same phase (see Fig. 2.4).

[1] More precisely, as discussed in Ref. [83], the distinction between the rung-singlet and rung-singlet* phases is protected by the Z_2 symmetry associated with the interchange of the legs and one-site translational invariance. In the language of the group cohomology classification [29], this distinction comes from the fact that the two phases take different elements of the first-group cohomology $H^1(Z_2, U(1)) = \mathbb{Z}_2$ (or equivalently, one-dimensional representations of Z_2) in a proper unit-cell. This is most easily seen in an extreme situation where the ground state is just a direct product of singlets on each rung (corresponding to a *fixed-point tensor*). The two singlets $(|\uparrow\downarrow\rangle - |\downarrow\uparrow\rangle)/\sqrt{2}$ and $(|\uparrow\downarrow\rangle + |\downarrow\uparrow\rangle)/\sqrt{2}$ obviously take different one-dimensional representations on each rung. On the other hand, the distinction between the Haldane and Haldane* phases is protected by the $\mathcal{D}_2$ and Z_2 symmetries. This comes from the fact that the two phases are associated with different elements of the second group cohomology $H^2(\mathcal{D}_2 \times Z_2, U(1)) = \mathbb{Z}_2^3$ (or equivalently, projective representations of $\mathcal{D}_2 \times Z_2$). This is related to representations of the $\mathcal{D}_2 \times Z_2$ symmetry on the edge states.

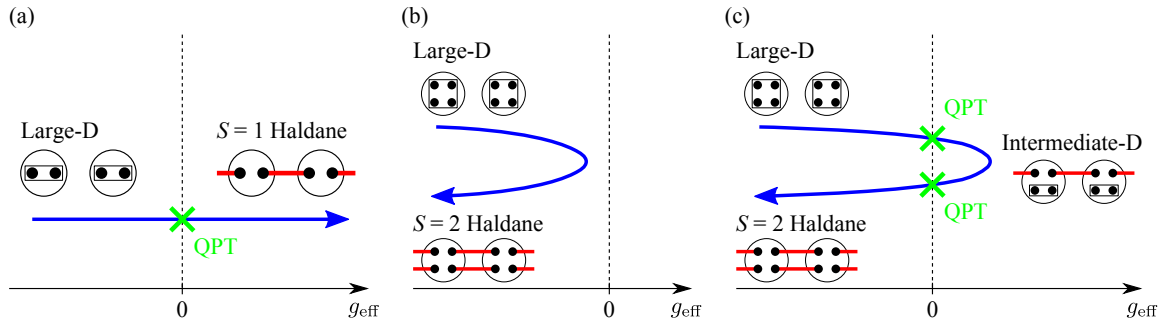

Figure 4.5: Phase diagrams of the effective Hamiltonian (3.24) on the $g_{\rm eff}$ line. The blue arrow represents an evolution of the parameters of the XXZ chain (4.24). If this arrow intersects the dashed line on which $g_{\rm eff} = 0$, the system undergoes a quantum phase transition that is marked by the green cross. (a) For $S = 1$, the blue arrow corresponds to the variation of D_z. For $S = 2$, there are two scenarios, depending on the choice of parameter paths: (b) the arrow does not intersect the $g_{\rm eff} = 0$ line, or (c) the arrow intersects the $g_{\rm eff} = 0$ line twice and undergoes an intermediate phase.

Such a difference between the $S = 1$ and $S = 2$ Haldane phases is generally recognized as the difference between the odd-S and even-S Haldane phases. The simple argument based on the number of singlets N_b under a cut suggests that the odd-S Haldane phase has odd N_b while the even-S Haldane phase has even N_b. Since the large-D phase has $N_b = 0$, we expect that the odd-S Haldane phase is separated from the large-D phase but the even-S Haldane phase is not.

Following the instruction in Sec. 3.2.2, this fact can be seen at the level of the effective Hamiltonian (3.24). Through the ladder mapping, the initial coupling g_1 is given by

$$g_1 = \frac{a_1^2}{a_0}(J\Delta - D_z). \tag{4.25}$$

In general, we cannot rely on the decoupling property of the Hamiltonian as seen in the $S = 1$ case. Thus, we assume that $\Delta \lesssim 1$ so that g_3 is most relevant and the relative fields can be integrated out. Applying S-th order perturbation theory, we obtain the effective Hamiltonian (3.24) with the coupling constant [17],

$$g_{\rm eff} \sim -A(D_z - J\Delta)^S, \tag{4.26}$$

where A is a nonuniversal constant. As demonstrated in Appendix 3.B, it is sensible to suppose that the prefactor A always takes some *positive* value.

If the effective coupling $g_{\rm eff}$ is relevant, the effective Hamiltonian leads to a unique gapped ground state without any symmetry breaking. We expect that this gapped ground state corresponds to the Haldane phase around $D_z = 0$ while the large-D phase for $D_z \gg J$. For odd S, increasing D_z from zero, the coupling constant $g_{\rm eff}$ can change its *sign*, since the power of $(D_z - J\Delta)$ is an odd integer. Thus, the Haldane and large-D phases are naturally identified as the $g_{\rm eff} > 0$ and $g_{\rm eff} < 0$ regimes, respectively, and there necessarily exists a Gaussian transition at $g_{\rm eff} = 0$ between those phases. For $S = 1$, a phase diagram on the $g_{\rm eff}$ line is shown in Fig. 4.5 (a). On the other hand, for even S, the coupling constant $g_{\rm eff}$ never changes its sign by increasing D_z; the Haldane and large-D phases share the same strong-coupling fixed point $g_{\rm eff} \to -\infty$ and belong to the same phase. From Eq. (4.26), it

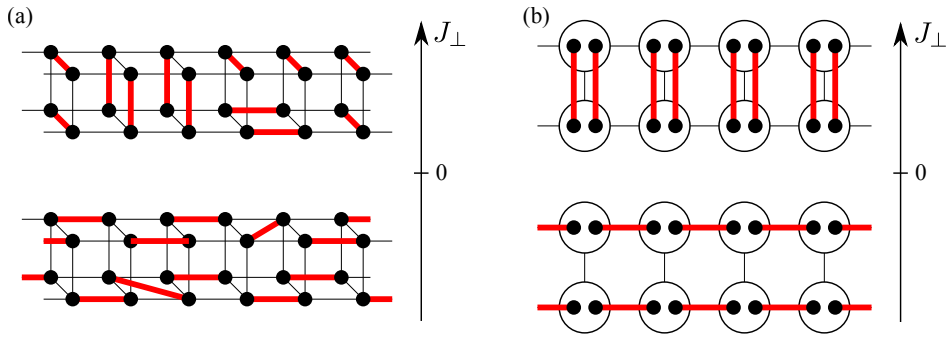

Figure 4.6: Typical configurations of the VBS phases realized in (a) the four-leg tube (4.27) and (b) the two-coupled spin-1 chains (4.29) by varying $J_\perp$.

appears that there is a gapless point at $D_z = J\Delta$, as predicted in Ref. [17]. But a finite g_{eff} is also generated from the coupling $g_4 \propto J$ and will open up a gap [97,98]. For $S = 2$, this is schematically explained in Fig. 4.5 (b).

From this observation, we expect that the odd-S Haldane phase has the different sign of g_{eff} from that of the large-D phase. Hence, there must be a Gaussian phase transition between those phases since we need to pass through the point $g_{\text{eff}} = 0$. In contrast, the even-S Haldane phase and the large-D phase share the same sign of g_{eff}. Thus they essentially belong to the same phase. A similar argument has been done by Nonne *et. al.* [108] in the context of 1D multi-component Hubbard models.

We also refer to the existence of the so-called intermediate-D phase [61], which is a realization of the spin-1 Haldane phase on spin-2 chains with uniaxial anisotropies. This phase is separated from the spin-2 Haldane and large-D phases [see Fig. 4.5 (c)]. Recent numerical simulations on the Hamiltonian (4.24) showed that it is absent [133] or restricted in a quite narrow region on the parameter space [58, 134]. At the level of the effective Hamiltonian, this subtlety on its existence can be seen from that it requires higher-order perturbations to change the sign of g_{eff}. However, once we introduce a quartic uniaxial anisotropy $D_4 \sum_i (S_i^z)^4$, the intermediate-D phase is stabilized for a broad range of D_4 [133,135]. Since D_4 contributes to g_{eff} at the first order, it is relatively easy to make the sign of g_{eff} positive, corresponding to the intermediate-D phase. This also provides a strong evidence that the sign of the effective coupling g_{eff} determines how VBS phases are distinguished, even for $S > 1$.

4.3 Spin tube with even legs

As the second example, we consider an N-leg spin tube with spin-1/2,

$$H = \sum_i \sum_{j=1}^{N} \left[J \vec{s}_{i,j} \cdot \vec{s}_{i+1,j} + J_\perp \vec{s}_{i,j} \cdot \vec{s}_{i,j+1} \right]. \tag{4.27}$$

We here consider the even N case. The ground state is in the rung-singlet phase for $J_\perp > 0$, which is smoothly connected to the direct product of singlet states formed on each rung, while in the spin-$N/2$ Haldane phase for $J_\perp < 0$. Qualitative properties of both phases can be understood in the strong-coupling limit $J_\perp \to \pm\infty$. Schematic picture of these phases are shown in Fig. 4.6 (a) for $N = 4$.

Again, as in the previous example of the XXZ chain, we can see the difference between the odd-$N/2$ and even-$N/2$ Haldane phases in terms of the sign of the effective coupling constant,

$$g_{\text{eff}} \sim -A'(J_\perp)^{N/2}, \tag{4.28}$$

where A' is a positive nonuniversal constant. For $N \in 4\mathbb{N}-2$, the rung-singlet phase takes the negative sign of g_{eff} whereas the Haldane phase takes the opposite sign. This indicates that the rung-singlet and odd-$N/2$ Haldane phases belong to the different phases separated by a quantum phase transition. On the other hand, for $N \in 4\mathbb{N}$, the rung-singlet and even-$N/2$ Haldane phases always share the same sign of g_{eff} and thus belong to the same phase.

In this model, to go from the $J_\perp < 0$ region to the $J_\perp > 0$ region, we have to pass through an obvious critical point at $J_\perp = 0$, corresponding to the N decoupled critical chains. However, whenever we take some continuous path of parameters, we have to observe a phase transition between the odd-$N/2$ Haldane and rung-singlet phases, according to the change of the sign of g_{eff} in the effective Hamiltonian (3.24). As we previously discussed, such nontrivial phase transitions have been observed for $N = 2$ by introducing a diagonal exchange coupling [116–121] or a uniaxial anisotropy [83]. In contrast, we can find some path that connects the even-$N/2$ Haldane and rung-singlet phases without gap closing. In the spin tube (4.27) with $N \geq 4$, a direct observation of this adiabatic continuity has not been reported. Instead, in the two-coupled spin-1 chains,

$$H = J \sum_i \sum_{j=1,2} \vec{T}_{i,j} \cdot \vec{T}_{i+1,j} + J_\perp \sum_i \vec{T}_{i,1} \cdot \vec{T}_{i,2}, \tag{4.29}$$

(here $\vec{T}_{i,j}$ is the spin-1 operator), the absence of the phase transition between the spin-2 Haldane and rung-singlet phases [see Fig. 4.6 (b)] has been observed [18, 127, 136]. This is again explained in terms of the effective Hamiltonian (3.24) through the ladder mapping: the effective coupling g_{eff} does not change its sign since it takes the form $g_{\text{eff}} \sim -A_0 J^2 - A_1 J_\perp^2$ with positive constants A_0 and A_1.

4.4 Dimerized spin ladder

The third example of interest is an open spin ladder with explicit dimerizations. As an example, we consider the N-leg spin ladder (4.27) with a "columnar" dimerization,

$$H' = \delta \sum_i \sum_{j=1}^{N} (-1)^i \vec{s}_{i,j} \cdot \vec{s}_{i+1,j}. \tag{4.30}$$

This term breaks both odd-site translational invariance and site-centered inversion symmetry. This external symmetry breaking does not affect the effective Hamiltonian for even N but does for odd N. It allows the vertex operator $\cos(\sqrt{2N}\Phi_0)$ to be added to the effective Hamiltonian (3.25). Therefore, we can here deal with both the odd-N and even-N cases in the same effective Hamiltonian (3.24).

Since the dimerization operator is bosonized as [99, 100]

$$(-1)^i \vec{s}_{i,j} \cdot \vec{s}_{i+1,j} \approx d \cos(\sqrt{2}\phi_j), \tag{4.31}$$

where d is a nonuniversal constant [125], Eq. (4.30) is bosonized as

$$H' \approx d\delta \sum_{j=1}^{N} \int dx \cos(\sqrt{2}\phi_j). \tag{4.32}$$

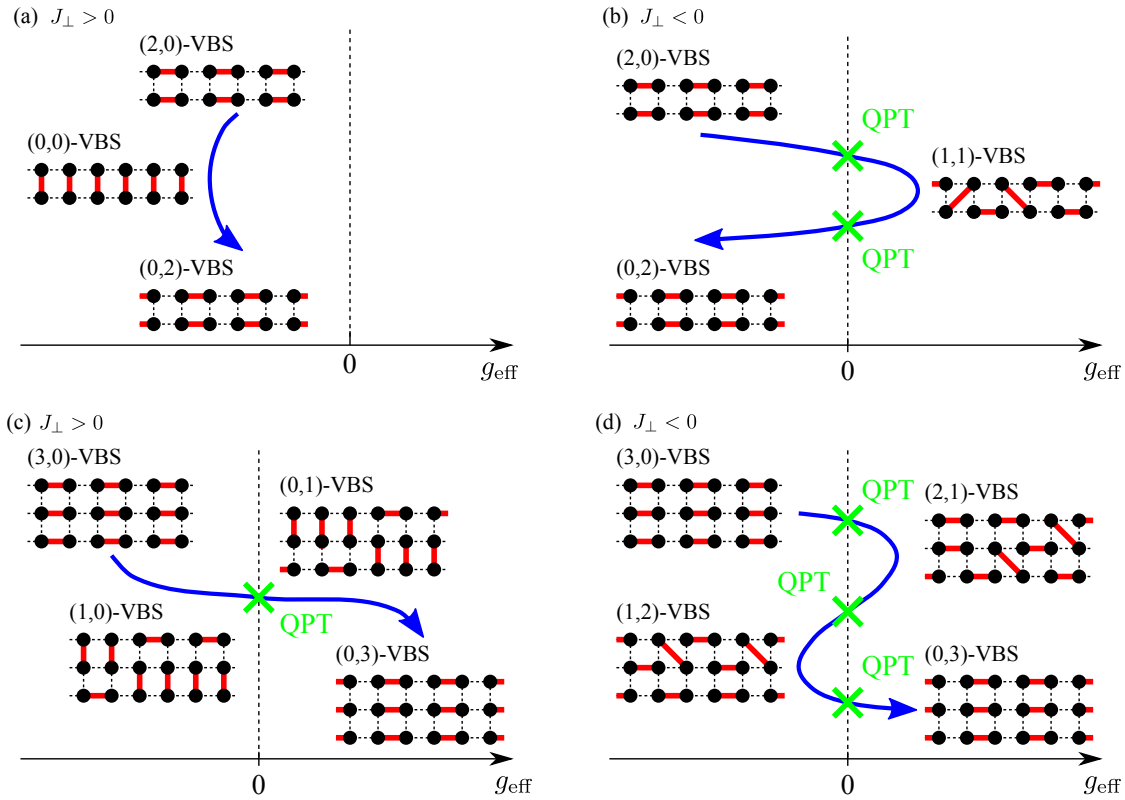

Figure 4.7: Phase diagrams of the effective Hamiltonian (3.24) on the $g_{\rm eff}$ line, corresponding to the open spin ladders with the columnar dimerization (4.30). The blue arrow represents an evolution of the dimerization parameter δ from $-\infty$ to $+\infty$ Each panel corresponds to (a) $N = 2$, $J_\perp > 0$, (b) $N = 2$, $J_\perp < 0$, (c) $N = 3$, $J_\perp > 0$, and (d) $N = 3$, $J_\perp < 0$.

For $N = 2$, the dimerization contributes to the effective coupling $g_{\rm eff}$ as [137]

$$g_{\rm eff} \sim -J_\perp - B\delta^2, \tag{4.33}$$

where B is a positive nonuniversal coefficient, according to a similar analysis in Appendix 3.B. This implies that, for $J_\perp > 0$, $g_{\rm eff}$ always takes negative values, and thus no phase transition is expected by varying δ. As illustrated in Fig. 4.7 (a), this follows that the parity of the number of singlets N_b under a cut does not change during the evolution of δ. If we denote a VBS phase as the (m, n)-VBS phase, which is adiabatically connected to the state with m singlets on each odd bond and n singlets on each even bond, we obtain the $(2, 0)$-VBS phase in the limit $\delta \to -\infty$ while the $(0, 2)$-VBS phase in the opposite limit $\delta \to \infty$. These phases share the same parities of m and n as the $(0, 0)$-VBS phase, i.e. the rung-singlet phase. On the other hand, for $J_\perp < 0$, we have to pass through the $(1, 1)$-VBS phase ($S = 1$ Haldane phase) between the $(2, 0)$-VBS and $(0, 2)$-VBS phases; thus we expect two phase transitions driven by the strong dimerization [138–140], as depicted in Fig. 4.7 (b).

For $N = 3$, the effective Hamiltonian takes the form of Eq. (3.24) by the dimerization and some VBS phases are expected to appear. The vertex operator in Eq. (3.24) is generated

from perturbations such as

$$\delta^3 \int dx_1 \int dx_2 \int dx_3 \cos(\sqrt{2}\phi_1(x_1)) \cos(\sqrt{2}\phi_2(x_2)) \cos(\sqrt{2}\phi_3(x_3)),$$
$$J_\perp \delta \int dx_1 \int dx_2 \cos\sqrt{2}(\phi_1(x_1) + \phi_2(x_1)) \cos(\sqrt{2}\phi_3(x_2)),$$

and therefore we obtain the effective coupling constant,

$$g_{\text{eff}} \sim B_0' J_\perp \delta + B_1' \delta^3, \tag{4.34}$$

with positive constants B_0' and B_1'. In the limits $\delta \to \pm\infty$, we obtain the $(0,3)$-VBS or $(3,0)$-VBS phases. For $J_\perp > 0$, we have only a single phase transition at $\delta = 0$ between these phases [see Fig. 4.7 (c)]. For $J_\perp < 0$, we can have two phase transitions at some finite value of δ, in addition to the trivial one at $\delta = 0$. These three phase transitions follow that, on the passage from the $(3,0)$-VBS to $(0,3)$-VBS phases, the ground state changes the parities of (m,n) three times, as illustrated in Fig. 4.7 (d). These results are consistent with numerical calculations [141–143].

We note that the behavior of a VBS phase under some spatial transformation is also reflected in the effective Hamiltonian (3.24). As expected, phase transitions between two VBS phases only occur when the parity of the number of singlets under a spatial cut is changed. Every VBS phase realized on the odd-N ladder changes this parity by odd-site translation or site-centered inversion. In the effective Hamiltonian (3.24), this boils down to the change of the sign of g_{eff}. By construction, the corresponding symmetry transformations in Table 3.1 indeed change the sign of g_{eff}, since $\cos(\sqrt{2N}\Phi_0)$ is odd under those transformations for odd N. This is not the case for even N; since the parity does not change under those transformation, g_{eff} is also not affected.

In general, the columnar dimerization (4.30) gives the following leading contributions to the effective coupling g_{eff}:

$$g_{\text{eff}} \sim \sum_{m=0}^{N/2} B_m J_\perp^{N/2-m} \delta^{2m}, \tag{4.35}$$

for even N, and

$$g_{\text{eff}} \sim \sum_{m=0}^{(N-1)/2} B_m' J_\perp^{(N-1)/2-m} \delta^{2m+1} \tag{4.36}$$

for odd N, where B_m and B_m' are positive nonuniversal constants. For $J_\perp < 0$, we can find at most N distinct solutions for $g_{\text{eff}} = 0$, although we have to determine the nonuniversal constants for the precise evaluation. This would coincide with the $2S$ phase transitions and the $2S+1$ VBS phases found in the dimerized spin-S chain [61, 109, 144–147]. The above discussion can also be applied to other shapes of the spin ladder and other configurations of the dimerization (e.g. staggered dimerization [139]).

Chapter 5

Symmetry protection of disordered phases

In Chapter 3, we derived an effective Hamiltonian for a large class of spin ladder models, which includes the spin-S chains through a ladder mapping. This Hamiltonian captures various essential properties of the spin ladders. In particular, it describes the phase transitions between VBS phases, as seen in Chapter 4. However, these phase are disordered and do not fit into the conventional classification based on the Landau theory.

In this chapter, we address that those phases are in fact protected by certain symmetries, based on the effective field theory (Sec. 5.1). Those symmetries are time reversal, bond-centered inversion, dihedral group of spin rotations, and site-centered inversion combined with a spin rotation. The first three are already known, but the last one is not. In Sec. 5.2, we propose a microscopic Hamiltonian that exhibits two different disordered phase protected by the combined inversion symmetry. We confirm that those phases are separated by a phase transition by perturbation theory and numerical simulations. We further prove the existence of such phases, based on the matrix-product state formalism without assuming translational invariance in Sec. 5.3. We also provide a brief review on the self-dual sine-Gordon models in Appendix. 5.A, which are used in Sec. 5.1.

5.1 Effective Hamiltonian and symmetry protection

Here, we address the consequence of symmetries for the effective Hamiltonian (3.24) and the distinction among VBS phases. The symmetries under consideration are listed in Table 3.1. We add some symmetry-breaking perturbation H' to the spin ladder model and consider the full Hamiltonian (3.1). However, H' is supposed to be small so that the effective Hamiltonian description with a single bosonic mode Φ_0 is still valid (i.e. g_3 is most relevant and the relative modes can be integrated out).

As discussed in Sec. 3.3, the effective Hamiltonians (3.24) and (3.25) were derived under the implicit assumption that all the symmetries in Table 3.1 and the U(1) spin-rotational symmetry exist. The effective Hamiltonian for even N, Eq. (3.24), gives VBS phases when g_{eff} is relevant, as demonstrated in the previous chapter. On the other hand, that for odd N, Eq. (3.25), only gives some symmetry-breaking ground state when g'_{eff} is relevant (see Sec. 3.4). To discuss the even-N and odd-N cases in the same ground, we assume that both odd-site translation invariance trs and site-centered inversion symmetry $\mathcal{I}_s$ are initially broken for the odd-N case, for example, by introducing a dimerization as demonstrated in

Sec. 4.4.

In the effective Hamiltonian (3.24), two distinct VBS phases are characterized by the different signs of g_{eff} and separated by an obvious phase transition at $g_{\text{eff}} = 0$. However, when some of symmetries are broken by introducing H', we can add new relevant vertex operators to the effective Hamiltonian (3.24), which may spoil the phase transition. In order to see the effects of symmetries on the distinction between two different VBS phases, we consider the stability of the phase transition between two gapped disordered phases associated with the different signs of g_{eff}, in the presence of such extra vertex operators. It will turn out that one of the following symmetries is sufficient to protect the distinction between two gapped phases with $g_{\text{eff}} > 0$ and $g_{\text{eff}} < 0$:

- time reversal $\mathcal{T}$,
- bond-centered inversion $\mathcal{I}_b$,
- dihedral group of spin rotations $\mathcal{D}_2$,
- site-centered inversion combined with a spin rotation by π, $\mathcal{I}_s \times \mathcal{R}_z$.

The first three are known to protect the Haldane phase and general VBS phases [13], whereas the last one is not understood to protect the VBS phases and discussed in Sec. 5.2.

5.1.1 With U(1) symmetry

We first consider the case where the U(1) spin-rotational symmetry around z axis is preserved. This symmetry forbids any vertex operator of Θ_0 and the analysis becomes much simpler. From Table 3.1, we find that three independent symmetry operations $\mathcal{T}$, $\mathcal{I}_b$, and $\mathcal{D}_2$ (since $\mathcal{R}_z$ is automatically assumed here, imposing $\mathcal{R}_x$ or $\mathcal{R}_y$ is to form $\mathcal{D}_2$) share the same transformation,

$$\Phi_0 \to -\Phi_0. \tag{5.1}$$

For even N, site-centered inversion $\mathcal{I}_s$ also has the same role since the shift $\pi\sqrt{N/2}$ can be absorbed in the compactification radius of Φ_0, given in Eq. (3.33). Once all these symmetries are broken, we can add vertex operators odd in Φ_0. Keeping only the most relevant operators, we obtain

$$H_{\text{eff}} = \frac{v_0}{2\pi}\int dx \left[K_0(\partial_x\Theta_0)^2 + \frac{1}{K_0}(\partial_x\Phi_0)^2\right] + g_{\text{eff}}\int dx \cos(\sqrt{2N}\Phi_0) + \tilde{g}\int dx \sin(\sqrt{2N}\Phi_0). \tag{5.2}$$

If g_{eff} is relevant, $\tilde{g}$ is also relevant, since they have the same scaling dimension. This Hamiltonian can be rewritten as

$$H_{\text{eff}} = \frac{v_0}{2\pi}\int dx \left[K_0(\partial_x\Theta_0)^2 + \frac{1}{K_0}(\partial_x\Phi_0)^2\right] + g'\int dx \cos(\sqrt{2N}\Phi_0 - \gamma), \tag{5.3}$$

where $g' = \sqrt{g_{\text{eff}}^2 + \tilde{g}^2}$ and $\gamma = \tan^{-1}(\tilde{g}/g_{\text{eff}})$. In the limit $g_{\text{eff}} \to +\infty$ $(-\infty)$, the field is locked into $\Phi_0 = 0$ $(\pi/\sqrt{2N})$ mod $\pi\sqrt{2/N}$. If we vary g_{eff} from $-\infty$ to $+\infty$ with fixed $\tilde{g}$, the presence of the last term in Eq. (5.2) implies that we can continuously connect the two minima $\Phi_0 = 0$ and $\pi/\sqrt{2N}$ without gap closing. Hence, the two disordered phases associated with

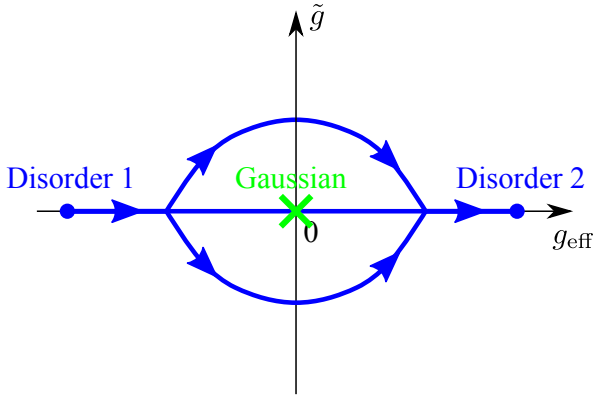

Figure 5.1: Phase diagram of the Hamiltonian (5.2). The blue arrow represents a continuous path of the parameters connecting $g_{\rm eff} \to -\infty$ and $g_{\rm eff} \to +\infty$. If $\tilde{g} = 0$, there has to be a Gaussian phase transition along such path. This transition can be avoided by considering a path with a nonvanishing $\tilde{g}$.

$g_{\rm eff} \to \pm\infty$ are smoothly connected. This is schematically explained in Fig. 5.1. One of the four symmetries, $\mathcal{T}$, $\mathcal{I}_b$, $\mathcal{I}_s$, and $\mathcal{D}_2$, together with the U(1) symmetry, is therefore required to protect a Gaussian phase transition between them and distinguish the two phases. This is a generalization of the discussion by Berg *et al.* [127], which indicated the importance of the inversion symmetry to stabilize the spin-1 Haldane phase in the context of a Bose-Hubbard model. Their result is now extended to specify the location of inversion center and to include time-reversal and dihedral-group symmetries for general N in the U(1)-symmetric case.

5.1.2 Without U(1) symmetry

Next we do not assume the presence of the U(1) spin-rotational symmetry. Then vertex operators of Θ_0 are generally allowed in the effective Hamiltonian (3.24). We again notice that $\mathcal{T}$, $\mathcal{I}_b$, and $\mathcal{D}_2$ share the same transformation property in Θ_0,

$$\Theta_0 \to \Theta_0 + \pi\sqrt{\frac{N}{2}}, \tag{5.4}$$

as well as that in Φ_0, namely $\Phi_0 \to -\Phi_0$. We note that one of the elements of $\mathcal{D}_2$ is insufficient to reproduce these transformation properties. In the presence of one of these symmetries, we would obtain an effective Hamiltonian,

$$H = \frac{v_0}{2\pi}\int dx \left[K_0(\partial_x\Theta_0)^2 + \frac{1}{K_0}(\partial_x\Phi_0)^2\right] + g_{\rm eff}\int dx \cos(\sqrt{2N}\Phi_0) + f\int dx \cos(\sqrt{\frac{8}{N}}\Theta_0). \tag{5.5}$$

Here we only keep the most relevant vertex operator among $\cos(q\sqrt{8/N}\Theta_0)$ with $q \geq 2$. When the spin-rotational symmetry in xy plane is broken, we can also add an additional vertex $\sin(\sqrt{8/N}\Theta_0)$, but it can be absorbed into the last term in Eq. (5.5) by an appropriate unitary transformation.

Let us assume that $\cos(\sqrt{2N}\Phi_0)$ is the only relevant vertex operator in Φ_0. Indeed, in order to make all the higher-order vertices $\cos(p\sqrt{2N}\Phi_0)$ with $p \geq 2$ irrelevant, we require that $1/N < K_0 < 4/N$. In this case, both of the couplings $g_{\rm eff}$ and f appearing in Eq. (5.5)

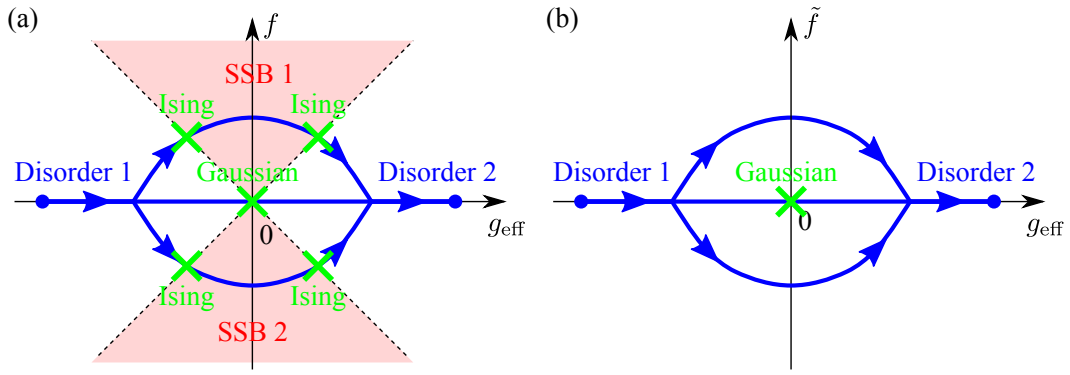

Figure 5.2: Phase diagrams of the Hamiltonians (5.5) and (5.8). The blue arrow represents a continuous path of the parameters connecting $g_{\rm eff} \to -\infty$ and $g_{\rm eff} \to +\infty$. If $f = 0$ ($\tilde{f} = 0$), there has to be a Gaussian phase transition along such path. (a) A nonvanishing f induces two Ising phase transitions along the path, and the system undergoes an intermediate phase with spontaneous Z_2-symmetry breaking. (b) The Gaussian phase transition can be avoided by considering a path with a nonvanishing $\tilde{f}$.

are relevant. Hence, if we vary $g_{\rm eff}$ from $-\infty$ to $+\infty$, we will find three phases: the first one is dominated by $g_{\rm eff} < 0$, the second one is governed by f around $g_{\rm eff} = 0$, and the third one is again dominated by $g_{\rm eff} > 0$. Along this continuous path of $g_{\rm eff}$, we will find two points where the dual fields Φ_0 and Θ_0 extremely compete each other. At such points, the two vertex operators would take the same scaling dimension and the same coupling constant under renormalization group. Such competitions are described by the $\beta^2 = 4\pi$ self-dual sine-Gordon Hamiltonian [148],

$$H_{\beta^2=4\pi} = \frac{v_0}{2}\int dx\left[(\partial_x\Theta_0)^2 + (\partial_x\Phi_0)^2\right] + G\int dx\left[\cos(\sqrt{4\pi}\Phi_0) + \cos(\sqrt{4\pi}\Theta_0)\right]. \tag{5.6}$$

It is known that this Hamiltonian describes the Ising phase transition with central charge $c = 1/2$ (see Appendix 5.A). This can be seen by refermionizing it in terms of two copies of the Majorana fermion (see, e.g. Refs. [79, 81]).

Therefore, we conclude that, in the presence of one of the three symmetries $\mathcal{T}$, $\mathcal{I}_b$, and $\mathcal{D}_2$, the disordered phase associated with $g_{\rm eff} < 0$ is separated from another with $g_{\rm eff} > 0$ by an intermediate phase governed by f, and its two phase boundaries are described by the Ising criticality [see Fig. 5.2 (a)]. In other words, a Gaussian transition that exists in the presence of the U(1) symmetry is now split into two Ising transitions. The intermediate phase must have some spontaneous Z_2-symmetry breaking, which is numerically observed in the absence of the U(1) symmetry [4, 13, 83].

If we assume that $K_0 < 1/N$, $\cos(\sqrt{8/N}\Theta_0)$ is irrelevant. However, the effective Hamiltonian naturally contains $\cos(\sqrt{8N}\Phi_0)$ and it becomes relevant. The Hamiltonian including this term,

$$H = \frac{v_0}{2\pi}\int dx\left[K_0(\partial_x\Theta_0)^2 + \frac{1}{K_0}(\partial_x\Phi_0)^2\right] + g_{\rm eff}\int dx\cos(\sqrt{2N}\Phi_0) + \tilde{g}_2\int dx\cos(\sqrt{8N}\Phi_0), \tag{5.7}$$

is known as the double-frequency sine-Gordon model [149, 150], and a similar result actually occurs along the continuous path of $g_{\rm eff}$ from $-\infty$ to $+\infty$; the two disordered phases are again separated by an intermediate phases whose boundaries correspond to the Ising transitions.

Finally, we consider the case where only the symmetry associated with $\Phi_0 \to -\Phi_0$, such as $\mathcal{R}_x$, $\mathcal{T} \times \mathcal{R}_z$, or $\mathcal{I}_s$ (for even N), is imposed, while we do not impose any symmetry constraint on Θ_0. In this case, possible vertex operators of Θ_0 are solely determined by the compactification radius in Eq. (3.33). Keeping only the most relevant vertex of Θ_0, we obtain an effective Hamiltonian,

$$H = \frac{v_0}{2\pi} \int dx \left[K_0 (\partial_x \Theta_0)^2 + \frac{1}{K_0} (\partial_x \Phi_0)^2 \right] + g_{\text{eff}} \int dx \cos(\sqrt{2N}\Phi_0) + \tilde{f} \int dx \cos(\sqrt{\frac{2}{N}}\Theta_0). \tag{5.8}$$

Along the same line argued above, when Φ_0 maximally competes with Θ_0, we here obtain the $\beta^2 = 2\pi$ self-dual sine-Gordon Hamiltonian [148],

$$H_{\beta^2=2\pi} = \frac{v_0}{2} \int dx \left[(\partial_x \Theta_0)^2 + (\partial_x \Phi_0)^2 \right] + G' \int dx \left[\cos(\sqrt{2\pi}\Phi_0) + \cos(\sqrt{2\pi}\Theta_0) \right], \tag{5.9}$$

where both of the vertex operators have the same scaling dimension 1/2. Since this Hamiltonian is known to be massive (see Appendix 5.A), we have no phase transition between the regime governed by g_{eff} and the other regime governed by $\tilde{f}$. As a result, two disordered phases associated with the different signs of g_{eff} are no longer distinguished and thus can be adiabatically connected.

We conclude that two disordered phases associated with the different signs of g_{eff} are separated by some phase transition only when the Hamiltonian is invariant under the symmetry operation,

$$\begin{aligned} &\Phi_0 \to -\Phi_0, \\ &\Theta_0 \to \Theta_0 + \pi\sqrt{\frac{N}{2}}. \end{aligned} \tag{5.10}$$

Such a symmetry operation includes time reversal $\mathcal{T}$, bond-centered inversion $\mathcal{I}_b$, and dihedral group of spin rotations $\mathcal{D}_2$. These symmetries are fully consistent with those obtained by the MPS representation and the projective representations of the symmetry groups on the spin-1 AKLT state [13]. Our result is also applied for any value of spin S, or equivalently, leg N (although we have required that odd-site translational invariance and site-centered inversion symmetry are explicitly broken for odd N). The present effective Hamiltonian approach concludes that there are essentially two different disordered phases protected by the above three symmetries. This is also compatible with the result of the more general classification [14, 15], which states that there exist two gapped disordered phases under $\mathcal{T}$ or $\mathcal{D}_2$. Although in Refs. [13–15], bond-centered inversion symmetry $\mathcal{I}_b$ is always together with translational invariance, $\mathcal{I}_b$ alone would suffice to produce two distinct disordered phases. Those three symmetries are expected to protect the distinction between different VBS phases.

5.1.3 Site-centered inversion with spin rotation

However, we can still have another symmetry operation that also reproduces Eq. (5.10). It is a symmetry under the combined operation of site-centered inversion and the π rotation around z axis, namely $\mathcal{I}_z \equiv \mathcal{I}_s \times \mathcal{R}_z$, which gives

$$\begin{aligned} &\Phi_0(x) \to -\Phi_0(-x) + \pi\sqrt{\frac{N}{2}}, \\ &\Theta_0(x) \to \Theta_0(-x) + \pi\sqrt{\frac{N}{2}}. \end{aligned} \tag{5.11}$$

This leads to the same symmetry operation as Eq. (5.10) for even N, since Θ_0 has the ambiguity of multiples of $\pi\sqrt{2/N}$ from its compactification. Therefore, under $\mathcal{I}_z$, we also have two distinct gapped phases associated with the different signs of g_{eff} in Eq. (3.24). One may consider that this is an artifact of our effective Hamiltonian approach. However, a matrix-product state formulation also confirms the existence of the gapped disordered phase protected by $\mathcal{I}_z$ in Sec. 5.3. Before that, we consider a specific example that exhibits such phases in the next section. In fact, those phases cannot be interpreted as VBS phases but some *trivial* phases, which can be smoothly connected to direct-product states.

For odd N or half-odd-integer S, the above discussion based on the effective Hamiltonian is not applicable since the combined symmetry $\mathcal{I}_z$ forbids $\cos(\sqrt{2N}\Phi_0)$. However, this instead allows $\sin(\sqrt{2N}\Phi_0)$. By replacing $\cos(\sqrt{2N}\Phi_0)$ by $\sin(\sqrt{2N}\Phi_0)$ in the effective Hamiltonian (3.24), it may be possible to proceed the same discussion as above and to show the existence of two gapped disordered phase protected by $\mathcal{I}_z$ for odd N. For a single $S = 1/2$ chain, this corresponds to two phases realized under the staggered magnetic field along the z axis, those are connected to direct-product states, $|\uparrow\downarrow\uparrow\downarrow\cdots\rangle$ and $|\downarrow\uparrow\downarrow\uparrow\cdots\rangle$.

5.2 Symmetry-protected trivial phase

In this section, we give a concrete microscopic model that gives two disordered phases protected by $\mathcal{I}_z$, as proposed above. We here show their existence by a simple argument based on perturbation theory and numerical simulations.

5.2.1 Model

As a model realizing such disordered phases protected by $\mathcal{I}_z$, we introduce an integer-S chain,

$$H = \sum_i \left[J\vec{S}_i \cdot \vec{S}_{i+1} + \sum_{n=1}^{S} D_{2n}^z (S_i^z)^{2n} - h(-1)^i S_i^z \right], \tag{5.12}$$

where D_{2n}^z are on-site uniaxial anisotropies and h is a staggered magnetic field. For $S = 1$, this model is simplified as

$$H = \sum_i \left[J\vec{S}_i \cdot \vec{S}_{i+1} + D_2^z (S_i^z)^2 - h(-1)^i S_i^z \right], \tag{5.13}$$

which has already been investigated in Refs. [151–153]. The staggered magnetic field breaks all the symmetries protecting the Haldane phase: $\mathcal{T}$, $\mathcal{I}_b$, and $\mathcal{D}_2$. Then the Haldane phase is now smoothly connected to a direct-product state realized in the limit $h \to \infty$,

$$|N\rangle \equiv |-+-+\cdots\rangle, \tag{5.14}$$

where $\pm$ represent the $S^z = \pm 1$ states, and thus in a trivial phase. However there still exists a phase transition between this trivial phase and the large-D phase that is also trivial and connected to another direct-product state,

$$|D\rangle \equiv |0000\cdots\rangle, \tag{5.15}$$

where 0 represents the $S^z = 0$ state. The phase diagrams obtained in Ref. [152] is shown in Fig. 5.3. Hereafter, we call the trivial phase connected to $|N\rangle$ as the "N phase" and that to $|D\rangle$ as the "D phase".

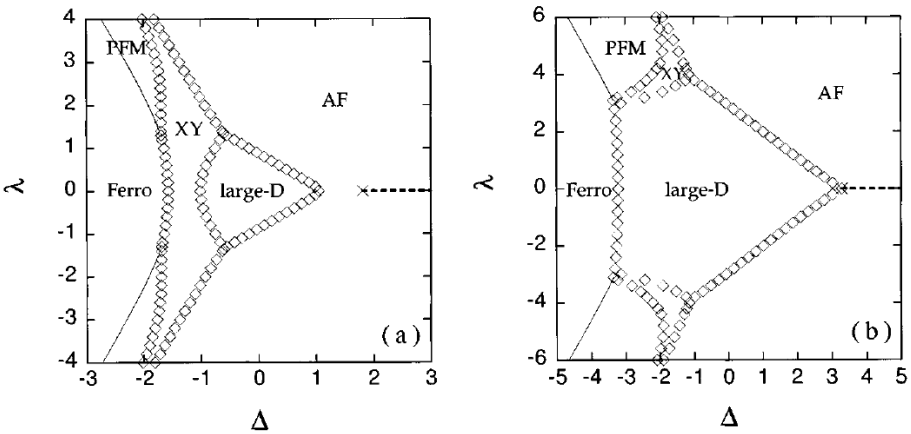

Figure 5.3: Phase diagrams of Eq. (5.13) obtained by exact diagonalization in Ref. [152], for (a) $D_2^z = 1$ and (b) $D_2^z = 3$. λ corresponds to the staggered magnetic field h, and Δ is an anisotropic coupling that is set to be unity in our model. The AF phase and large-D phases correspond to the N and D phases in our terminology. Phase boundaries between the large-D and AF phases are the Gaussian phase transitions.

From the point of view of the effective Hamiltonian, through the ladder mapping, the staggered magnetic field is bosonized as

$$-h\sum_i(-1)^i S_i^z \approx a_1 h \sum_{j=1}^{2S} \int dx \sin(\sqrt{2}\phi_j). \tag{5.16}$$

For integer S, this contributes to the effective Hamiltonian (3.24) at the even order and thus does not generate the $\sin(\sqrt{2N}\Phi_0)$ term. According to a similar mechanism to that by the dimerization in Sec. 4.4, the staggered field also induces several phase transitions.

The model (5.13) will be experimentally realized in the cold atom system on an optical lattice. The corresponding Hamiltonian is a Bose-Hubbard model with the staggered on-site potential,

$$H = \sum_i \left[-t(b_i^\dagger b_{i+1} + \text{h.c.}) + \frac{U}{2} n_i(n_i - 1) + \Delta(-1)^i n_i \right], \tag{5.17}$$

where b_i is the boson creation operator at site i and $n_i = b_i^\dagger b_i$. This model can be achieved in one-dimensional cold atom systems with two periodic potentials with wave lengths k_1 and $k_2 = 2k_1$ [154,155]. If the one-site repulsion U is sufficiently strong, the single site occupation is strongly suppressed and may be truncated to be $n_i = 0, 1, 2$. Then we can map Eq. (5.17) onto a spin-1 chain [127, 156]. As numerically shown in Ref. [153], for $\langle n_i \rangle = 1$, this model also exhibits the phase transition between two trivial phases protected by $\mathcal{I}_s$ and the particle number conservation. Now the D phase corresponds to a Mott insulator with one particle per one site for $U \gg \Delta$, while the N phase to another insulator where two particles alternatively occupy one site for $\Delta \gg U$. Those phases are illustrated in Fig. 5.4. The phase transition will be observed by controlling strengths of the periodic potentials and measuring the particle distribution, as done in Ref. [157]. Only at the transition, the system behaves as a superfluid.

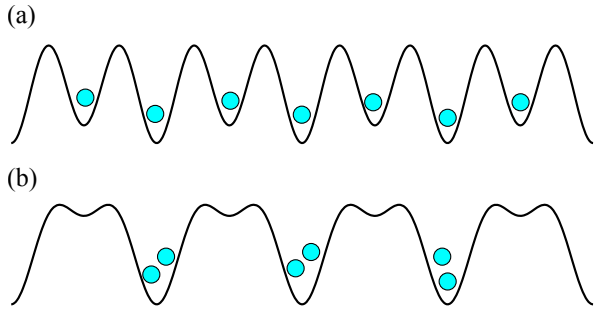

Figure 5.4: Schematic pictures of two Mott-insulating phases realized in the Bose-Hubbard model with a double periodic potential (5.17). (a) If the potential with a period k_1 is dominant, the system is in the D phase. (b) If the potential with a period $k_2 = 2k_1$ is dominant, the system is in the N phase.

5.2.2 Perturbative expansion

Here, we show a simple way to see the phase transition between the D and N phases by means of perturbation theory. First we consider the $S = 1$ model in Eq. (5.13). Now the only uniaxial anisotropy in this model is D_2^z. In the limit of isolated spins $J = 0$ and for $D_2^z = h$, two states $|+\rangle$ and $|0\rangle$ are degenerate on each odd site, while $|-\rangle$ and $|0\rangle$ are degenerate on each even site. If we regard these states as the two basis states of spin-1/2,

$$\begin{aligned} &|\uparrow\rangle \equiv |+\rangle\,, \qquad |\downarrow\rangle \equiv |0\rangle \qquad \text{for even sites,} \\ &|\uparrow\rangle \equiv |0\rangle\,, \qquad |\downarrow\rangle \equiv |-\rangle \qquad \text{for odd sites,} \end{aligned} \tag{5.18}$$

we can write down the strong-coupling Hamiltonian up to the first order in J,

$$H_{\mathrm{SC}} = \sum_i \left[2J\left(s_i^x s_{i+1}^x + s_i^y s_{i+1}^y\right) + J s_i^z s_{i+1}^z + \left(J + h - D_2^z\right)(-1)^i s_i^z\right], \tag{5.19}$$

where $\vec{s}_i$ is the spin-1/2 operator. If the last term corresponding to a staggered magnetic field is absent, this model is nothing but an easy-plane XXZ chain and described by a gapless Tomonaga-Luttinger liquid. The staggered magnetic field is now a relevant perturbation, and a finite h immediately opens up an excitation gap. Therefore, we have a Gaussian phase transition when $J = D_2^z - h$ and D_2^z, $h \gg J$. Although this result is only applied to the parameter region close to the isolated spins, this phase transition between trivial phases continues for an arbitrary value of J, as we will demonstrate later.

We can proceed similar analyses for general integer-S chains where higher-order uniaxial anisotropies D_{2n}^z are allowed. Starting from the isolated spins and appropriately tuning D_{2n}^z and h, two states $|S-l\rangle$ and $|S-l-1\rangle$ become degenerate on each odd site, while $|-S+l\rangle$ and $|-S+l+1\rangle$ on each even site, where $l = 0, \cdots, S-1$. Applying first-order perturbation theory in J to this "spin-1/2" Hilbert space, we can again obtain an easy-plane XXZ chain with a staggered magnetic field as in the form (5.19). Thus, for $D_{2n}^z, h \gg J$, we can see a Gaussian phase transition between two trivial phases that are smoothly connected to direct-product states, $|S-l, -S+l, \cdots\rangle$ and $|S-l-1, -S+l+1, \cdots\rangle$, respectively. We expect that there is a continuity between a state $|S-k, -S+k, \cdots\rangle$ with $k = 0, \cdots, S$ and the spin-$(S-k)$ Haldane (or intermediate-D) phase [61], since $\mathcal{T}$, $\mathcal{I}_b$, and $\mathcal{D}_2$ are explicitly broken in the present cases. Nevertheless, there are still S phase transitions between trivial phases protected by $\mathcal{I}_z$. Their distinction follows that those direct-product states take two

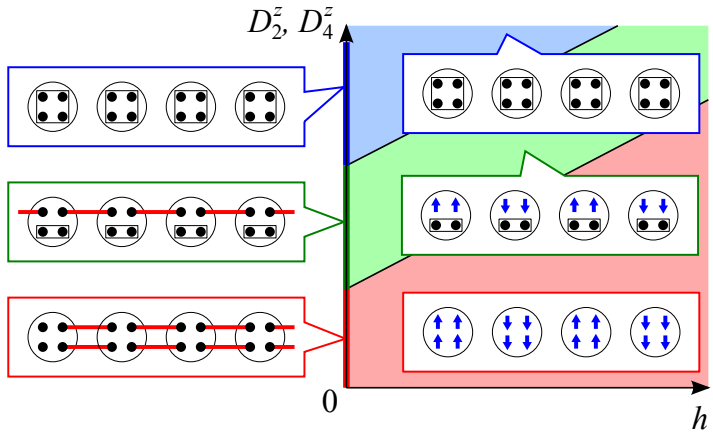

Figure 5.5: An expected phase diagram for the spin-2 chain (5.12). The horizontal and vertical axes correspond to the staggered magnetic field h and some function of D_{2n}^z, respectively. The VBS pictures for three Haldane phases realized at $h = 0$ are shown in the left, while those for three trivial phases realized in the presence of h are shown in the right. The arrows in the VBS pictures represent polarized spin-1/2's along the staggered magnetic field.

different one-dimensional representations of $\mathcal{R}_z$ on each site, as discussed in Sec. 5.3. A naively expected phase diagram of Eq. (5.12) for $S = 2$ is shown in Fig. 5.5.

5.2.3 Numerical simulations

We numerically show the existence of the phase transition between the D and N phases. The bosonization analysis suggests that we can introduce microscopic models with less symmetries than Eq. (5.13), but with the symmetry under $\mathcal{I}_z$, to maintain the two distinct trivial phases. To this end, we consider the following Hamiltonian:

$$H = \sum_i \left[\vec{S}_i \cdot \vec{S}_{i+1} + D_2^z (S_i^z)^2 - h(-1)^i S_i^z + d_x \left(S_i^y S_{i+1}^z - S_i^z S_{i+1}^y \right) \right]. \tag{5.20}$$

The new term d_x represents the (uniform) Dzyaloshinskii-Moriya (DM) interaction with the DM vector parallel to the x axis. This term breaks not only the U(1) spin-rotational symmetry about the z axis, but also both $\mathcal{I}_s$ and $\mathcal{R}_z$ as individual symmetries. However, the Hamiltonian (5.20) with a nonvanishing d_x still preserves the symmetry $\mathcal{I}_z$ under the composite operation.

We study the Hamiltonian (5.20) using infinite density-matrix renormalization group (iDMRG) [133, 158, 159]. This method numerically approximates the ground state of an infinite-size quantum system in the MPS form (2.28) with a finite bond dimension χ. Since the Hamiltonian (5.20) has two-site translational invariance, we can also assume the two-site translational invariance on the MPS. Thus, we need to know only two sets of matrices $\{\Gamma^A, \Lambda^A\}$ and $\{\Gamma^B, \Lambda^B\}$ to represent the MPS for the infinite systems size.

The correlation length ξ is easily evaluated from the second largest eigenvalue of the transfer matrix [see Eq. (2.39)]. It is plotted in Fig. 5.6 as functions of D_2^z, for different bond dimension χ and parameters of the model. A divergent correlation length with increasing χ indicates a critical point. For $h = d_x = 0$, we observed two sharp peaks in the correlation length by increasing D_2^z. Those are shown in Fig. 5.6 (a). These transitions are already known (for example, see Ref. [57]); one at $D_2^z \sim -0.3$ corresponds to the Ising transition between

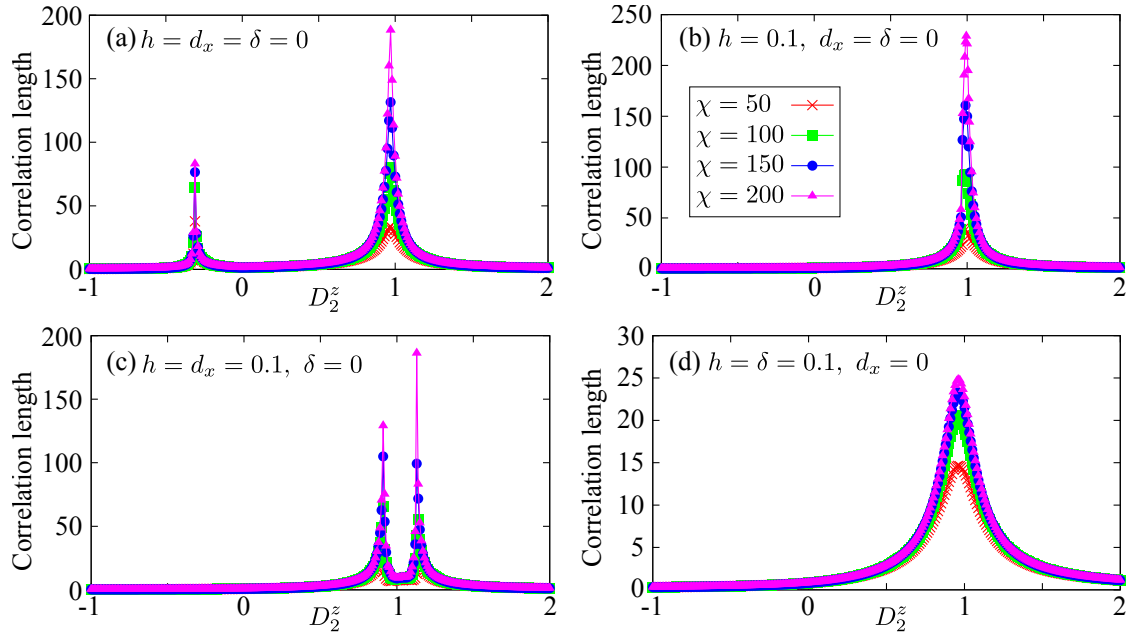

Figure 5.6: Correlation lengths calculated for the spin-1 chain (5.20) with the dimerization (5.23) are plotted against D_2^z. The parameters are varied as (a) $h = d_x = \delta = 0$, (b) $h = 0.1$, $d_x = \delta = 0$, (c) $h = d_x = 0.1$, $\delta = 0$, and (d) $h = \delta = 0.1$, $d_x = 0$. Each color and symbol denotes the different bond dimensions χ from 50 to 200.

the Ising antiferromagnetic and Haldane phases, and the other at $D_2^z \sim 1$ corresponds to the Gaussian transition between the Haldane and D (large-D) phases.

When introducing the staggered field $h = 0.1$ but still setting $d_x = 0$, as seen from Fig. 5.6 (b), we find that the Haldane and Ising antiferromagnetic phases are merged into the single N phase since all of the three symmetries protecting the Haldane phase are broken. However, as found in Refs. [152, 153], the transition at $D_2^z \sim 1$ still exists. This indicates that there is a phase transition between two trivial phases corresponding to the N and D phases. As suggested by the bosonization analysis, this transition should be of the Gaussian type. This is easily checked by examining the von Neumann entanglement entropy S [see Eq. (2.10)], [1] which behaves as [133, 160]

$$S = \frac{c}{6} \log \xi + c_1, \tag{5.22}$$

where c is the central charge and c_1 is a nonuniversal constant, for an infinite system with a large correlation length ξ. The von Neumann entanglement entropy is plotted in Fig. 5.7 (a) for $D_2^z = 1$ and several correlation lengths. From this, the central charge is estimated as $c \approx 1.02$ and is compatible with the ideal value at the Gaussian phase transition, $c = 1$.

To further confirm that this transition is protected by $\mathcal{I}_z$ alone, we further introduce d_x in Fig. 5.6 (c). A single transition in Fig. 5.6 (b) is now split into two transitions, but

[1] Since eigenvalues of the reduced density matrix ρ_A is nothing but squares of the entries of Λ, $\{\lambda_\alpha^2\}$, the von Neumann entanglement entropy is straightforwardly calculated as

$$S = -\mathrm{Tr}_A \rho_A \log \rho_A = -\sum_{\alpha=1}^{\chi} \lambda_\alpha^2 \log(\lambda_\alpha^2). \tag{5.21}$$

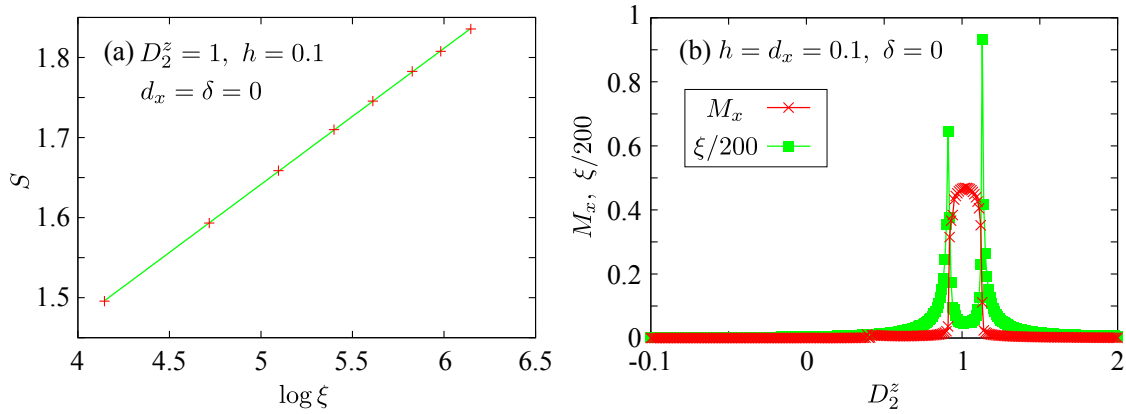

Figure 5.7: (a) von Neumann entanglement entropy as a function of the correlation length ξ for $D_2^z = 1$, $h = 0.1$, and $d_x = \delta = 0$. The solid line is a logarithmic fitting function $S = 0.170 \log \xi + 0.792$. (b) Staggered magnetization in the x axis as a function of D_2^z for $\chi = 200$, $h = d_x = 0.1$, and $\delta = 0$. The correlation length (divided by 200) is again shown for comparison.

the N and D phases are still separated by (two) transitions and thus are distinct. In the intermediate phase between them, an Ising antiferromagnetic order along the x axis occurs and thus $\mathcal{I}_z$ is spontaneously broken. In Fig. 5.7 (b), we plot the staggered magnetization $M_x \equiv \langle (-1)^i S_i^x \rangle$ against D_2^z. Obviously, it takes a finite value in the intermediated regime sandwiched between the two transitions. M_x is now meaningful since the Hamiltonian still preserves the spin reversal symmetry $S_i^x \to -S_i^x$, besides $\mathcal{I}_z$. These results coincide with the prediction by the bosonization approach in Sec. 5.1.2, which states that the two trivial phases are separated by two Ising transition and an intermediate phase with spontaneous Z_2-symmetry breaking.

Finally we introduce an explicit dimerization,

$$H' = \delta \sum_i (-1)^i \vec{S}_i \cdot \vec{S}_{i+1}, \tag{5.23}$$

with $\delta \neq 0$, and consider $H + H'$. This breaks the inversion symmetry $\mathcal{I}_z$ without affecting any other symmetries in the Hamiltonian (5.20), and there will be only one trivial phase. As shown in Fig. 5.6 (d), we observe that the correlation length remains finite (order of 10) for all values of D_2^z when $d_x = 0$. In fact, this can also be shown analytically by considering the limit of $\delta = 1$ with $d_x = 0$. In this limit, the Hamiltonian with $d_x = 0$ is reduced to the sum of independent two-site Hamiltonians,

$$H_{\text{two-site}} = 2\vec{S}_1 \cdot \vec{S}_2 + D_2^z[(S_1^z)^2 + (S_2^z)^2] + h(S_1^z - S_2^z). \tag{5.24}$$

Again we can obtain the two trivial states $|D\rangle$ and $|N\rangle$ in the limits $D_2^z \to \infty$ and $h \to \infty$, respectively. Therefore, the continuity between $|D\rangle$ and $|N\rangle$ is confirmed by finding a path on which no level crossing occurs in the lowest energy spectrum between these limits. In Fig. 5.8, we plot energy spectra of the two-site Hamiltonian. Obviously, the singlet state at $D_2^z = h = 0$ is adiabatically connected to both the states $|00\rangle$ and $|-+\rangle$. We conclude that, by breaking the site-centered inversion symmetry, the D and N phases are adiabatically connected and thus no longer distinguished. This fact also rules out a possibility that the two trivial phases are distinct under the two-site translation invariance and some on-site symmetry, as indicated in Refs. [14, 15].

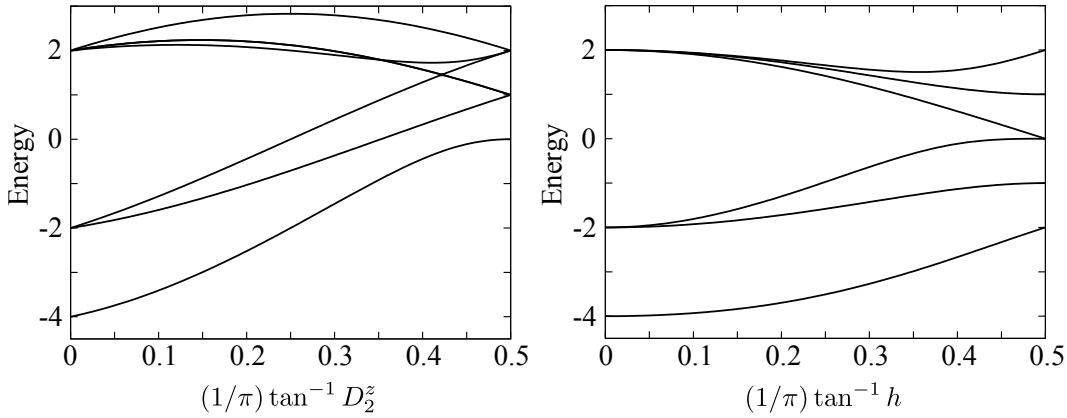

Figure 5.8: Energy spectra of the two-site Hamiltonian (5.24). D_2^z are varied and $h = 0$ on the left panel, while h_z are varied and $D_2^z = 0$ on the right panel.

5.3 MPS formulation

The existence of distinct disordered phases protected by site-centered inversion symmetry combined with a spin rotation seems plausible as shown by a field-theoretical approach in Sec. 5.1.3 and numerical simulations in Sec. 5.2.3. In this section, we provide a more rigorous proof based on the MPS formalism without assuming translational invariance.

5.3.1 Non-translation-invariant MPS and its pureness

In Sec. 2.3, we mainly considered the translation-invariant MPS and reviewed the classification of SPT phases. However, in order to only consider the role of the inversion symmetry, we need to work on the non-translation-invariant MPS. Specifically, if we have one-site (or generally, odd-site) translational invariance, we cannot distinguish the site-centered and bond-centered inversion symmetries (see Fig. 3.2). To investigate how the position of the inversion center affects the classification of SPT phases, it is essential to consider the non-translational-invariant MPS.

Thus we begin with the general MPS [67, 69], without assuming any translational invariance:

$$|\psi\rangle = \sum_{\{m_n\}} \cdots \Gamma^{[n-1]}_{m_{n-1}} \Lambda^{[n-\frac{1}{2}]} \Gamma^{[n]}_{m_n} \Lambda^{[n+\frac{1}{2}]} \Gamma^{[n+1]}_{m_{n+1}} \cdots |\cdots m_{n-1} m_n m_{n+1} \cdots\rangle \,, \tag{5.25}$$

where $\Lambda^{[a]}$ is a $\chi_a \times \chi_a$ positive diagonal matrix, $\Gamma^{[n]}$ is a $\chi_{n-1/2} \times \chi_{n+1/2}$ matrix, and m_n represents the physical degrees of freedom on site n. An MPS representation is not unique for a given state but we can always fix it by the canonical condition [67, 68],

$$\mathrm{Tr}[(\Lambda^{[a]})^2] = 1 \tag{5.26}$$

and

$$\begin{aligned} \sum_m \Gamma^{[n]}_m \left(\Lambda^{[n+1/2]}\right)^2 \left(\Gamma^{[n]}_m\right)^\dagger &= \mathbb{I}_{\chi_{n-1/2}}, \\ \sum_m \left(\Gamma^{[n]}_m\right)^\dagger \left(\Lambda^{[n-1/2]}\right)^2 \Gamma^{[n]}_m &= \mathbb{I}_{\chi_{n+1/2}}, \end{aligned} \tag{5.27}$$

where $\mathbb{I}_\chi$ is the $\chi \times \chi$ identity matrix. Here we dropped the site index n from m_n for brevity. In Sec. 2.3.1, we interpret these relations in terms of transfer matrices. The transfer matrices introduced by the MPS correspond to the following completely positive maps [64, 68],

$$\begin{aligned} \mathcal{E}_R^{[n]}(X) &= \sum_m \Gamma_m^{[n]} \Lambda^{[n+1/2]} X \Lambda^{[n+1/2]} \left(\Gamma_m^{[n]}\right)^\dagger, \\ \mathcal{E}_L^{[n]}(Y) &= \sum_m \left(\Gamma_m^{[n]}\right)^\dagger \Lambda^{[n-1/2]} Y \Lambda^{[n-1/2]} \Gamma_m^{[n]}. \end{aligned} \tag{5.28}$$

They can be understood as linear mappings between the spaces of $\chi_{n+1/2} \times \chi_{n+1/2}$ and $\chi_{n-1/2} \times \chi_{n-1/2}$ matrices, with the metric defined by the norm,

$$|X|^2 \equiv \mathrm{Tr}\left[X(\Lambda^{[a]})^2 X^\dagger\right]. \tag{5.29}$$

Given the metric, we can introduce the singular value decomposition of $\mathcal{E}_R^{[n]}$ and $\mathcal{E}_L^{[n]}$. The canonical condition (5.27) means that the identity matrices are left/right eigenvectors of $\mathcal{E}_R^{[n]}$ and $\mathcal{E}_L^{[n]}$ belonging to the largest singular value 1, that is,

$$\begin{aligned} \mathcal{E}_R^{[n]}(\mathbb{I}_{\chi_{n+1/2}}) &= \mathbb{I}_{\chi_{n-1/2}}, \\ \mathcal{E}_L^{[n]}(\mathbb{I}_{\chi_{n-1/2}}) &= \mathbb{I}_{\chi_{n+1/2}}. \end{aligned} \tag{5.30}$$

Furthermore, we require the MPS to be pure, that is the largest singular value 1 is nondegenerate. As we saw in Sec. 2.3.1, the pureness of a translation-invariant MPS is equivalent to the uniqueness of the ground state (or absence of any long-range order). If a translation-invariant MPS in not pure, that is, the largest singular value of $\mathcal{E}_R^{[n]}$ or $\mathcal{E}_L^{[n]}$ is degenerate, this immediately leads to the presence of some long-range order. In a non-translation-invariant MPS, the pureness is a sufficient but *not* a necessary condition for the uniqueness of the ground state [14]. However, it is still physically reasonable to assume that the MPS is pure. In the rest of this section, we argue this point.

For the non-translation-invariant MPS, the matrices and correspondingly the completely positive maps are site-dependent. One can still calculate correlation functions $\langle P(0)Q(r)\rangle$ by the transfer-matrix method as demonstrated in Sec. 2.3.1, but we cannot obtain a complete set of eigenvectors for all $\mathcal{E}_R^{[n]}$ at the same time. Nevertheless, the canonical condition (5.30) ensures that the left eigenvector $\mathbb{I}_{\chi_{n+1/2}}$ of $\mathcal{E}_L^{[n]}$ with the largest singular value 1 is also the right eigenvector of $\mathcal{E}_L^{[n+1]}$ with the largest singular value 1. Using this fact successively from site to site, one can prove that any correlation function decays exponentially if the largest singular value 1 of $\mathcal{E}_R^{[n]}$ is nondegenerate, as in the case of the translation-invariant MPS.

There could be other eigenvectors with the singular value 1. Supposing that the largest singular value 1 is two-fold degenerate, we denote the corresponding left/right eigenvectors of $\mathcal{E}_L^{[n]}$, different from $\mathbb{I}$, as $L^{[a]}$ and $R^{[a]}$. They satisfy the normalization $|L^{[a]}| = |R^{[a]}| = 1$ and

$$\mathcal{E}_L^{[n]}(R^{[n-1/2]}) = L^{[n+1/2]}. \tag{5.31}$$

If the left eigenvector of $\mathcal{E}_L^{[n]}$, $L^{[n+1/2]}$, matches with the right eigenvector of $\mathcal{E}_L^{[n+1]}$, $R^{[n+1/2]}$, for all $n \in \mathbb{Z}$, correlation functions do not decay and imply some long-range order. Precisely, a finite number of the mismatching in left/right eigenvectors is acceptable to show the presence

of the long-range order for a sufficiently large r. However, if mismatches between the left eigenvector $L^{[a]}$ and the right eigenvector $R^{[a]}$, that is $|L^{[a]}-R^{[a]}| > \epsilon\ (>0)$, occur many times $[\sim \mathcal{O}(r)]$, correlation functions decay exponentially, even though the MPS is not pure. Note that, "mismatch" only means that $L^{[a]}$ and $R^{[a]}$ are different; it does not necessarliy indicates $L^{[a]}$ and $R^{[a]}$ are orthogonal. Therefore, the pureness of a non-translation-invariant MPS is sufficient but not necessary condition for the exponential decays of correlation functions.

Even if a non-translational-invariant MPS is pure, the completely positive map on each site could have degeneracy in the largest singular value 1. However, if we glue a sufficiently large but finite number of consecutive sites into a single "supersite", it becomes difficult to maintain that the completely positive map on that supersite has the degenerate largest singular value, in the following sense. Let us introduce the completely positive map on a supersite consisting of AB by $\mathcal{E}_L^{AB}(X) \equiv \mathcal{E}_L^A(\mathcal{E}_L^B(X))$. In order to have degeneracy in the largest singular value of $\mathcal{E}_L^{AB}$, we have to require that both $\mathcal{E}_L^A$ and $\mathcal{E}_L^B$ have degeneracy and their corresponding eigenvectors match each other. A similar consideration continues to larger supersites. Then it turns out that, to maintain degeneracy in the largest singular value of the completely positive map on the supersite, all constituent sites must have degeneracy and matching eigenvectors from site to site.

Although it seems harder as we take a larger supersite, in principle, the completely positive map can still possesses degeneracy for an arbitrary large supersite. However, in that case, there is a local operator that does not decay at arbitrary distance. In other words, there must be a ground-state degeneracy in the thermodynamic limit. Since we focus on the SPT phase, this situation is not of our interest. Thus, as far as we are interested in the unique gapped ground state, we assume that one can divide the system into finite-size supersites in which the completely positive map has the nondegenerate largest singular value 1, even for a non-translation-invariant MPS. Then we can always make the MPS to be pure. In the following, what we call "site" is taken to be such a supersite.

5.3.2 SPT phase protected by inversion symmetry

We here consider inversion symmetry on a non-translation-invariant MPS. We always take the inversion center at the origin 0. Thus, in order to represent the site-centered inversion, the sites are defined on integral points $n \in \mathbb{Z}$. Then, the inversion center is at $n = 0$. On the other hand, in the case of the bond-centered inversion, the bonds are defined on integral points $n - 1/2 \in \mathbb{Z}$, while the sites are on half-odd-integral point $n \in \mathbb{Z} - 1/2$. Now the inversion center is at $n - 1/2 = 0$. For a while, we do not specify the position of the inversion center.

Following Refs. [13, 70], if $|\psi\rangle$ is invariant under an inversion symmetry $\mathcal{I}$, it satisfies

$$\sum_{m'} u_{mm'} \left(\Gamma_{m'}^{[n]}\right)^T = e^{i\theta^{[n]}(\mathcal{I})} \left(U^{[-n-\frac{1}{2}]}(\mathcal{I})\right)^\dagger \Gamma_m^{[-n]} U^{[-n+\frac{1}{2}]}(\mathcal{I}), \tag{5.32}$$

where $u_{mm'}$ is the unitary representation of some Z_2 symmetry acting on the physical Hilbert space of each site, $\theta^{[n]}(\mathcal{I})$ is a phase, and $U^{[a]}(\mathcal{I})$ is a $\chi_a \times \chi_a$ unitary matrix commuting with $\Lambda^{[a]}$. The inversion symmetry also implies that

$$\Lambda^{[a]} = \Lambda^{[-a]}, \tag{5.33}$$

and this yields $\chi_a = \chi_{-a}$. Using the above relation twice, we obtain

$$\Gamma_m^{[n]} = e^{i(\theta^{[n]}(\mathcal{I})+\theta^{[-n]}(\mathcal{I}))} \left(U^{[-n+1/2]}(\mathcal{I})\right)^T \left(U^{[n-1/2]}(\mathcal{I})\right)^\dagger \Gamma_m^{[n]} U^{[n+1/2]}(\mathcal{I}) \left(U^{[-n-1/2]}(\mathcal{I})\right)^*. \tag{5.34}$$

Substituting into the canonical condition (5.27), we have

$$\begin{aligned}&\sum_m (\Gamma_m^{[n]})^\dagger \Lambda^{[n-1/2]} U^{[n-1/2]}(\mathcal{I}) \left(U^{[-n+1/2]}(\mathcal{I})\right)^* \Lambda^{[n-1/2]} \Gamma_m^{[n]} \\ &= e^{i(\theta^{[n]}(\mathcal{I})+\theta^{[-n]}(\mathcal{I}))} U^{[n+1/2]}(\mathcal{I}) \left(U^{[-n-1/2]}(\mathcal{I})\right)^*.\end{aligned} \tag{5.35}$$

Using the completely positive map, this implies

$$\mathcal{E}_L^{[n]} \left(U^{[n-1/2]}(\mathcal{I}) \left(U^{[-n+1/2]}(\mathcal{I})\right)^*\right) = e^{i(\theta^{[n]}(\mathcal{I})+\theta^{[-n]}(\mathcal{I}))} U^{[n+1/2]}(\mathcal{I}) \left(U^{[-n-1/2]}(\mathcal{I})\right)^*. \tag{5.36}$$

Introducing

$$A^{[a]}(\mathcal{I}) \equiv U^{[a]}(\mathcal{I}) \left(U^{[-a]}(\mathcal{I})\right)^*, \tag{5.37}$$

this can be rewritten as

$$\mathcal{E}_L^{[n]} \left(A^{[n-1/2]}(\mathcal{I})\right) = e^{i(\theta^{[n]}(\mathcal{I})+\theta^{[-n]}(\mathcal{I}))} A^{[n+1/2]}(\mathcal{I}). \tag{5.38}$$

As defined in Eq. (5.29), the matrix $A^{[a]}(\mathcal{I})$ has a unit norm:

$$|A^{[a]}(\mathcal{I})|^2 = \mathrm{Tr}\left[U^{[a]}(\mathcal{I}) \left(U^{[-a]}(\mathcal{I})\right)^* \left(\Lambda^{[a]}\right)^2 \left(U^{[-a]}(\mathcal{I})\right)^T \left(U^{[a]}(\mathcal{I})\right)^\dagger\right] = 1, \tag{5.39}$$

since $[U^{[a]}(\mathcal{I}), \Lambda^{[a]}] = 0$ and $\Lambda^{[a]} = \Lambda^{[-a]}$.

Thus $A^{[n-1/2]}(\mathcal{I})$ $[A^{[n+1/2]}(\mathcal{I})]$ is a left (right) eigenvector belonging to the singular value 1 of $\mathcal{E}_L^{[n]}$. By the assumption of the pure MPS, $A^{[n\pm1/2]}(\mathcal{I})$ is proportional to the identity matrix with some phase factor:

$$A^{[a]}(\mathcal{I}) = e^{i\phi^{[a]}(\mathcal{I})} \mathbb{I}_{\chi_a}. \tag{5.40}$$

This means

$$U^{[a]}(\mathcal{I}) = e^{i\phi^{[a]}(\mathcal{I})} \left(U^{[-a]}(\mathcal{I})\right)^T. \tag{5.41}$$

Using this relation twice, we obtain

$$\phi^{[a]}(\mathcal{I}) + \phi^{[-a]}(\mathcal{I}) = 0 \mod 2\pi. \tag{5.42}$$

Substitute Eq. (5.40) back into Eq. (5.38), we obtain

$$\mathcal{E}_L^{[n]} \left(\mathbb{I}_{\chi_{n-1/2}}\right) = e^{i(\theta^{[n]}(\mathcal{I})+\theta^{[-n]}(\mathcal{I}))} e^{i(\phi^{[n+1/2]}(\mathcal{I})-\phi^{[n-1/2]}(\mathcal{I}))} \mathbb{I}_{\chi_{n+1/2}}. \tag{5.43}$$

Since $\mathbb{I}_{\chi_{n\pm1/2}}$ are the right/left eigenvectors belonging to the largest singular value 1, this yields

$$\theta^{[n]}(\mathcal{I}) + \theta^{[-n]}(\mathcal{I}) + \phi^{[n+1/2]}(\mathcal{I}) - \phi^{[n-1/2]}(\mathcal{I}) = 0 \mod 2\pi. \tag{5.44}$$

The implications of these relations depend on the position of the inversion center, namely, whether we impose the site-centered or bond-centered inversion symmetry. If we choose the bond-centered inversion $\mathcal{I} \equiv \mathcal{I}_b$, the unitary matrix in Eq. (5.32) is $u = 1$ and the bond index is integral, $a = n - 1/2 \in \mathbb{Z}$. For most values of a, the bond-centered inversion symmetry gives no constraint on the phases. However, at $a = 0$, Eq. (5.42) gives

$$\phi^{[0]}(\mathcal{I}_b) = 0,\ \pi \mod 2\pi. \tag{5.45}$$

This implies that $U^{[a]}(\mathcal{I}_b)$ at the inversion center, $U^{[0]}(\mathcal{I}_b)$, can form a projective representation with $\phi^{[0]}(\mathcal{I}_b) = \pi$. If this is the case, $U^{[0]}(\mathcal{I}_b)$ becomes an antisymmetric matrix obeying,

$$U^{[0]}(\mathcal{I}_b) = -\left(U^{[0]}(\mathcal{I}_b)\right)^T. \tag{5.46}$$

Since this commutes with $\Lambda^{[0]}$, the entanglement spectrum at the cut $a = 0$ becomes two-fold degenerate [13]. This degeneracy cannot be lifted unless the system undergoes a phase transition. Thus, two gapped phases associated with different $\phi^{[a]}(\mathcal{I}_b)$ are distinct. This is a more rigorous discussion than that of Ref. [13], since we use the non-translational-invariant MPS.

Now let us move to the case of the site-centered inversion symmetry $\mathcal{I} \equiv \mathcal{I}_s$. In this case, the unitary matrix in Eq. (5.32) is $u = 1$ and the site index is integral, $n \in \mathbb{Z}$. Again, the constraints on $\phi^{[a]}(\mathcal{I}_s)$ and $\theta^{[n]}(\mathcal{I}_s)$ are not restrictive for most values of n, but at $n = 0$, Eq. (5.44) gives

$$2\theta^{[0]}(\mathcal{I}_s) + \phi^{[+1/2]}(\mathcal{I}_s) - \phi^{[-1/2]}(\mathcal{I}_s) = 0 \mod 2\pi. \tag{5.47}$$

Using Eq. (5.42), we obtain

$$\theta^{[0]}(\mathcal{I}_s) + \phi^{[1/2]}(\mathcal{I}_s) = 0,\ \pi \mod 2\pi. \tag{5.48}$$

Yet this phase cannot be interpreted as the one related to the projective representation, the gapped phases associated with different values of $\theta^{[0]}(\mathcal{I}_s) + \phi^{[1/2]}(\mathcal{I}_s)$ gives distinct phases. As the following example shows, this phase is rather related to the one-dimensional representation of $\mathcal{I}_s$ on a block (with odd sites) respecting that symmetry.

It is straightforward to generalize the above result to the site-centered inversion combined with a spin rotation about the z axis, $\mathcal{I} \equiv \mathcal{I}_z = \mathcal{I}_s \times \mathcal{R}_z$. We just replace the unitary matrix u by $\mathcal{R}_z = e^{i\pi S^z}$ in Eq. (5.32), and the remaining discussion is exactly the same as that for $\mathcal{I}_s$. Thus the phase $\theta^{[0]}(\mathcal{I}_z) + \phi^{[1/2]}(\mathcal{I}_z)$ is quantized to 0 or π. Let us consider the two direct-product states, $|D\rangle$ and $|N\rangle$, realized in the model (5.12) introduced in Sec. 5.2.1. For a direct-product state, all the matrices $\Gamma^{[n]}$, $\Lambda^{[a]}$, and $U^{[a]}(\mathcal{I}_z)$ are just scalars (1×1 matrices) and commute with each other. For $|D\rangle$, we have

$$\Gamma_0^{[n]} = 1, \quad \Gamma_\pm^{[n]} = 0, \quad \Lambda^{[a]} = 1. \tag{5.49}$$

We easily find $\theta^{[0]}(\mathcal{I}_z) = 0$ and $\phi^{[1/2]}(\mathcal{I}_z) = 0$, and thus $\theta^{[0]}(\mathcal{I}_z) + \phi^{[1/2]}(\mathcal{I}_z) = 0$. On the other hand, for $|N\rangle$, we have

$$\Gamma_0^{[n]} = 0, \quad \Gamma_\pm^{[n]} = 1, \quad \Lambda^{[a]} = 1. \tag{5.50}$$

Then we find $\theta^{[0]}(\mathcal{I}_z) + \phi^{[1/2]}(\mathcal{I}_z) = \pi$. This establishes that, under the $\mathcal{I}_z$ symmetry, the two states $|D\rangle$ and $|N\rangle$ belong to distinct phases, which are always separated by a quantum phase transition.

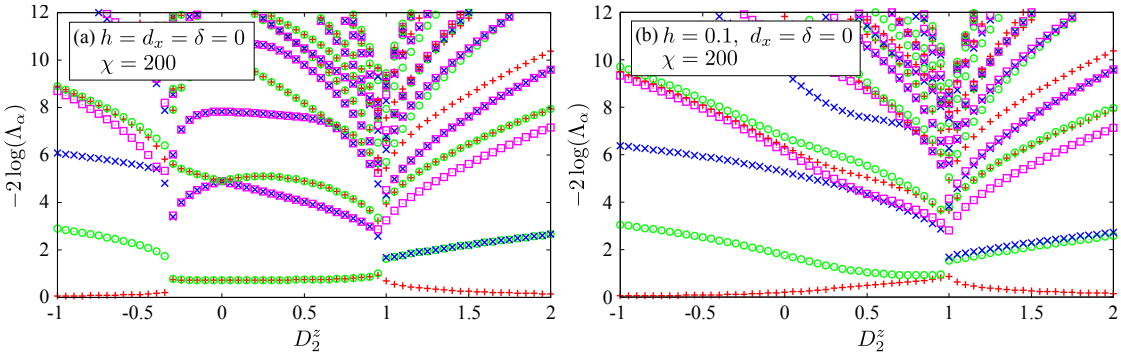

Figure 5.9: Low-lying entanglement spectra as functions of D_2^z for (a) $h = d_x = \delta = 0$ and (b) $h = 0.1$, $d_x = \delta = 0$ in the spin-1 model (5.20). Both data are obtained with $\chi = 200$.

One can also extract $\theta^{[0]}(\mathcal{I}_z) + \phi^{[1/2]}(\mathcal{I}_z)$ from the AKLT state. Under the $\mathcal{I}_z$ symmetry, the matrices $\Gamma^{[n]}$ given in Sec. 2.3.4 transform as

$$\Gamma_x^{[n]} \to -\sigma_x, \quad \Gamma_y^{[n]} \to \sigma_y, \quad \Gamma_z^{[n]} \to \sigma_z. \tag{5.51}$$

These transformations are brought together in a single expression,

$$\Gamma_m^{[n]} \to -\sigma_x \Gamma_m^{[n]} \sigma_x. \tag{5.52}$$

From this we can read $e^{i\theta^{[0]}(\mathcal{I}_z)} = -1$ and $U^{[a]}(\mathcal{I}_z) = \sigma_x$. Finally, we obtain $\theta^{[0]}(\mathcal{I}_z) = \pi$ and $\phi^{[1/2]}(\mathcal{I}_z) = 0$, and thus $\theta^{[0]}(\mathcal{I}_z) + \phi^{[1/2]}(\mathcal{I}_z) = \pi$. Thus, the AKLT state and $|D\rangle$ belong to distinct phases separated by a phase transition under $\mathcal{I}_z$. Under $\mathcal{I}_x \equiv \mathcal{I}_s \times \mathcal{R}_x$ and $\mathcal{I}_y \equiv \mathcal{I}_s \times \mathcal{R}_y$, the AKLT state also has $\theta^{[0]}(\mathcal{I}_x) = \theta^{[0]}(\mathcal{I}_y) = \pi$.

As the symmetry $\mathcal{I}_z$ is not related to the projective representation formed by $U^{[a]}(\mathcal{I}_z)$, the elements of $\Lambda^{[a]}$, i.e. the entanglement spectrum [see Eq. (2.77)] under a bipartition does not show any nontrivial degenerate structure. This can be seen from the numerical simulation on the spin-1 model (5.20). For $h = 0$ [see Fig. 5.9 (a)], the Haldane phase ($-0.3 \lesssim D_2^z \lesssim 1$) exhibits two-fold degeneracy in the entanglement spectrum since they are associated with nontrivial projective representations of $\mathcal{T}$, $\mathcal{I}_b$, and $\mathcal{D}_2$. On the other hand, there is no particular feature in the antiferromagnetic phase ($D_2^z \lesssim -0.3$) and the large-D phase ($D_2^z \gtrsim 1$). Once $h \neq 0$ is turned on [see Fig. 5.9 (b)], the nontrivial degenerate structure in the entanglement spectrum is completely absent in the whole phase diagram, since there is no symmetry associated with nontrivial projective representations.

5.3.3 Construction of string order parameter

As in the case of the Haldane phase, no local order parameter distinguishes these trivial phases. However, using the MPS framework, we can directly derive *non-local* order parameters [161] that are sensitive to the phase factor $\theta^{[0]}(\mathcal{I}_z) + \phi^{[1/2]}(\mathcal{I}_z)$. In particular, we can define an operator $\mathcal{I}_z(2p+1)$ that inverts a block of $2p+1$ consecutive sites and applies $\mathcal{R}_z$ on it. For p much larger than the correlation length, we find that

$$\mathcal{O}_s(p) = \langle\psi|\mathcal{I}_z(2p+1)|\psi\rangle \approx e^{i(\theta^{[0]}(\mathcal{I}_z)+\phi^{[1/2]}(\mathcal{I}_z))}\mathrm{Tr}\left[\Lambda^4\right]. \tag{5.53}$$

Here we have assumed two-site translational invariance for the actual numerical simulation using iDMRG.

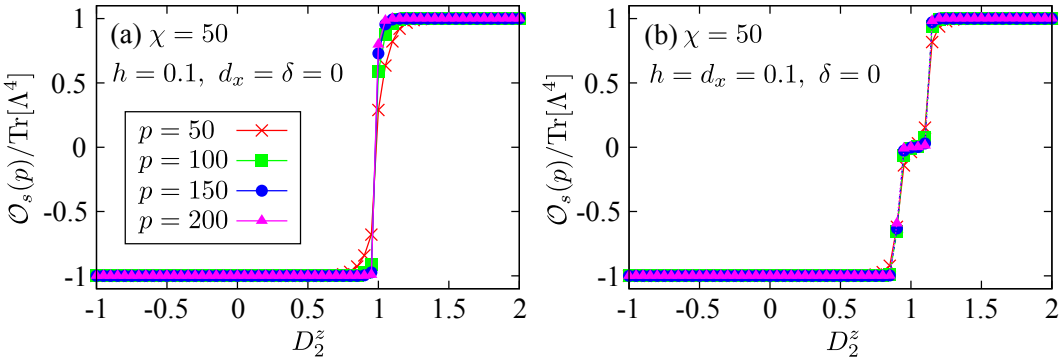

Figure 5.10: String order parameters $\mathcal{O}_s(p)$ defined in Eq. (5.53) are calculated for the spin-1 chain (5.20), as functions of D_2^z. They are normalized by $\mathrm{Tr}[\Lambda^4]$. We fix the bond dimension $\chi = 50$ and vary the length of block from $p = 50$ to 200. We use the parameters (a) $h = 0.1$, $d_x = \delta = 0$ and (b) $h = d_x = 0.1$, $\delta = 0$.

In the spin-1 model (5.20), Fig. 5.10 shows that the two different trivial phases are indeed distinguished by $\mathcal{O}_s(p)/\mathrm{Tr}[\Lambda^4]$. In the one phase that is smoothly connected to the Haldane phase or $|N\rangle$, $\mathcal{O}_s(p) = -1$ since $\theta^{[0]}(\mathcal{I}_z) + \phi^{[1/2]}(\mathcal{I}_z) = \pi$, while in the other phase connected to $|D\rangle$, $\mathcal{O}_s(p) = 1$ since $\theta^{[0]}(\mathcal{I}_z) + \phi^{[1/2]}(\mathcal{I}_z) = 0$. For $d_x \neq 0$, an intermediate phase appears between those phases, where the symmetry $\mathcal{I}_z$ is spontaneously broken. In that phase, $\mathcal{O}_s(p) = 0$ since the overlap between $\mathcal{I}_z(2p+1)\,|\psi\rangle$ and $|\psi\rangle$ goes to zero in the limit $p \to \infty$.

In the following, we graphically explain how this string order parameter detects $\theta^{[0]}(\mathcal{I}_z) + \phi^{[1/2]}(\mathcal{I}_z)$. The matrices Γ and Λ are graphically represented as

$$(\Gamma_m)_{\alpha\beta} =$$ 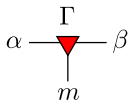 $$,\qquad \Lambda_\alpha =$$ 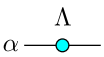 $$. \tag{5.54}$$

In general, the horizontal and vertical lines respectively correspond to the indices of the bond dimension (α, β) and the physical dimension (m). The state $|\psi\rangle$ in the MPS form (5.25) is represented as

$$|\psi\rangle = \sum_{\{m_n\}} \left(\cdots \Lambda\Gamma_{m_{-1}}\Lambda\Gamma_{m_0}\Lambda\Gamma_{m_1}\Lambda\cdots\right) |\cdots m_{-1}m_0m_1\cdots\rangle$$

$$=$$ 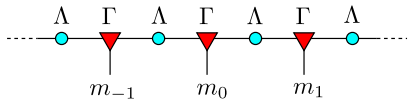 $$. \tag{5.55}$$

Here we prescribe that the connected line represents the summation over its index. Then the canonical condition (5.27) is denoted as

$$\sum_m \Gamma_m \Lambda^2 (\Gamma_m)^\dagger = \mathbb{I}_\chi \quad \Leftrightarrow$$ 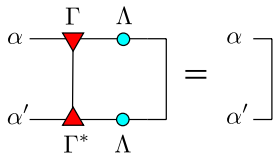 $$,$$

$$\sum_m (\Gamma_m)^\dagger \Lambda^2 \Gamma_m = \mathbb{I}_\chi \quad \Leftrightarrow$$ 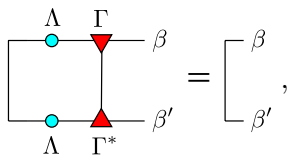 $$, \tag{5.56}$$

where the upside-down triangle represents the complex conjugation of the matrix Γ.

Now it is ready to write down the string order parameter (5.53). Applying $\mathcal{I}_z(2p+1)$ on $|\psi\rangle$ and taking an inner product with $\langle\psi|$, we obtain

$\mathcal{O}_s(p) =$ 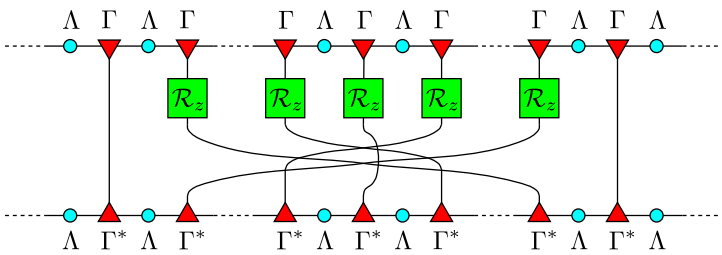

. (5.57)

Using Eq. (5.32), we obtain

$\mathcal{O}_s(p) =$ 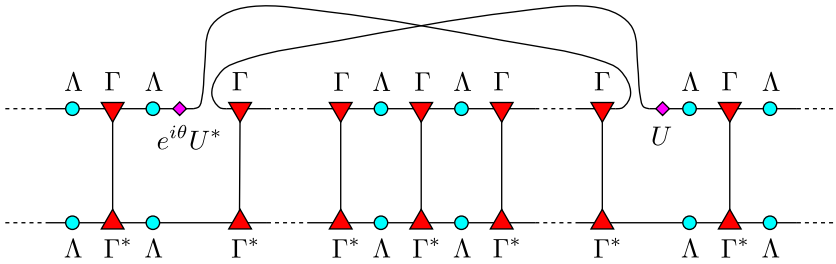

. (5.58)

Two-site translational invariance ensures that $\theta^{[n]}(\mathcal{I}_z)$ cancels with $\theta^{[-n]}(\mathcal{I}_z)$ except for $n=0$. For a sufficiently large system, using Eq. (5.56), we can contract the transfer matrices with the identities from the outer sides. Thus, we have

$\mathcal{O}_s(p) \approx$ 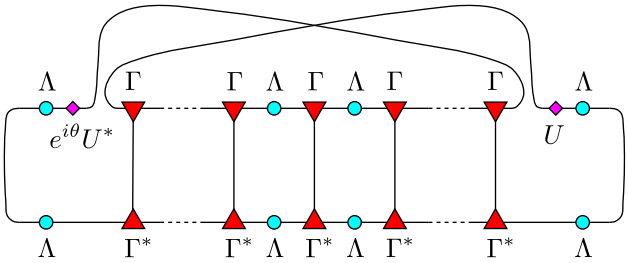

. (5.59)

For a large block size $2p+1$, we can also contract the transfer matrices with the identities from the inner sides and then obtain

$\mathcal{O}_s(p) \approx$ 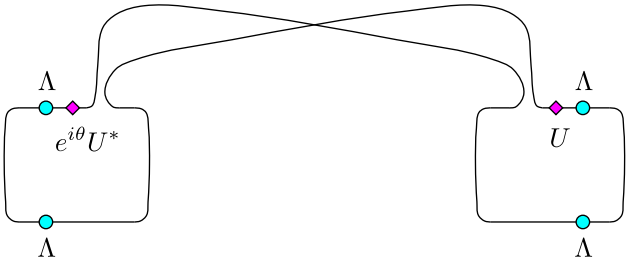

. (5.60)

Thus we reach

$$\begin{aligned}\mathcal{O}_s(p) &\approx e^{i\theta^{[0]}(\mathcal{I}_z)}\mathrm{Tr}\left[\left(\Lambda^{[-p-1/2]}\right)^2 U^{[p+1/2]}(\mathcal{I}_z)\left(U^{[-p-1/2]}(\mathcal{I}_z)\right)^*\left(\Lambda^{[p+1/2]}\right)^2\right]\\ &= e^{i(\theta^{[0]}(\mathcal{I}_z)+\phi^{[p+1/2]}(\mathcal{I}_z))}\mathrm{Tr}\left[(\Lambda^{[p+1/2]})^4\right].\end{aligned} \tag{5.61}$$

From two-site translational invariance, for even p, we obtain

$$\mathcal{O}_s(p) \approx e^{i(\theta^{[0]}(\mathcal{I}_z)+\phi^{[1/2]}(\mathcal{I}_z))}\mathrm{Tr}\left[(\Lambda^{[1/2]})^4\right]. \tag{5.62}$$

5.3.4 Remarks on lattice symmetries and finite systems

As reviewed in Sec. 2.3.4, three symmetries $\mathcal{T}$, $\mathcal{D}_2$, and $\mathcal{I}_b$, which protect the Haldane phase, form the nontrivial projective representations on a virtual space living on each bond. These projective representations result from the formation of spin singlets (or generally entangled pairs) in the ground state. For $\mathcal{T}$ and $\mathcal{D}_2$, the corresponding projective representations can be seen as the representations on spin-1/2's constituting the spin singlets. For bond-centered inversion $\mathcal{I}_b$, the projective representation comes from the odd parity of a singlet wave function. If we put the AKLT state on a finite periodic chain with an *odd* number of sites, the wave function takes the odd parity under $\mathcal{I}_b$ since the reflection plane cut one singlet bond. [2] On the other hand, the product state $|D\rangle$ has the even parity. Therefore, if the ground state of a Hamiltonian $H(g)$ is smoothly connected to the AKLT state for $g = 0$ while to the product state $|D\rangle$ for $g = 1$, there must be a level crossing in the ground-state energy between $g = 0$ and 1 since the two states have different parities (see also Ref. [18]). This is not the case for the periodic chain with an *even* number of sites. Since the two states share the same parity in this case, the two energy levels in general do not cross each other.

A similar discussion can be applied to the case of the combined symmetry $\mathcal{I}_z$. Here let us put the system on a open chain with an odd number of sites. Under $\mathcal{I}_z$, the product state $|D\rangle$ has the even parity while the other product state $|N\rangle$ takes the odd parity. Thus we again expect the level crossing between two ground states connected to these product states. For an even number of sites, these two states share the same even parity and no level crossing occurs.

In general, it is not obvious that this level crossings on finite chains continue or are replaced by continuous phase transitions in the thermodynamic limit. Above analyses based on the effective field theory and the MPS formalism directly dealt with the infinite system and indeed showed that these naive expectations are correct. However we can also construct a counterexample. Even without site-centered inversion $\mathcal{I}_s$, the two states $|D\rangle$ and $|N\rangle$ have different parities on odd-site chains under only $\mathcal{R}_z$, which is the π spin rotation around the z axis. Thus there must be a level crossing between the two states. But the above numerical analysis showed that the two states are adiabatically connected each other by introducing the dimerization even if we keep $\mathcal{R}_z$.

As known for symmetry breaking phases, we have to carefully analyze the ground state in the thermodynamic limit from the knowledge on finite-size systems. For example, the Majumdar-Ghosh model on an open chain has the four-fold degenerate ground state for odd sites while five-fold for even sites. Nevertheless, the ground state in the thermodynamic limit has only two-fold degeneracy, as discussed in Ref. [8]. Roughly speaking, this is because the recombination of the degenerate ground state can happen in the thermodynamic limit. This may also apply to the above discussions on the level crossing in finite-size systems but we do not proceed further discussions in this thesis.

We also note that the bond-centered and site-centered inversion symmetries cannot coexist on an open chain with a finite number of sites. The former is only allowed for even sites while the latter is allowed for odd sites. This means that two operations $\mathcal{I}_b$ and $\mathcal{I}_s$ do not close among themselves; to obtain a closed form, we need to add translation (see also Sec. 3.3.2) and it conflicts with the open boundary condition on finite chains. To resume the situation

[2] The open boundary condition creates two free spin-1/2's at the ends of the chain for the AKLT state. Since they can form either singlet or triplet, the parity of the wave function can be even or odd. To avoid this ambiguity, we here consider the periodic boundary condition, which ensures that the two spin-1/2's form triplet and the resulting parity becomes odd.

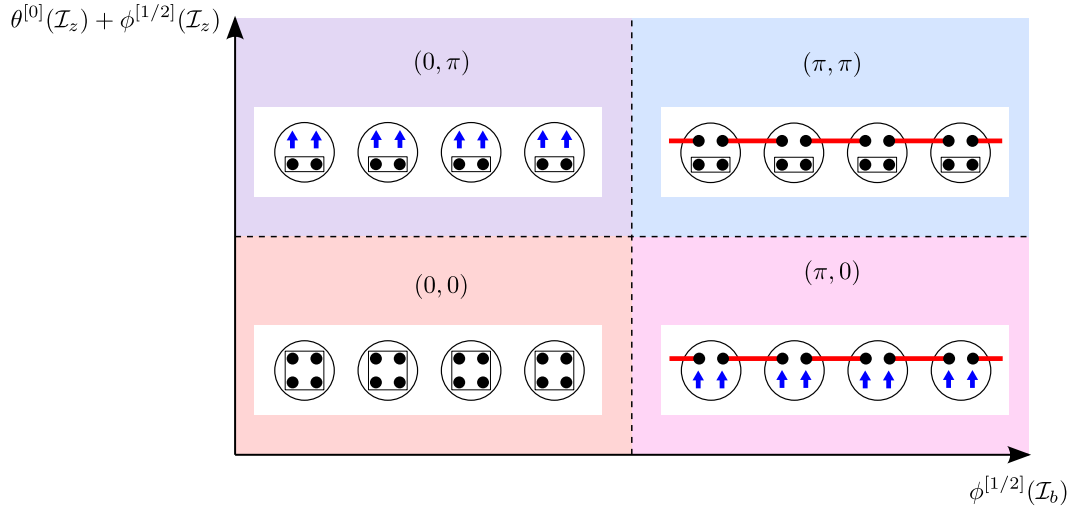

Figure 5.11: Four SPT phases realized under the two inversion symmetries $\mathcal{I}_b$ and $\mathcal{I}_z$. They are distinguished by two phases $(\phi^{[1/2]}(\mathcal{I}_b), \theta^{[0]}(\mathcal{I}_z) + \phi^{[1/2]}(\mathcal{I}_z))$. We adopted the representations of the states in Fig. 5.5.

in which both inversion symmetries exist, we need to consider the infinite chain. This is also true for any space-group symmetry, which is only meaningful in infinite lattice systems. Therefore, even if the Hamiltonian for a finite system only possesses one of the two inversion symmetries $\mathcal{I}_b$ or $\mathcal{I}_s$, it does not necessarily mean that an SPT phase is only protected by either of them in the *thermodynamic limit*, where the full space-group symmetry is recovered. In our case, the distinction between the Haldane and large-D phases, in the sense that they are separated by a gap closing, is protected by both $\mathcal{I}_b$ and $\mathcal{I}_z$. However they can in principle take different roles. Indeed, we can have at least $2 \times 2 = 4$ distinct SPT phases in the presence of both $\mathcal{I}_b$ and $\mathcal{I}_z$. Those examples on a spin-2 chain are shown in Fig. 5.11.

5.3.5 Lieb-Schultz-Mattis theorem on MPS

We prove a generalization of the Lieb-Schultz-Mattis theorem predicted by the bosonization approach in Sec. 3.4. It states that the ground state of a half-odd-integer spin system with (i) translational invariance and either time reversal or $Z_2 \times Z_2$ symmetries or (ii) site-centered inversion symmetry and either time reversal or $Z_2 \times Z_2$ symmetry is gapless or degenerate with spontaneous symmetry breaking. In Ref. [14], Chen, Gu, and Wen argued that a translational-invariant system with an on-site symmetry with a projective representation has a gapless or degenerate ground state. This includes the statement (i). Along the same line as they discussed, we can also prove that a system with site-centered inversion symmetry and an on-site symmetry with a projective representation has a gapless or degenerate ground state. This is a stronger statement than (ii). In the following, we refer to Appendix D of Ref. [14].

First, we consider an on-site symmetry G that may form a projective representation on the physical Hilbert space,

$$u^{[n]}(g_1)u^{[n]}(g_2) = e^{-i\rho^{[n]}(g_1,g_2)}u^{[n]}(g_1 g_2), \tag{5.63}$$

where $g_1, g_2 \in G$. Here, we do not assume any lattice symmetry such as translational invari-

ance or inversion symmetry. Acting $u^{[n]}(g_1g_2)$ on the matrix $\Gamma^{[n]}$, we obtain

$$\begin{aligned}
&\sum_m u^{[n]}_{mm'}(g_1g_2)\Gamma^{[n]}_{m'} \\
&= \sum_{m',m''} e^{i\rho^{[n]}(g_1,g_2)} u^{[n]}_{mm'}(g_1) u^{[n]}_{m'm''}(g_2)\Gamma^{[n]}_{m''} \\
&= \sum_{m'} e^{i\rho^{[n]}(g_1,g_2)} u^{[n]}_{mm'}(g_1) e^{i\theta^{[n]}(g_2)} \left(U^{[n-1/2]}(g_2)\right)^\dagger \Gamma^{[n]}_{m'} U^{[n+1/2]}(g_2) \\
&= e^{i\rho^{[n]}(g_1,g_2)} e^{i(\theta^{[n]}(g_1)+\theta^{[n]}(g_2))} \left(U^{[n-1/2]}(g_2)\right)^\dagger \left(U^{[n-1/2]}(g_1)\right)^\dagger \Gamma^{[n]}_{m} U^{[n+1/2]}(g_1) U^{[n+1/2]}(g_2).
\end{aligned} \tag{5.64}$$

On the other hand, we also obtain

$$\sum_m u^{[n]}_{mm'}(g_1g_2)\Gamma^{[n]}_{m'} = e^{i\theta^{[n]}(g_1g_2)} \left(U^{[n-1/2]}(g_1g_2)\right)^\dagger \Gamma^{[n]}_{m} U^{[n+1/2]}(g_1g_2). \tag{5.65}$$

Equating the left-hand sides of Eqs. (5.64) and (5.65), we have

$$\begin{aligned}
&e^{i\rho^{[n]}(g_1,g_2)} \left(U^{[n-1/2]}(g_2)\right)^\dagger \left(U^{[n-1/2]}(g_1)\right)^\dagger \Gamma^{[n]}_{m} U^{[n+1/2]}(g_1) U^{[n+1/2]}(g_2) \\
&= \left(U^{[n-1/2]}(g_1g_2)\right)^\dagger \Gamma^{[n]}_{m} U^{[n+1/2]}(g_1g_2).
\end{aligned} \tag{5.66}$$

Since $e^{i\theta^{[n]}(g)}$ is a 1D linear representation of G, we used

$$\theta^{[n]}(g_1g_2) = \theta^{[n]}(g_1) + \theta^{[n]}(g_2). \tag{5.67}$$

The substitution of Eq. (5.66) into the canonical condition (5.30) yields

$$\begin{aligned}
&\mathcal{E}^{[n]}_L \left(U^{[n-1/2]}(g_1)U^{[n-1/2]}(g_2) \left(U^{[n-1/2]}(g_1g_2)\right)^\dagger\right) \\
&= e^{i\rho^{[n]}(g_1,g_2)} U^{[n+1/2]}(g_1)U^{[n+1/2]}(g_2) \left(U^{[n+1/2]}(g_1g_2)\right)^\dagger.
\end{aligned} \tag{5.68}$$

As discussed in Sec. 5.3.2, the assumption of the pure MPS implies that

$$U^{[n-1/2]}(g_1)U^{[n-1/2]}(g_2) = e^{i\rho^{[n-1/2]}(g_1,g_2)} U^{[n-1/2]}(g_1g_2), \tag{5.69}$$

$$U^{[n+1/2]}(g_1)U^{[n+1/2]}(g_2) = e^{i\rho^{[n+1/2]}(g_1,g_2)} U^{[n+1/2]}(g_1g_2), \tag{5.70}$$

where $\rho^{[n\pm1/2]}(g_1,g_2)$ are some phases. These relations are nothing but the multiplication rule of the projective representation $U^{[n\pm1/2]}(g)$. Each projective representation is related by

$$\rho^{[n]}(g_1,g_2) = \rho^{[n-1/2]}(g_1,g_2) - \rho^{[n+1/2]}(g_1,g_2). \tag{5.71}$$

Let us assume that $u^{[n]}(g)$ forms a nontrivial projective representation with $\rho^{[n]}(g_1,g_2) \neq 0$. If we impose translational invariance on the state $|\psi\rangle$, we have

$$U^{[n-1/2]}(g) = U^{[n+1/2]}(g), \tag{5.72}$$

and correspondingly

$$\rho^{[n-1/2]}(g_1, g_2) = \rho^{[n+1/2]}(g_1, g_2). \tag{5.73}$$

This contradicts with $\rho^{[n]}(g_1, g_2) \neq 0$. Thus a state with translational invariance and an on-site symmetry with a projective representation cannot be unique and gapped. Similarly, if there is site-centered inversion symmetry with respect to the site $n = 0$, we have

$$U^{[-n-1/2]}(g) = U^{[n+1/2]}(g). \tag{5.74}$$

This leads to

$$\rho^{[-1/2]}(g_1, g_2) = \rho^{[+1/2]}(g_1, g_2), \tag{5.75}$$

and contradicts with $\rho^{[0]}(g_1, g_2) \neq 0$. Therefore, a state with site-centered inversion symmetry and an on-site symmetry with a projective representation cannot be unique and gapped.

Next, we consider time reversal symmetry that satisfies $(\mathcal{T}^{[n]})^2 = \alpha^{[n]}(\mathcal{T})$ with $\alpha^{[n]}(\mathcal{T}) = \pm 1$ on the physical Hilbert space of each site. Applying $\mathcal{T}$ twice on $\Gamma^{[n]}$, we obtain

$$\alpha^{[n]}(\mathcal{T})\Gamma_m^{[n]} = \left(U^{[n-1/2]}(\mathcal{T})\right)^T \left(U^{[n-1/2]}(\mathcal{T})\right)^\dagger \Gamma_m^{[n]} U^{[n+1/2]}(\mathcal{T}) \left(U^{[n+1/2]}(\mathcal{T})\right)^*. \tag{5.76}$$

Substituting this into the canonical condition (5.30), we have

$$\mathcal{E}_L^{[n]}\left(U^{[n-1/2]}(\mathcal{T})\left(U^{[n-1/2]}(\mathcal{T})\right)^*\right) = \alpha^{[n]}(\mathcal{T})U^{[n+1/2]}(\mathcal{T})\left(U^{[n+1/2]}(\mathcal{T})\right)^*. \tag{5.77}$$

From the assumption of the pure MPS, we should have

$$U^{[n-1/2]}(\mathcal{T})\left(U^{[n-1/2]}(\mathcal{T})\right)^* = \beta^{[n-1/2]}(\mathcal{T})\mathbb{I}_{\chi_{n-1/2}}, \tag{5.78}$$

$$U^{[n+1/2]}(\mathcal{T})\left(U^{[n+1/2]}(\mathcal{T})\right)^* = \beta^{[n+1/2]}(\mathcal{T})\mathbb{I}_{\chi_{n+1/2}}, \tag{5.79}$$

where $\beta^{[n-1/2]}(\mathcal{T}) = \pm 1$ and $\beta^{[n+1/2]}(\mathcal{T}) = \pm 1$. These relations are the multiplication rule of the projective representation of time reversal symmetry. They also satisfy

$$\alpha^{[n]}(\mathcal{T}) = \beta^{[n-1/2]}(\mathcal{T})\beta^{[n+1/2]}(\mathcal{T}). \tag{5.80}$$

Let us suppose $\alpha^{[n]}(\mathcal{T}) = -1$ as time reversal symmetry acts on half-odd-integer spin. As in the previous case, if the state $|\psi\rangle$ is translational invariant, we have

$$\beta^{[n-1/2]}(\mathcal{T}) = \beta^{[n+1/2]}(\mathcal{T}). \tag{5.81}$$

This contradicts with $\alpha^{[n]}(\mathcal{T}) = -1$. Also for the state $|\psi\rangle$ invariant under site-centered inversion with respect to $n = 0$, we have

$$\beta^{[-1/2]}(\mathcal{T}) = \beta^{[+1/2]}(\mathcal{T}), \tag{5.82}$$

This contradicts with $\alpha^{[0]}(\mathcal{T}) = -1$. Therefore, a half-odd-integer spin system with time reversal symmetry cannot have a unique gapped ground state if the systems is translational invariant or has site-centered inversion symmetry.

5.A Self-dual sine-Gordon models

In this appendix, following [148], we supplement the physical properties on the self-dual sine-Gordon model with $\beta^2 = 4\pi$ [Eq. (5.6)] and $\beta^2 = 2\pi$ [Eq. (5.9)]. For the $\beta^2 = 4\pi$ self-dual sine-Gordon model,

$$H_{\beta^2=4\pi} = \frac{v}{2}\int dx\left[(\partial_x\theta)^2 + (\partial_x\phi)^2\right] + g\int dx\left[\cos(\sqrt{4\pi}\phi) + \cos(\sqrt{4\pi}\theta)\right], \tag{5.83}$$

both the vertex operators have the same scaling dimension 1. Since this is the same as the scaling dimension of a fermionic field, introducing the refermionization formulas [see Eq. (3.58)],

$$\frac{\xi_1 + i\xi_2}{\sqrt{2}} = \frac{1}{\sqrt{2\pi a_0}}e^{-i\sqrt{\pi}(\phi-\theta)}, \quad \frac{\bar{\xi}_1 + i\bar{\xi}_2}{\sqrt{2}} = \frac{1}{\sqrt{2\pi a_0}}e^{i\sqrt{\pi}(\phi+\theta)}, \tag{5.84}$$

one can rewrite the vertex operators as

$$\begin{aligned}\cos(\sqrt{4\pi}\phi) &= -i\pi a_0(\xi_1\bar{\xi}_1 + \xi_2\bar{\xi}_2),\\ \cos(\sqrt{4\pi}\theta) &= -i\pi a_0(\xi_1\bar{\xi}_1 - \xi_2\bar{\xi}_2),\end{aligned} \tag{5.85}$$

where ξ_α ($\bar{\xi}_\alpha$) is a right-moving (left-moving) Majorana fermion. The free part of Eq. (5.83) is also rewritten by the Majorana fermions, through the relation with a Dirac fermion (3.43), as

$$\frac{v}{2}\int dx\left[(\partial_x\theta)^2 + (\partial_x\phi)^2\right] = -\frac{iv}{2}\int dx\sum_{\alpha=1}^{2}(\xi_\alpha\partial_x\xi_\alpha - \bar{\xi}_\alpha\partial_x\bar{\xi}_\alpha). \tag{5.86}$$

Then we find

$$H_{\beta^2=4\pi} = -\frac{iv}{2}\int dx\sum_{\alpha=1}^{2}(\xi_\alpha\partial_x\xi_\alpha - \bar{\xi}_\alpha\partial_x\bar{\xi}_\alpha) - i2\pi a_0 g\int dx\ \xi_1\bar{\xi}_1. \tag{5.87}$$

Thus one Majorana fermion is massive while the other is massless. Since the former corresponds to the off-critical two-dimensional Ising model while the latter to the critical Ising model, the $\beta^2 = 4\pi$ self-dual sine-Gordon model represents the Ising critical point with central charge $c = 1/2$.

For the $\beta^2 = 2\pi$ self-dual sine-Gordon model,

$$H_{\beta^2=2\pi} = \frac{v}{2}\int dx\left[(\partial_x\theta)^2 + (\partial_x\phi)^2\right] + g\int dx\left[\cos(\sqrt{2\pi}\phi) + \cos(\sqrt{2\pi}\theta)\right], \tag{5.88}$$

both the vertex operators have the same scaling dimension 1/2. One easiest way to recognize that this model is massive is to consider the $s = 1/2$ Heisenberg model with a dimerization and staggered magnetic field along the x axis,

$$H = \sum_i\left[J\vec{s}_i\cdot\vec{s}_{i+1} + \delta(-1)^i\vec{s}_i\cdot\vec{s}_{i+1} + h(-1)^i s_i^x\right]. \tag{5.89}$$

Using the bosonization formulas for the spin operator (3.14) and dimerization operator (4.31), for $\delta = h \ll J$, we obtain

$$H = \frac{v_s}{2}\int dx\left[(\partial_x\theta)^2 + (\partial_x\phi)^2\right] + b_0 h\int dx\left[\cos(\sqrt{2\pi}\phi) + \cos(\sqrt{2\pi}\theta)\right]. \tag{5.90}$$

where $v_s = \pi J a_0/2$ and $b_0 = d$ at the SU(2) symmetric point. By making a unitary transformation $e^{i(\pi/2)s^y}$, s^x is transformed into s^z and then we find

$$\begin{aligned} H &= \frac{v_s}{2}\int dx\left[(\partial_x\theta)^2 + (\partial_x\phi)^2\right] + b_0 h\int dx\left[\cos(\sqrt{2\pi}\phi) - \sin(\sqrt{2\pi}\phi)\right] \\ &= \frac{v_s}{2}\int dx\left[(\partial_x\theta)^2 + (\partial_x\phi)^2\right] + \sqrt{2}b_0 h\int dx\cos(\sqrt{2\pi}\phi + \frac{\pi}{4}). \end{aligned} \tag{5.91}$$

Thus one can immediately see that this model is massive.

Chapter 6

Summary

In this thesis, we considered the phase transition between different disordered phases, realized in 1D quantum spin systems, from the point of view of symmetry. We refined the field-theoretical argument based on the Abelian bosonization approach, originally given by Schulz. Indeed, we clarified the following facts on his effective field theory:

(i) It is consistent with the compactification of the bosonic field and symmetries of the Hamiltonian and not necessarily relying on perturbation theory.

(ii) It describes the phase transitions between VBS phases realized in various 1D spin systems.

(iii) Those phase transitions are protected by one of four symmetries: time reversal, bond-centered inversion, dihedral group of spin rotations, and site-centered inversion combined with a spin rotation.

Regarding (i), we carefully considered the compactification condition on multi-component bosonic fields and identified the condition for a single bosonic field entering the effective field theory. We further listed the transformation laws of the bosonic field under the symmetries relevant in our ladder model. These physical requirements are all consistent with the effective field theory obtained by perturbation theory. As a bonus, we also proposed an extension of the Lieb-Schultz-Mattis theorem:

(v) The ground states of half-odd-integer spin systems with (a) translational invariance and either time reversal or dihedral group symmetries or (b) site-centered inversion symmetry and either time reversal or dihedral group symmetry are either gapless or degenerate.

Regarding (ii), we showed that, for the integer-spin-S XXZ chain with an on-site uniaxial anisotropy, there must be a phase transition between the odd-S Haldane and large-D phases, while the even-S and large-D phases can be adiabatically connected. Similar conclusion was also made for the distinction between the Haldane phase and the rung-singlet phase on the even-N-leg spin-1/2 ladder. For the dimerized ladders systems, we found that the phase transition between VBS phases occurs when the parity of the number of singlets under a certain spatial cut is changed. All these results are explained by the presence or absence of the sign change in the coupling constant of the effective field theory, combined with perturbation theory.

Regarding (iii), we identified the four symmetries protecting the distinction between VBS phases on the effective field theory, by considering the interactions allowed by the symmetry

and using the knowledge on self-dual sine-Gordon models. We also proposed a microscopic Hamiltonian that has two distinct phases protected by the site-centered inversion symmetry combined with a spin rotation. We examined this model and confirmed the existence of the two distinct phases, by perturbation theory and numerical simulations using infinite density-matrix renormalization group. We further proved their existence by a more rigorous approach based on the MPS. We clarified the meaning of a pure MPS as a physical requirement in the absence of translational invariance. By using the pure MPS, we showed the existence of two distinct trivial phases; they are trivial in the sense that they do not have nontrivial entanglement structure, yet they are always separated by a quantum phase transition under the site-centered inversion symmetry. The corresponding nonlocal order parameter was constructed to detect these phases. The statement (iv) under (b) was also proven in this formalism.

These results indicate that two apparently different approaches, *field* theory and the MPS defined on a *lattice*, give perfectly consistent results on the symmetry-protected nature of the Haldane phase and general VBS phase. Such an interesting connection between field and lattice theories may be found for other 1D SPT phases. Although there are no ifs in history, this also suggest that one could find the SPT phase in even more earlier stage, without waiting for the revaluation of the MPS. Another interesting remark is the role of point-group symmetries on the classification of topological phases in higher dimensions. There are not only inversion but many point-group symmetries such as lattice rotations and reflections. They may lead to other nontrivial but distinct "trivial" phases (in the above sense), as proposed in Refs. [49, 50], and a consistency condition on the existence of certain topological order [162].

Bibliography

[1] F. Verstraete, J. I. Cirac, J. I. Latorre, E. Rico, and M. M. Wolf, *Renormalization-Group Transformations on Quantum States*, Phys. Rev. Lett. **94**, 140601 (2005).

[2] X. Chen, Z.-C. Gu, and X.-G. Wen, *Local unitary transformation, long-range quantum entanglement, wave function renormalization, and topological order*, Phys. Rev. B **82**, 155138 (2010).

[3] N. Schuch, D. Perez-Garcia, and I. Cirac, *Classifying quantum phases using matrix product states and projected entangled pair states*, Phys. Rev. B **84**, 165139 (2011).

[4] Z.-C. Gu and X.-G. Wen, *Tensor-entanglement-filtering renormalization approach and symmetry-protected topological order*, Phys. Rev. B **80**, 155131 (2009).

[5] F. D. M. Haldane, *Continuum dynamics of the 1-D Heisenberg antiferromagnet: Identification with the $O(3)$ nonlinear sigma model*, Phys. Lett. A **93**, 464 (1983).

[6] F. D. M. Haldane, *Nonlinear Field Theory of Large-Spin Heisenberg Antiferromagnets: Semiclassically Quantized Solitons of the One-Dimensional Easy-Axis Néel State*, Phys. Rev. Lett. **50**, 1153 (1983).

[7] I. Affleck, T. Kennedy, E. H. Lieb, and H. Tasaki, *Rigorous results on valence-bond ground states in antiferromagnets*, Phys. Rev. Lett. **59**, 799 (1987).

[8] I. Affleck, T. Kennedy, E. H. Lieb, and H. Tasaki, *Valence bond ground states in isotropic quantum antiferromagnets*, Comm. Math. Phys. **115**, 477 (1988).

[9] M. den Nijs and K. Rommelse, *Preroughening transitions in crystal surfaces and valence-bond phases in quantum spin chains*, Phys. Rev. B **40**, 4709 (1989).

[10] T. Kennedy and H. Tasaki, *Hidden $Z_2 \times Z_2$ symmetry breaking in Haldane-gap antiferromagnets*, Phys. Rev. B **45**, 304 (1992).

[11] T. Kennedy and H. Tasaki, *Hidden symmetry breaking and the Haldane phase in $S = 1$ quantum spin chains*, Comm. Math. Phys. **147**, 431 (1992).

[12] T. Kennedy, *Exact diagonalisations of open spin-1 chains*, J. Phys.: Condens. Matter **2**, 5737 (1990).

[13] F. Pollmann, A. M. Turner, E. Berg, and M. Oshikawa, *Entanglement spectrum of a topological phase in one dimension*, Phys. Rev. B **81**, 064439 (2010).

[14] X. Chen, Z.-C. Gu, and X.-G. Wen, *Classification of gapped symmetric phases in one-dimensional spin systems*, Phys. Rev. B **83**, 035107 (2011).

[15] X. Chen, Z.-C. Gu, and X.-G. Wen, *Complete classification of one-dimensional gapped quantum phases in interacting spin systems*, Phys. Rev. B **84**, 235128 (2011).

[16] K. Duivenvoorden and T. Quella, *Topological phases of spin chains*, Phys. Rev. B **87**, 125145 (2013).

[17] H. J. Schulz, *Phase diagrams and correlation exponents for quantum spin chains of arbitrary spin quantum number*, Phys. Rev. B **34**, 6372 (1986).

[18] F. Pollmann, E. Berg, A. M. Turner, and M. Oshikawa, *Symmetry protection of topological phases in one-dimensional quantum spin systems*, Phys. Rev. B **85**, 075125 (2012).

[19] E. Lieb, T. Schultz, and D. Mattis, *Two soluble models of an antiferromagnetic chain*, Ann. Phys. (N. Y.) **16**, 407 (1961).

[20] I. Affleck and E. H. Lieb, *A proof of part of Haldane's conjecture on spin chains*, Lett. Math. Phys. **12**, 57 (1986).

[21] N. Goldenfeld, *Lectures on phase transitions and the renormalization group* (Addison-Wesley, Reading, 1992)

[22] L. Onsager, *Crystal Statistics. I. A Two-Dimensional Model with an Order-Disorder Transition*, Phys. Rev. **65**, 117 (1944).

[23] X. G. Wen, *Vacuum degeneracy of chiral spin states in compactified space*, Phys. Rev. B **40**, 7387 (1989).

[24] A. Kitaev and J. Preskill, *Topological Entanglement Entropy*, Phys. Rev. Lett. **96**, 110404 (2006).

[25] M. Levin and X.-G. Wen, *Detecting Topological Order in a Ground State Wave Function*, Phys. Rev. Lett. **96**, 110405 (2006).

[26] L. Kong and X.-G. Wen, *Braided fusion categories, gravitational anomalies, and the mathematical framework for topological orders in any dimensions*, arXiv:1405.5858 (unpublished).

[27] X.-G. Wen, *Construction of bosonic symmetry-protected-trivial states and their topological terms via $G \times SO(\infty)$ non-linear σ-models*, arXiv:1410.8477 (unpublished).

[28] Y.-M. Lu and A. Vishwanath, *Theory and classification of interacting integer topological phases in two dimensions: A Chern-Simons approach*, Phys. Rev. B **86**, 125119 (2012).

[29] X. Chen, Z.-C. Gu, Z.-X. Liu, and X.-G. Wen, *Symmetry protected topological orders and the group cohomology of their symmetry group*, Phys. Rev. B **87**, 155114 (2013).

[30] O. M. Sule, X. Chen, and S. Ryu, *Symmetry-protected topological phases and orbifolds: Generalized Laughlin's argument*, Phys. Rev. B **88**, 075125 (2013).

[31] Z.-C. Gu and X.-G. Wen, *Symmetry-protected topological orders for interacting fermions: Fermionic topological nonlinear σ models and a special group supercohomology theory*, Phys. Rev. B **90**, 115141 (2014).

[32] Y.-Z. You and C. Xu, *Symmetry-protected topological states of interacting fermions and bosons*, Phys. Rev. B **90**, 245120 (2014).

[33] C. Wang and M. Levin, *Topological invariants for gauge theories and symmetry-protected topological phases*, arXiv:1412.1781 (unpublished).

[34] M. B. Hastings and T. Koma, *Spectral Gap and Exponential Decay of Correlations*, Comm. Math. Phys. **265**, 781 (2006).

[35] C. L. Kane and E. J. Mele, *Z_2 Topological Order and the Quantum Spin Hall Effect*, Phys. Rev. Lett. **95**, 146802 (2005).

[36] B. A. Bernevig, T. L. Hughes, and S.-C. Zhang, *Quantum Spin Hall Effect and Topological Phase Transition in HgTe Quantum Wells*, Science **314**, 1757 (2006).

[37] X. Chen, Z.-X. Liu, and X.-G. Wen, *Two-dimensional symmetry-protected topological orders and their protected gapless edge excitations*, Phys. Rev. B **84**, 235141 (2011).

[38] M. Levin and Z.-C. Gu, *Braiding statistics approach to symmetry-protected topological phases*, Phys. Rev. B **86**, 115109 (2012).

[39] X. Chen, Z.-C. Gu, Z.-X. Liu, and X.-G. Wen, *Symmetry-Protected Topological Orders in Interacting Bosonic Systems*, Science **338**, 1604 (2012).

[40] T. Senthil and M. Levin, *Integer Quantum Hall Effect for Bosons*, Phys. Rev. Lett. **110**, 046801 (2013).

[41] S. Furukawa and M. Ueda, *Integer Quantum Hall State in Two-Component Bose Gases in a Synthetic Magnetic Field*, Phys. Rev. Lett. **111**, 090401 (2013).

[42] L. Fu, C. L. Kane, and E. J. Mele, *Topological Insulators in Three Dimensions*, Phys. Rev. Lett. **98**, 106803 (2007).

[43] J. Moore and L. Balents, *Topological invariants of time-reversal-invariant band structures*, Phys. Rev. B **75**, 121306 (2007).

[44] H. Li and F. D. M. Haldane, *Entanglement Spectrum as a Generalization of Entanglement Entropy: Identification of Topological Order in Non-Abelian Fractional Quantum Hall Effect States*, Phys. Rev. Lett. **101**, 010504 (2008).

[45] L. Fidkowski, *Entanglement Spectrum of Topological Insulators and Superconductors*, Phys. Rev. Lett. **104**, 130502 (2010).

[46] A. M. Turner, F. Pollmann, and E. Berg, *Topological phases of one-dimensional fermions: An entanglement point of view*, Phys. Rev. B **83**, 075102 (2011).

[47] X.-L. Qi, H. Katsura, and A. W. W. Ludwig, *General Relationship between the Entanglement Spectrum and the Edge State Spectrum of Topological Quantum States*, Phys. Rev. Lett. **108**, 196402 (2012).

[48] R. Lundgren, Y. Fuji, S. Furukawa, and M. Oshikawa, *Entanglement spectra between coupled Tomonaga-Luttinger liquids: Applications to ladder systems and topological phases*, Phys. Rev. B **88**, 245137 (2013).

[49] H. Yao, W.-F. Tsai, and S. A. Kivelson, *Myriad phases of the checkerboard Hubbard model*, Phys. Rev. B **76**, 161104 (2007).

[50] H. Yao and S. A. Kivelson, *Fragile Mott Insulators*, Phys. Rev. Lett. **105**, 166402 (2010).

[51] E. Fradkin, *Field Theories of Condensed Matter Physics*, Second edition (Cambridge University Press, Cambridge, 2013).

[52] R. Botet and R. Jullien, *Ground-state properties of a spin-1 antiferromagnetic chain*, Phys. Rev. B **27**, 613 (1983).

[53] R. Botet, R. Jullien, and M. Kolb, *Finite-size-scaling study of the spin-1 Heisenberg-Ising chain with uniaxial anisotropy*, Phys. Rev. B **28**, 3914 (1983).

[54] U. Glaus and T. Schneider, *Critical properties of the spin-1 Heisenberg chain with uniaxial anisotropy*, Phys. Rev. B **30**, 215 (1984).

[55] M. P. Nightingale and H. W. J. Blöte, *Gap of the linear spin-1 Heisenberg antiferromagnet: A Monte Carlo calculation*, Phys. Rev. B **33**, 659 (1986).

[56] H. J. Schulz and T. Ziman, *Finite-length calculations of η and phase diagrams of quantum spin chains*, Phys. Rev. B **33**, 6545 (1986).

[57] W. Chen, K. Hida, and B. C. Sanctuary, *Ground-state phase diagram of $S = 1$ XXZ chains with uniaxial single-ion-type anisotropy*, Phys. Rev. B **67**, 104401 (2003).

[58] T. Tonegawa, K. Okamoto, H. Nakano, T. Sakai, K. Nomura, and M. Kaburagi, *Haldane, Large-D, and Intermediate-D States in an $S = 2$ Quantum Spin Chain with On-Site and XXZ Anisotropies*, J. Phys. Soc. Jpn. **80**, 043001 (2011).

[59] G. Sierra, *The nonlinear sigma model and spin ladders*, J. Phys. A: Math. Gen. **29**, 3299 (1996).

[60] S. Dell'Aringa, E. Ercolessi, G. Morandi, P. Pieri, and M. Roncaglia, *Effective Actions for Spin Ladders*, Phys. Rev. Lett. **78**, 2457 (1997).

[61] M. Oshikawa, *Hidden $Z_2 \times Z_2$ symmetry in quantum spin chains with arbitrary integer spin*, J. Phys.: Condens. Matter **4**, 7469 (1992).

[62] P. W. Anderson, *Resonating valence bonds: A new kind of insulator?*, Mat. Res. Bull. **8** (1973).

[63] S. R. White, R. M. Noack, and D. J. Scalapino, *Resonating Valence Bond Theory of Coupled Heisenberg Chains*, Phys. Rev. Lett. **73**, 886 (1994).

[64] M. Fannes, B. Nachtergaele, and R. F. Werner, *Finitely correlated states on quantum spin chains*, Comm. Math. Phys. **144**, 443 (1992).

[65] A. Klümper, A. Schadschneider, and J. Zittartz, *Equivalence and solution of anisotropic spin-1 models and generalized t-J fermion models in one dimension*, J. Phys. A: Math. Gen. **24**, L955 (1991).

[66] A. Klümper, A. Schadschneider, and J. Zittartz, *Groundstate properties of a generalized VBS-model*, Z. Phys. B **87**, 281 (1992).

[67] G. Vidal, *Efficient Classical Simulation of Slightly Entangled Quantum Computations*, Phys. Rev. Lett. **91**, 147902 (2003).

[68] D. Perez-Garcia, F. Verstraete, M. M. Wolf, and J. I. Cirac, *Matrix product state representations*, Quantum Inf. Comput. **7**, 401 (2007).

[69] R. Orús and G. Vidal, *Infinite time-evolving block decimation algorithm beyond unitary evolution*, Phys. Rev. B **78**, 155117 (2008).

[70] D. Perez-Garcia, M. M. Wolf, M. Sanz, F. Verstraete, and J. I. Cirac, *String Order and Symmetries in Quantum Spin Lattices*, Phys. Rev. Lett. **100**, 167202 (2008).

[71] M. M. Wolf, G. Ortiz, F. Verstraete, and J. I. Cirac, *Quantum Phase Transitions in Matrix Product Systems*, Phys. Rev. Lett. **97**, 110403 (2006).

[72] A. M. Tsvelik, *Two weakly coupled Heisenberg chains – Solution in continuous limit*, Mod. Phys. Lett. B **05**, 1973 (1991).

[73] S. P. Strong and A. J. Millis, *Competition between singlet formation and magnetic ordering in one-dimensional spin systems*, Phys. Rev. Lett. **69**, 2419 (1992).

[74] T. Barnes, E. Dagotto, J. Riera, and E. S. Swanson, *Excitation spectrum of Heisenberg spin ladders*, Phys. Rev. B **47**, 3196 (1993).

[75] S. Gopalan, T. M. Rice, and M. Sigrist, *Spin ladders with spin gaps: A description of a class of cuprates*, Phys. Rev. B **49**, 8901 (1994).

[76] Y. Nishiyama, N. Hatano, and M. Suzuki, *Phase Transition and Hidden Orders of the Heisenberg Ladder Model in the Ground State*, J. Phys. Soc. Jpn. **64**, 1967 (1995).

[77] S. P. Strong and A. J. Millis, *Competition between singlet formation and magnetic ordering in one-dimensional spin systems*, Phys. Rev. B **50**, 9911 (1994).

[78] D. Sénéchal, *Semiclassical description of spin ladders*, Phys. Rev. B **52**, 15319 (1995).

[79] D. G. Shelton, A. A. Nersesyan, and A. M. Tsvelik, *Antiferromagnetic spin ladders: Crossover between spin $S = 1/2$ and $S = 1$ chains*, Phys. Rev. B **53**, 8521 (1996).

[80] E. Orignac and T. Giamarchi, *Weakly disordered spin ladders*, Phys. Rev. B **57**, 5812 (1998).

[81] P. Lecheminant and E. Orignac, *Magnetization and dimerization profiles of the cut two-leg spin ladder*, Phys. Rev. B **65**, 174406 (2002).

[82] K. Hijii, A. Kitazawa, and K. Nomura, *Phase diagram of $S = 1/2$ two-leg XXZ spin-ladder systems*, Phys. Rev. B **72**, 014449 (2005).

[83] Z.-X. Liu, Z.-B. Yang, Y.-J. Han, W. Yi, and X.-G. Wen, *Symmetry-protected topological phases in spin ladders with two-body interactions*, Phys. Rev. B **86**, 195122 (2012).

[84] M. Reigrotzki, H. Tsunetsugu, and T. M. Rice, *Strong-coupling expansions for antiferromagnetic Heisenberg spin-one-half ladders*, J. Phys.: Condens. Matter **6**, 9235 (1994).

[85] N. Hatano and Y. Nishiyama, *Scaling theory of antiferromagnetic Heisenberg ladder models*, J. Phys. A: Math. Gen. **28**, 3911 (1995).

[86] H. J. Schulz, *Coupled Luttinger Liquids*, p. 81, (Editions Frontières, Gif-sur-Yvette, 1996), see also e-print arXiv:condmat/9605075.

[87] M. Greven, R. J. Birgeneau, and U. J. Wiese, *Monte Carlo Study of Correlations in Quantum Spin Ladders*, Phys. Rev. Lett. **77**, 1865 (1996).

[88] D. C. Cabra, A. Honecker, and P. Pujol, *Magnetization Curves of Antiferromagnetic Heisenberg Spin-1/2 Ladders*, Phys. Rev. Lett. **79**, 5126 (1997).

[89] D. C. Cabra, A. Honecker, and P. Pujol, *Magnetization plateaux in N-leg spin ladders*, Phys. Rev. B **58**, 6241 (1998).

[90] F. B. Ramos and J. C. Xavier, *N-leg spin-S Heisenberg ladders: A density-matrix renormalization group study*, Phys. Rev. B **89**, 094424 (2014).

[91] M. den Nijs, *The critical exponent η of the planar model from one-dimensional quantum field theory*, Physica A **111**, 273 (1982).

[92] J. Timonen and A. Luther, *Continuum-limit correlation functions for the spin-one anisotropic Heisenberg chain*, J. Phys. C **18**, 1439 (1985).

[93] J. Timonen, J. Sólyom, and J. B. Parkinson, *Critical behaviour of coupled spin chains*, J. Phys.: Condens. Matter **3**, 3343 (1991).

[94] S. R. White, *Equivalence of the antiferromagnetic Heisenberg ladder to a single $S = 1$ chain*, Phys. Rev. B **53**, 52 (1996).

[95] Ö. Legeza, G. Fáth, and J. Sólyom, *Phase diagram of magnetic ladders constructed from a composite-spin model*, Phys. Rev. B **55**, 291 (1997).

[96] Ö. Legeza and J. Sólyom, *Stability of the Haldane phase in anisotropic magnetic ladders*, Phys. Rev. B **56**, 14449 (1997).

[97] E. H. Kim and J. Sólyom, *Opening of the Haldane gap in anisotropic two- and four-leg spin ladders*, Phys. Rev. B **60**, 15230 (1999).

[98] P. Lecheminant, T. Jolicoeur, and P. Azaria, *Phase transitions in the one-dimensional spin-S J_1-J_2 XY model*, Phys. Rev. B **63**, 174426 (2001).

[99] T. Giamarchi, *Quantum Physics in One Dimension*, (Oxford University Press, New York, 2003).

[100] A. O. Gogolin, A. A. Nersesyan, and A. M. Tsvelik, *Bosonization and Strongly Correlated Systems*, (Cambridge University Press, Cambridge, 1998).

[101] D. C. Cabra and P. Pujol, "Field-Theoretical Methods in Quantum Magnetism," in *Quantum Magnetism*, edited by U. Schollwöck, J. Richter, D. J. J. Farnell, and R. F. Bishop (Springer-Verlag, Berlin, 2004) Chap. 6.

[102] S. Eggert, *Numerical evidence for multiplicative logarithmic corrections from marginal operators*, Phys. Rev. B **54**, R9612 (1996).

[103] S. Lukyanov and A. Zamolodchikov, *Exact expectation values of local fields in the quantum sine-Gordon model*, Nucl. Phys. B **493**, 571 (1997).

[104] S. Lukyanov, *Low energy effective Hamiltonian for the XXZ spin chain*, Nucl. Phys. B **522**, 533 (1998).

[105] S. Lukyanov, *Correlation amplitude for the XXZ spin chain in the disordered regime*, Phys. Rev. B **59**, 11163 (1999).

[106] S. Lukyanov and V. Terras, *Long-distance asymptotics of spin-spin correlation functions for the XXZ spin chain*, Nucl. Phys. B **654**, 323 (2003).

[107] D. C. Cabra, P. Pujol, and C. von Reichenbach, *Non-Abelian bosonization and Haldane's conjecture*, Phys. Rev. B **58**, 65 (1998).

[108] H. Nonne, P. Lecheminant, S. Capponi, G. Roux, and E. Boulat, *Competing orders in one-dimensional half-filled multicomponent fermionic cold atoms: The Haldane-charge conjecture*, Phys. Rev. B **84**, 125123 (2011).

[109] I. Affleck and F. D. M. Haldane, *Critical theory of quantum spin chains*, Phys. Rev. B **36**, 5291 (1987).

[110] M. Oshikawa, M. Yamanaka, and I. Affleck, *Magnetization Plateaus in Spin Chains: "Haldane Gap" for Half-Integer Spins*, Phys. Rev. Lett. **78**, 1984 (1997).

[111] T. Hirano, H. Katsura, and Y. Hatsugai, *Degeneracy and consistency condition for Berry phases: Gap closing under a local gauge twist*, Phys. Rev. B **78**, 054431 (2008).

[112] I. Affleck, *Exact critical exponents for quantum spin chains, non-linear σ-models at $\theta = \pi$ and the quantum hall effect*, Nucl. Phys. B **265**, 409 (1986).

[113] T. Hikihara and A. Furusaki, *Correlation amplitudes for the spin-1/2 XXZ chain in a magnetic field*, Phys. Rev. B **69**, 064427 (2004).

[114] E. Witten, *Non-abelian bosonization in two dimensions*, Comm. Math. Phys. **92**, 455 (1984).

[115] H. Tasaki, *Quantum liquid in antiferromagnetic chains: A stochastic geometric approach to the Haldane gap*, Phys. Rev. Lett. **66**, 798 (1991).

[116] Z. Weihong, V. Kotov, and J. Oitmaa, *Two-chain spin ladder with frustrating second-neighbor interactions*, Phys. Rev. B **57**, 11439 (1998).

[117] E. H. Kim, G. Fáth, J. Sólyom, and D. J. Scalapino, *Phase transitions between topologically distinct gapped phases in isotropic spin ladders*, Phys. Rev. B **62**, 14965 (2000).

[118] G. Fáth, Ö. Legeza, and J. Sólyom, *String order in spin liquid phases of spin ladders*, Phys. Rev. B **63**, 134403 (2001).

[119] A. A. Nersesyan and A. M. Tsvelik, *Spinons in more than one dimension: Resonance valence bond state stabilized by frustration*, Phys. Rev. B **67**, 024422 (2003).

[120] O. A. Starykh and L. Balents, *Dimerized Phase and Transitions in a Spatially Anisotropic Square Lattice Antiferromagnet*, Phys. Rev. Lett. **93**, 127202 (2004).

[121] E. H. Kim, Ö. Legeza, and J. Sólyom, *Topological order, dimerization, and spinon deconfinement in frustrated spin ladders*, Phys. Rev. B **77**, 205121 (2008).

[122] T. Hikihara and O. A. Starykh, *Phase diagram of the frustrated spin ladder*, Phys. Rev. B **81**, 064432 (2010).

[123] A. A. Nersesyan and A. M. Tsvelik, *One-Dimensional Spin-Liquid without Magnon Excitations*, Phys. Rev. Lett. **78**, 3939 (1997).

[124] A. K. Kolezhuk and H.-J. Mikeska, *Non-Haldane Spin-Liquid Models with Exact Ground States*, Phys. Rev. Lett. **80**, 2709 (1998).

[125] S. Takayoshi and M. Sato, *Coefficients of bosonized dimer operators in spin-1/2 XXZ chains and their applications*, Phys. Rev. B **82**, 214420 (2010).

[126] M. Nakamura, *Identification of topologically different valence bond states in spin ladders*, Physica B **329 - 333**, 1000 (2003).

[127] E. Berg, E. G. Dalla Torre, T. Giamarchi, and E. Altman, *Rise and fall of hidden string order of lattice bosons*, Phys. Rev. B **77**, 245119 (2008).

[128] A. M. Tsvelik, *New fermionic description of quantum spin liquid state*, Phys. Rev. Lett. **69**, 2142 (1992).

[129] U. Schollwöck and T. Jolicoeur, *Haldane Gap and Hidden Order in the $S = 2$ Antiferromagnetic Quantum Spin Chain*, Europhys. Lett. **30**, 493 (1995).

[130] U. Schollwöck, O. Golinelli, and T. Jolicœur, *$S = 2$ antiferromagnetic quantum spin chain*, Phys. Rev. B **54**, 4038 (1996).

[131] K. Nomura and A. Kitazawa, *$SU(2)/Z_2$ symmetry of the BKT transition and twisted boundary condition*, J. Phys. A: Math. Gen. **31**, 7341 (1998).

[132] H. Aschauer and U. Schollwöck, *Absence of string order in the anisotropic $S = 2$ Heisenberg antiferromagnet*, Phys. Rev. B **58**, 359 (1998).

[133] J. A. Kjäll, M. P. Zaletel, R. S. K. Mong, J. H. Bardarson, and F. Pollmann, *Phase diagram of the anisotropic spin-2 XXZ model: Infinite-system density matrix renormalization group study*, Phys. Rev. B **87**, 235106 (2013).

[134] Y.-C. Tzeng, *Parity quantum numbers in the density matrix renormalization group*, Phys. Rev. B **86**, 024403 (2012).

[135] K. Okamoto, T. Tonegawa, T. Sakai, and M. Kaburagi, *Edge Modes in the Intermediate-D and Large-D Phases of the $S = 2$ Quantum Spin Chain with XXZ and On-Site Anisotropies*, JPS Conf. Proc. **3**, 014022 (2014).

[136] S. Todo, M. Matsumoto, C. Yasuda, and H. Takayama, *Plaquette-singlet solid state and topological hidden order in a spin-1 antiferromagnetic Heisenberg ladder*, Phys. Rev. B **64**, 224412 (2001).

[137] D. C. Cabra and M. D. Grynberg, *Massive and Massless Behavior in Dimerized Spin Ladders*, Phys. Rev. Lett. **82**, 1768 (1999).

[138] K. Totsuka and M. Suzuki, *The spin-1/2 Heisenberg spin ladder with bond alternation*, J. Phys.: Condens. Matter **7**, 6079 (1995).

[139] M. A. Martín-Delgado, R. Shankar, and G. Sierra, *Phase Transitions in Staggered Spin Ladders*, Phys. Rev. Lett. **77**, 3443 (1996).

[140] J. Almeida, M. A. Martin-Delgado, and G. Sierra, *Density-matrix renormalization group study of the bond-alternating $S = 1/2$ Heisenberg ladder with ferro-antiferromagnetic couplings*, Phys. Rev. B **76**, 184428 (2007).

[141] J. Almeida, M. A. Martin-Delgado, and G. Sierra, *Critical lines and massive phases in quantum spin ladders with dimerization*, Phys. Rev. B **77**, 094415 (2008).

[142] J. Almeida, M. A. Martin-Delgado, and G. Sierra, *Twisted-order parameter applied to dimerized ladders*, J. Phys. A: Math. Theor. **41**, 485301 (2008).

[143] S. J. Gibson, R. Meyer, and G. Y. Chitov, *Numerical study of critical properties and hidden orders in dimerized spin ladders*, Phys. Rev. B **83**, 104423 (2011).

[144] Y. Kato and A. Tanaka, *Numerical Study of the $S = 1$ Antiferromagnetic Spin Chain with Bond Alternation*, J. Phys. Soc. Jpn. **63**, 1277 (1994).

[145] M. Yajima and M. Takahashi, *$S = 3/2$ Antiferromagnetic Spin Chain with Bond Alternation*, J. Phys. Soc. Jpn. **65**, 39 (1996).

[146] M. Yamanaka, M. Oshikawa, and S. Miyashita, *Hidden Order and Dimerization Transition in $S = 2$ Chains*, J. Phys. Soc. Jpn. **65**, 1562 (1996).

[147] S. Yamamoto, *Phase transitions in antiferromagnetic quantum spin chains with bond alternation*, Phys. Rev. B **55**, 3603 (1997).

[148] P. Lecheminant, A. O. Gogolin, and A. A. Nersesyan, *Criticality in self-dual sine-Gordon models*, Nucl. Phys. B **639**, 502 (2002).

[149] G. Delfino and G. Mussardo, *Non-integrable aspects of the multi-frequency sine-Gordon model*, Nucl. Phys. B **516**, 675 (1998).

[150] M. Fabrizio, A. O. Gogolin, and A. A. Nersesyan, *Critical properties of the double-frequency sine-Gordon model with applications*, Nucl. Phys. B **580**, 647 (2000).

[151] M. Tsukano and K. Nomura, *Berezinskii-Kosterlitz-Thouless Transition of Spin-1 XXZ Chains in a Staggered Magnetic Field*, J. Phys. Soc. Jpn. **67**, 302 (1998).

[152] M. Tsukano and K. Nomura, *Spin-1 XXZ chains in a staggered magnetic field*, Phys. Rev. B **57**, R8087 (1998).

[153] X. Deng, R. Citro, E. Orignac, A. Minguzzi, and L. Santos, *Polar bosons in one-dimensional disordered optical lattices*, Phys. Rev. B **87**, 195101 (2013).

[154] L. Fallani, J. E. Lye, V. Guarrera, C. Fort, and M. Inguscio, *Ultracold Atoms in a Disordered Crystal of Light: Towards a Bose Glass*, Phys. Rev. Lett. **98**, 130404 (2007).

[155] G. Roux, T. Barthel, I. P. McCulloch, C. Kollath, U. Schollwöck, and T. Giamarchi, *Quasiperiodic Bose-Hubbard model and localization in one-dimensional cold atomic gases*, Phys. Rev. A **78**, 023628 (2008).

[156] E. Altman and A. Auerbach, *Oscillating Superfluidity of Bosons in Optical Lattices*, Phys. Rev. Lett. **89**, 250404 (2002).

[157] M. Endres, M. Cheneau, T. Fukuhara, C. Weitenberg, P. Schaus, C. Gross, L. Mazza, M. C. Banuls, L. Pollet, I. Bloch, and S. Kuhr, *Observation of Correlated Particle-Hole Pairs and String Order in Low-Dimensional Mott Insulators*, Science **334**, 200 (2011).

[158] S. R. White, *Density matrix formulation for quantum renormalization groups*, Phys. Rev. Lett. **69**, 2863 (1992).

[159] I. P. McCulloch, *Infinite size density matrix renormalization group, revisited*, arXiv:0804.2509 (unpublished).

[160] P. Calabrese and J. Cardy, *Entanglement entropy and quantum field theory*, J. Stat. Mech. P06002 (2004).

[161] F. Pollmann and A. M. Turner, *Detection of symmetry-protected topological phases in one dimension*, Phys. Rev. B **86**, 125441 (2012).

[162] M. P. Zaletel and A. Vishwanath, *Constraints on topological order in Mott Insulators*, arXiv:1410.2894 (unpublished).